The role of the novel synthetic microneurotrophin BNN27 in glial cells in health and demyelination

UNIVERSITY OF CRETE

Department of Medicine

Laboratory of Basic Sciences

and

INSTITUTE OF MOLECULAR BIOLOGY AND BIOTECHNOLOGY

Foundation of Research and Technology (IMBB - FoRTH)

Heraklion

July 2017

PhD Thesis

Giulia Bonetto

Ο ρόλος της νέας συνθετικής νευροτροφίνης BNN27 σε κύτταρα της γλοίας σε φυσιολογικές και απομυελινωτικές συνθήκες

ΠΑΝΕΠΙΣΤΗΜΙΟ ΚΡΗΤΗΣ

Τμήμα Ιατρικής

Εργαστήριο Βασικών Επιστημών

και

ΙΝΣΤΙΤΟΥΤΟ ΜΟΡΙΑΚΗΣ ΒΙΟΛΟΓΙΑΣ ΚΑΙ ΒΙΟΤΕΧΝΟΛΟΓΙΑΣ

ΙΔΡΥΜΑ ΤΕΧΝΟΛΟΓΙΑΣ ΚΑΙ ΕΡΕΥΝΑΣ (IMBB - FoRTH)

Ηράκλειο

Ιούλιος 2017

Διδακτορική Διατριβή

Giulia Bonetto

ACKNOWLEDGMENTS

This dissertation would not have been possible without the help of several people who contributed in the preparation and completion of this project.

I owe my deepest gratitude to my supervisor, Professor Domna Karagogeos, for the continuous support of my PhD study and related research, for her patience and motivation. Her guidance helped me in all the time of research and writing of this thesis. I could not have imagined having a better advisor and mentor for my PhD study.

Also, my sincere thanks go to the members of my supervising committee, Professor Achille Gravanis and Doctor Kleio Spanaki, for their feedback and their valuable comments on my work.

I am particularly grateful to Assistant Professor Ioannis Charalampopoulos for his contributions to the study and for freely giving of his time, resources and expertise.

PhD candidates often talk about loneliness during the course of their studies, but this is something I never experienced. My fellow colleagues, Kostas, Lida, Maria, Katerina, Zouzanna and Ilias, have all extended their support in a very special way, and I gained a lot from them, through their personal and scholarly interactions, and their suggestions at various points of my research programme. I must also express my gratitude to the B.S./M.S. students Sofia, Vassiliki and Marina, which put their time and expertise into my research: without your contributions, it is likely that I would not have been able to handle all the work associated with my project.

A heartfelt thanks to my friends and previous labmates, Simona and Marilena, for keeping me motivated throughout the experiments and the writing.

A special thanks to my family, especially to my mother and grandmother: words cannot express how grateful I am for all of the sacrifices that you have made on my behalf. You have given me the motivation and direction with your unfaltering support throughout the good and bad years of my education.

I would also like to thank all of my friends who supported me in writing, and incented me to strive towards my goal. Thank you all for helping me to become who I am today.

Finally, I would like to express appreciation to my beloved Tommaso, who was always my support in the moments when there was no one to answer my queries.

Table of Contents

SUMMARY

In the first part of this doctoral thesis we investigated the activity of BNN27, a member of a chemical library of C17-spiroepoxy derivatives of the neurosteroid DHEA. BNN27 has been shown to regulate neuronal survival through its selective interaction with NGF receptors (TrkA and $p75^{NTR}$), but its role on glial populations has not been studied. Here we report that BNN27 provides trophic action (i.e. rescue from apoptosis), in a TrkA-dependent manner, to mature oligodendrocytes when they are challenged with the cuprizone toxin in culture. BNN27 treatment also increases oligodendrocyte maturation and diminishes microglia activation *in vitro*. The effect of BNN27 in the cuprizone mouse model of demyelination *in vivo* has also been investigated. In this model, that does not directly involve the adaptive immune system, BNN27 is able to protect from demyelination without affecting the remyelinating process. BNN27 preserves mature oligodendrocyte during demyelination, while reducing microgliosis and astrogliosis. Our findings suggest that BNN27 may serve as a lead molecule to develop neurotrophin-like, blood brain barrier (BBB)-permeable protective agents of oligodendrocyte populations and myelin, with potential applications in the treatment of demyelinating disorders. In the second part of the research, we focused on the identification of novel partners of TAG-1. TAG-1 is a GPI-anchored protein interacting with the transmembrane protein Caspr2 and the voltage-gated potassium channels expressed on the axon, forming a cluster in the juxtaparanodal area. Four putative TAG-1 interactors (MAP1B, MAP2, Reelin and TenascinR) were selected. These proteins were identified using a new computational tool called UniReD, which is able to predict new protein-protein interactions not yet documented in the literature. We describe that TAG-1 interacts (directly or indirectly) with MAP1B and Reelin, while no interaction was visible with MAP2 and TenascinR. MAP1B holds an important role in the regulation of microtubule dynamics, and microtubule-actin interactions, and it mediates growth cone as well as neuronal migration. Reelin is a large secreted extracellular matrix glycoprotein that regulates processes of neuronal migration and positioning in the developing brain by controlling cell-cell interactions. These novel identified interactions may not be associated with the juxtaparanodal partners of TAG-1, but they may be important for its developmental functions.

A. INTRODUCTION I

A.1. Myelin origin and functions

Over the course of evolution, vertebrates experienced a dramatic increase in body size, which corresponded to the need of action potential propagation along bigger distances. The signal propagation could be facilitated by two possible mechanisms: either the increase in axonal diameter, observed in many large invertebrate species, including cephalopods, which axons can reach several millimeters in diameter (Zalc and Colman 2000), or a decrease in axonal capacitance and increase in axial resistance by means of physical insulation. The vertebrates adopted the second strategy, producing specialized glial cells that could insulate regular intervals (internodes) along large caliber axons (Zalc and Colman 2000). This insulation, called myelin, prompted saltatory conduction between ion channels clustered at the nodes of Ranvier rather than continuous membrane depolarization, which is both energetically unfavorable and slow (Nave 2010). Myelination benefits are twofold: first, in non-myelinated fibers, the restoration of ion gradients by the Na^+/K^+-ATPase consumes a large fraction of available ATP. Myelination strongly reduces this energy consumption, because action potentials and ion currents are restricted to less than 0.5% of the axon's surface. Second, the increase in conduction velocity for myelinated neurons allows complex yet compact higher nervous systems to evolve (Nave 2010).

Myelin is not only essential for the fast conduction of the action potential but also to maintain axonal integrity (Yin, Baek et al. 2006). For instance, proteolipid protein (PLP)-null mice have reduced anterograde and retrograde axonal transport that manifest as organelle accumulations at nodes of Ranvier (Edgar, McLaughlin et al. 2004). Mice chimeric for the X-linked PLP-null allele (50% of myelin internodes lack PLP) have numerically 50% of the axonal ovoids present in PLP-null mice (Edgar, McLaughlin et al. 2004). This implies that PLP facilitates paranodal axonal cytoskeletal organization at the level of individual myelin internodes. Moreover, nucleotide-3′-phosphodiesterase (CNP)-null mice have earlier and more extensive axonal pathology, decreased motor performance at earlier ages, and reduced life spans (Lappe-Siefke, Goebbels et al. 2003).

Furthermore, signals from the myelinating glia induce specialisations in the axonal membrane such as the distribution of ion channels at the nodes and paranodes, essential for rapid conduction (Schafer and Rasband 2006).

Myelin is formed by glial cells: oligodendrocytes (OL) are the myelinating cells of the central nervous system (CNS), while this task is performed by Scwhann cell in the peripheral nervous system (PNS) (Fig.1). To properly myelinate, these cells have to extend many processes that will contact and envelope a stretch of axon (Barateiro and Fernandes 2014).

Myelin is composed of 70-80% lipids (mainly galactosylceramide or cerebroside), and 15-30% myelin-specific proteins. The increased composition of myelin in lipids is opposed to other biological membranes, which have a bigger protein-to-lipid ratio (Farrer and Quarles 1999).

The distinct composition of the cell membrane of the two glial types (OLs and Schwann cells), results in unique myelin proteins in the CNS and the PNS. CNS myelin is composed of the myelin basic protein (MBP), PLP, CNP and myelin-associated glycoprotein (MAG). In the PNS, myelin shares some common proteins with the CNS, such as MBP and MAG, while others, such as P0 and peripheral myelin protein-22 (PMP-22), are specifically expressed only in this system (Farrer and Quarles 1999). Myelin in the PNS has a similar structure and fulfills similar functions as CNS myelin, yet surprisingly there are fundamental differences in its formation, best underscored by the fact that crucial molecular regulators of axon–Schwann cell interactions are by and large not required for axon-OL interactions (Brinkmann, Agarwal et al. 2008, Monk, Naylor et al. 2009). Moreover, the cell-cell interactions that lead to myelination of peripheral nerves by Schwann cells are quite distinct from those in the CNS. Schwann cells require axons for almost all stages of their early development, including myelination *in vitro* and *in vivo* (Jessen and Mirsky 2005). In contrast, OLs can develop and differentiate in cell culture in the absence of axons (Knapp, Bartlett et al. 1987) and they can myelinate inert structures including paraformaldehyde (PFA)-fixed axons (Rosenberg, Kelland et al. 2008) and polystyrene nanofibers (Lee, Leach et al. 2012). Furthermore, while one OL myelinates up to 40 axonal segments, each Schwann cell wraps only a single axon (Pfeiffer, Warrington et al. 1993). In conclusion, the differences in cell biology and origin of the two types of glial cells may account for the functional differences as well. We will not discuss further the biology of Schwann cells as this thesis focuses on the CNS and OLs.

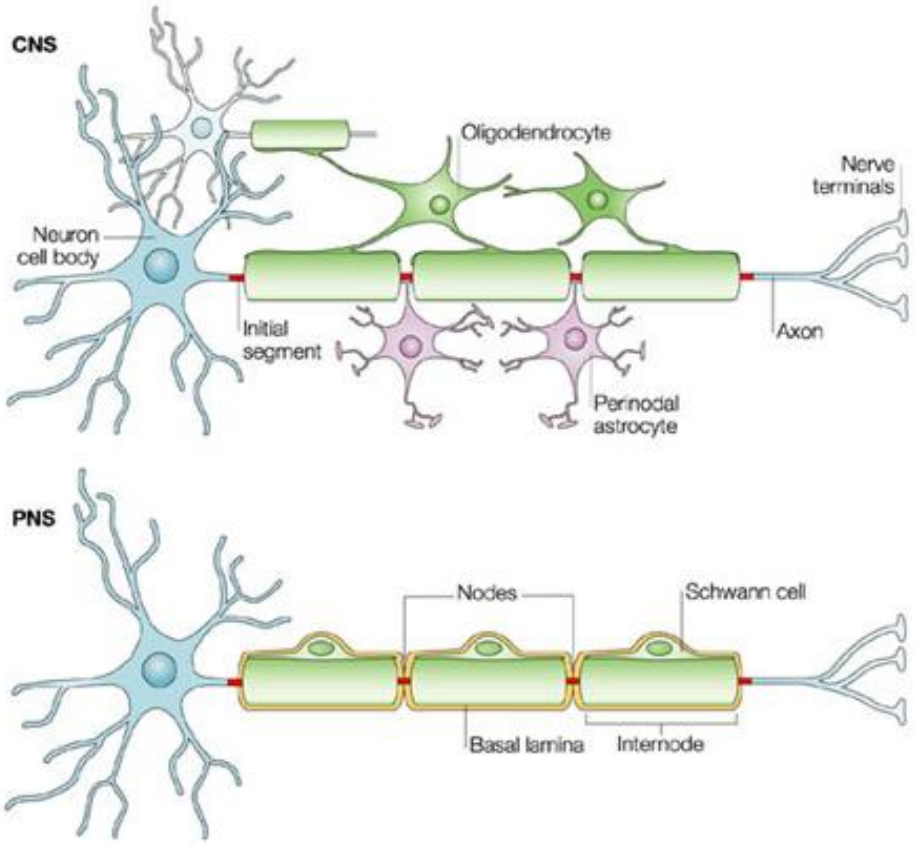

Figure 1. Structure of myelinated axons in CNS and PNS. Myelinating glial cells, OLs in the CNS or Schwann cells in the PNS, form the myelin sheath by enwrapping their membrane several times around the axon. Myelin covers the axon at intervals (internodes), leaving gaps called nodes of Ranvier. OLs can myelinate different axons and several internodes per axon, whereas Schwann cells myelinate a single internode in a single axon. Adapted from Poliak & Peles (Poliak and Peles 2003).

A.2. Oligodendrocyte origin

As mentioned before, in the CNS, OLs are responsible for the production of myelin, consisting of oligodendroglial plasma membrane loops tightly wound concentrically around the axon. Oligodendrocyte progenitor cells (OPCs) are generated in the ventral neuroepithelium of the neural tube in early embryonic life, more specifically from the motor neuron progenitor (pMN) domain (Pringle, Guthrie et al. 1998), and in the dorsal spinal cord and hindbrain/telencephalon of the brain, in late embryonic development and early post-natal life (Cai, Qi et al. 2005, Kessaris, Fogarty et al. 2006).

In the spinal cord, OPCs initially arise in ventral regions of the neural tube at embronic day 12.5 (E12.5) (Fig. 2b), and then migrate dorsally during development (Warf, Fok-Seang et al. 1991). During subsequent development (E15.5), the dorsal regions acquire the capacity for oligodendrogenesis, probably both intrinsically and through the ventral to dorsal migration of OPCs (Rowitch and Kriegstein 2010).

The initial restricted localization of OPCs in the ventral plate of the neural tube appears not to be limited to the spinal cord but is also observed in mid- and forebrain (Fig. 2a). The earliest cortical oligodendrocytes arise from Nkx2.1 expressing precursors in the ventricular zone of the medial ganglionic eminence (MGE) and the anterior entopeduncular area (AEP), starting at E12.5, migrating to the entire dorsal and ventral telencephalon to populate the cerebral cortex by E16. The second and third waves of OPCs arise from Gsh2-expressing precursors in the lateral and caudal ganglionic eminences (LGE and CGE) at E16, and Emx1-expressing precursors in the postnatal dorsal cortex (Rowitch and Kriegstein 2010). Paradoxically, most of the early born OPCs disappear after birth, such that majority of the oligodendrocytes in the adult dorsal cortex are derived from later arising Emx1-expressing cells (Kessaris, Fogarty et al. 2006).

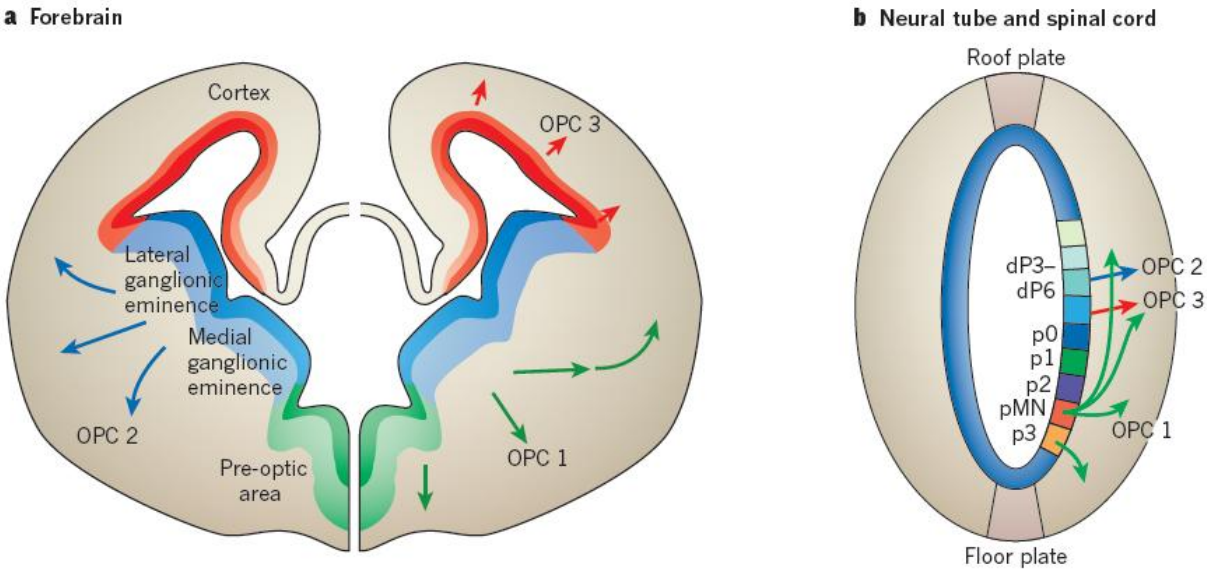

Figure 2. OPC production in the mammalian CNS. (A) Three sequential waves of OPCs are generated from different regions of the forebrain ventricular zone: OPC 1 (green arrows) arises from Nkx2.1-expressing precursors in the MGE, starting at E12.5; OPC 2 (blue arrows) arises from precursors expressing the homeobox gene Gsx2 in the LGE and MGE, starting at E15.5; and OPC 3 (red arrows) arises from precursors expressing the homeobox gene Emx1 in the cortex, starting at birth. (B) Two distinct waves of OPCs emanate from the ventral and the dorsal region of the spinal cord in the embryo and fetus, respectively. A third wave begins after birth. In the first wave (OPC 1, green arrows), ventral OPCs arise from Olig2-expressing progenitor cells in the pMN domain at E12.5 and subsequently migrate to populate the entire neural tube. The development of these cells depends on Sonic Hedgehog (SHH)-mediated signaling. In the second wave (OPC 2, blue arrows), dorsal OPCs develop from Olig2-expressing cells of the dP3, dP4, dP5 and dP6 domains during the fetal phase (at day E15.5) in an SHH-independent manner. The origins of the third wave (OPC 3, red arrows), which occurs after birth, remain unclear. These OPCs might arise from progenitor cells, which remain around the central canal, or from proliferative Ng2-expressing precursor cells throughout the parenchyma. OPCs from ventral and dorsal regions are intermixed in the spinal cord at birth, with a heavy predominance of pMN-derived cells. Adapted from Rowitch & Kriegestein (Rowitch and Kriegstein 2010).

OPCs migrate extensively throughout the CNS before their final differentiation into myelin-forming OLs (Mitew, Hay et al. 2014, Ackerman, Garcia et al. 2015). Moreover, OLs have to extend processes in a similar fashion to the extension of neurites from neuronal cell bodies. As for neurons, a number of extracellular matrix (ECM) molecules play an instructive role in the control of migrating OPCs. For example, tenascin-C is expressed at high levels at the rat retina-

optic nerve junction, an area through which OPCs do not migrate, so preventing access of myelin-forming cells to the retina. Therefore, it has been proposed that tenascin-C might provide a barrier to OPC migration at the retinal end of the optic nerve (Bartsch, Faissner et al. 1994). Moreover, to find their way and to regulate the extension of their processes along the astrocyte-produced ECM, oligodendrocytes use metalloproteinases (MMP). With the use of explant cultures of newborn rat neurohypophysis, it was shown that migrating OPCs express a polysialylated (PSA) form of NCAM (Wang, Rougon et al. 1994). Removal of PSA-NCAM from the surface of progenitors by an endoneuraminidase treatment results in the complete blockade of the dispersion of the OPCs from the explant. As shown for neurons and astrocytes, the expression of PSA-NCAM does not itself provide a specific signal for migration, but its expression appears to open a permissive gate that allows cells to respond to external cues at the appropriate time and space (Rutishauser and Landmesser 1996). Thus migrating OPCs may use distinct and discrete mechanisms to navigate specific migrational pathways.

When they reach their destination, OPCs become post-mitotic and acquire a pre-myelinating identity as $Nkx2.2^{+}$ cells, mainly in white matter regions. Pre-myelinating OPCs are able to wrap axons with their plasma membrane but do not form mature myelin (Snaidero and Simons 2014). Not all OPCs that are generated differentiate into myelinating OLs: some OPCs that appear to commit to the myelination pathways but fail to associate with a target axon, undergo programed cell death or apoptosis, while others remain undifferentiated and form a significant population of adult OPCs, whose functions are not well defined (Trapp, Nishiyama et al. 1997).

A.3. Myelination during adulthood and remyelination in the damaged CNS

Myelination in the CNS refers to the ensheathment of axons by the plasma membranes of OLs in a spiral fashion (wrapping), with compaction into segments of compact myelin to form internodes. Internodal segments alternate with nodes of Ranvier (unwrapped axonal membranes) (Fig. 3), where an accumulation of voltage-gated sodium (Na_v) channels allows for action potential propagation (Sherman and Brophy 2005). Immediately adjacent to nodes of Ranvier, on either side are segments of paranodal myelin, where interactions between cell adhesion molecules and the extracellular matrix help to define and may initiate the formation of nodes of Ranvier (Susuki and Rasband 2008). Beyond the paranodes are juxtaparanodal regions of myelin, which express voltage-gated potassium (K_v) channels that are thought to maintain neuronal resting potential in internodal segments and to mediate axoglial communication (Poliak and Peles 2003). Myelin insulates the internodal regions to decrease membrane capacitance and increase membrane resistance, thereby facilitating fast saltatory propagation of action potentials (Hartline and Colman 2007).

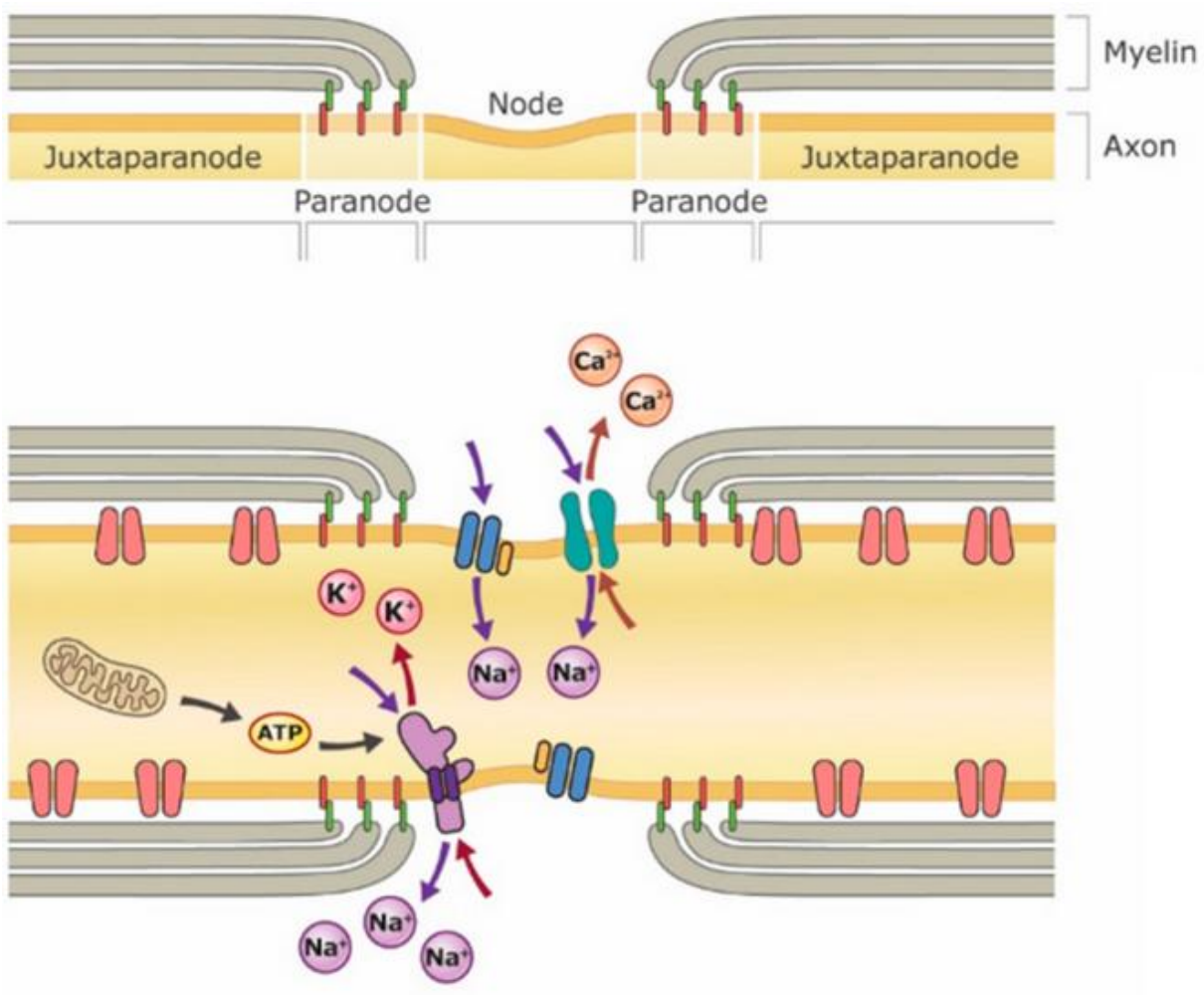

Figure 3. An intact node of Ranvier with paranodal and juxtaparanodal regions. Depicted are Na^+, K^+ and Ca^{2+} ions flowing through their respective channels, with mitochondria supplying the ATP for energy-dependent $Na^{+/}K^+$ ATPases that re-establish the ion gradients depleted by ion flux through channels. Adapted from Coggan et al. (Coggan, Bittner et al. 2015).

OPCs remain proliferative throughout life, dividing in adult mice every 20-40 days on average when raised in a non-enriched environment (Simon, Gotz et al. 2011, Young, Psachoulia et al. 2013). Despite the inherent capacity of forebrain OPCs for self-renewal (Psachoulia, Jamen et al. 2009), a population of OPCs derived from SVZ progenitors has been found in the postnatal rodent forebrain (Levison and Goldman 1993), mobilizing especially after demyelinating injury (Xing, Roth et al. 2014). These cells account for 5-8% of all cells in the CNS (Levine, Reynolds et al. 2001) and exist throughout regions such as the optic nerve (Shi, Marinovich et al. 1998), motor cortex, corpus callosum (CC) (Clarke, Young et al. 2012), and cerebellum (Levine, Stincone et al. 1993), providing a substantial source of new oligodendrocytes and thus a

potential reservoir for remyelination. Adult OPC are oligodendrocyte precursors with restricted lineage potential, generating myelinating OLs, but not astrocytes or neurons, not even during disease (Psachoulia, Jamen et al. 2009). Interestingly, these cells are constantly proliferating in the CNS to maintain their homeostatic cell density (Hughes, Kang et al. 2013), though at slower rate than during development or injury (McTigue, Wei et al. 2001).

OPCs can extend filopodia to continuously survey their environment, and they are capable of migrating to areas of demand to replace injured or dying cells (Hughes, Kang et al. 2013). Through a combination of growth and trophic factor exposure (Bansal, Kumar et al. 1996) and epigenetic modifications (Shen, Li et al. 2005), OPCs can withdraw from the cell cycle, express OL proteins, including MBP and PLP, and differentiate into myelinating OLs. OLs in the mammalian brain myelinate axons of diameters greater than 0.2 mm, but unmyelinated axons between diameters of 0.2 mm and 0.8 mm can also be found (Snaidero and Simons 2014). Given an axon or axon-like substrate (e.g. polystyrene nanofibers or silica micropillars), oligodendroglial cells *in vitro* appear to follow an innate program of differentiation and myelin wrapping even in the absence of exogenous signaling (Mei, Fancy et al. 2014). While this inherent propensity to wrap fibers of appropriate size is evident *in vitro*, the presence in the brain of appropriately sized yet unmyelinated fibers suggests a more complicated interplay of modulating factors *in vivo*.

Following injury and myelin damage, NG2/PDGFRα-expressing adult progenitors differentiate into OLs capable of remyelinating axons and restoring nearly normal nerve conduction (Zawadzka, Rivers et al. 2010). Remyelination at large requires the activation, recruitment and maturation of OPCs present throughout the CNS and/or derived from stem/progenitor cells located within the SVZ (Hesp, Goldstein et al. 2015). However, this regenerative process, in particular with progression of disease and/or age, is often limited and only partially able to fully restore axonal conduction velocity and the neuroprotective functions of the myelin sheath (Franklin and Gallo 2014). Impairment of myelin regeneration under pathological conditions has been attributed to a decrease in both OPC recruitment and differentiation, whereby the latter is currently considered to play a more prominent role in determining the rate of remyelination (Franklin and Goldman 2015).While the exact reasons for impaired remyelination are not fully understood, there is increasing evidence for a critical role of the extracellular environment (Berezin, Walmod et al. 2014), which likely acts upstream of transcriptional and epigenetic mechanisms regulating OL differentiation (Hernandez and Casaccia 2015). Thus, enhancing remyelination is considered a promising strategy toward the regenerative/protective treatment of diseases in which the myelin sheath is lost (Lubetzki and Stankoff 2014).

A.4. Oligodendrocyte, astrocyte and microglia crosstalk in myelin development, damage and repair

Glial cells in the adult mammalian CNS comprise astrocytes, OLs and microglia. The roles of glial cells in health and in disease have been partially neglected because many basic aspects of their physiology and pathophysiology are still not completely understood. However, it is becoming more evident that glia-glia crosstalk plays several important roles in brain function during development and disease. Glial cells play many roles, including the modulation of homeostatic and synaptic functions, myelination, nerve signal propagation and responses to neural injury (Herculano-Houzel 2014). Astrocytes have star-shape morphology and are the most abundant CNS glial cell type. They play essential functions in blood brain barrier (BBB) maintenance, neuronal survival and in synapse formation, strength and turnover (Barres 2008). While OLs and astrocytes originate from a common lineage of neural progenitor cells within the neuroectoderm, microglia are the main innate immune cells of the CNS and arise from hematopoietic stem cells in the yolk sac during early embryogenesis that populate the CNS. Being ontogenetically different from other tissue-macrophages they have longevity and capacity for self-renewal (Prinz and Priller 2014).

Astrocytes originate from neural embryonic progenitor cells that line the lumen of the embryonic neural tube. However, they can be formed indirectly via radial glia, which in addition to function as scaffolding for newborn neuron migration, can serve as progenitor cells giving rise to astrocytes (Kessaris, Pringle et al. 2008). Type 1 astrocytes (protoplasmic astrocytes) are localized in the gray matter and ensheath synapses and blood vessels to promote synapse and BBB functions, respectively. Type 2 astrocytes (fibrous astrocytes) are localized in the white matter and contact the nodes of Ranvier and the blood vessels (Sofroniew and Vinters 2010). In addition, astrocytes range from inactive or quiescent, to active and reactive. Quiescent astrocytes exist in the normal resting CNS tissue. Upon injury or insult, astrocytes become activated by various mechanisms that result in mild astrogliosis. Reactive astrocytes are closer to the injury site and are responsible for the glial scar formation (Nash, Ioannidou et al. 2011).

There are several pieces of evidence about the interplay between astrocytes and oligodendrocytes and their impact on myelination (Fig. 4): for instance, type 1 astrocytes were identified to expand O-2A progenitors from neonatal rat optic nerve. Such expansion was found to be mediated by unidentified soluble growth factors (Noble and Murray 1984), later identified as platelet-derived growth factor (PDGF) (Noble, Murray et al. 1988) and basic fibroblast growth factor (FGF2) (Bogler, Wren et al. 1990). PDGF and FGF2 are both potent mitogens for OPCs and inhibit premature oligodendrocyte differentiation. Other soluble factors secreted by astrocytes have been implicated in enhancing myelination, such as the leukemia inhibitory factor-like protein (LIF), which is able to promote OL survival and to maintain them in a mature myelinogenic state (Gard, Burrell et al. 1995). Other examples are neuregulin-1 (Taveggia, Thaker et al. 2008), gamma-secretase (Watkins, Emery et al. 2008), ciliary neurotrophic factor

(CNTF) (Stankoff, Aigrot et al. 2002), insulin-like growth factor 1 (IGF-1) (Zeger, Popken et al. 2007), and neurotrophin-3 (NT3) (Kumar, Biancotti et al. 2007). Physical contact with astrocytes can also facilitate the maturation of oligodendrocytes (Sakurai, Nishimura et al. 1998). Astrocytes were found to promote adult mouse OL survival through a cell-contact dependent mechanism involving the interaction of a6b1 integrin on OLs with laminin on astrocytes (Corley, Ladiwala et al. 2001). In addition to promoting OL survival and differentiation, astrocytes also affect other aspects of OL biology, such as process extension through FGF2 in combination with the ECM proteins fibronectin and laminin (Oh and Yong 1996).

It has been shown, taking advantage of remyelinating models (such as the cuprizone), that *in vivo* transplantation of type 1 astrocytes potentiated OL remyelination and increased the thickness of myelin sheaths (Franklin, Crang et al. 1991). The expression of TNFR2 in astrocytes resulted in the autocrine expression of CXCL12, which acted at its receptor CXCR4 on OPCs, inducing their proliferation and differentiation, therefore enabling remyelination (Patel, Williams et al. 2012). Furthermore, it has been shown that astrocyte ablation during cuprizone-induced demyelination did not prevent myelin damage but rather inhibited the removal of the myelin debris and delayed remyelination (Skripuletz, Hackstette et al. 2013). Altogether, these results suggest that the astrocyte free regions of the lesion either contained inhibitory signals preventing terminal differentiation of OPCs or lack appropriate signals necessary for OPCs to undergo terminal differentiation.

Astrocytes have been initially described to have detrimental effects on oligodendrocyte differentiation, in particular those within the glial scar, which appear to inhibit regeneration and impacted negatively on remyelination (Silver and Miller 2004). *In vitro* studies showed that type 1 astrocytes inhibited myelination of dorsal root ganglion axons by OLs (Rosen, Bunge et al. 1989). Astrocytes also secrete factors implicated in the inhibition of myelination and remyelination. Besides the above mentioned PDGF and FGF2 (Bogler, Wren et al. 1990), which promote OPC proliferation and inhibit premature differentiation, others such as tenascin C (Nash, Ioannidou et al. 2011), BMP 2/4 (Wang, Cheng et al. 2011), and hyaluronan (Sloane, Batt et al. 2010) have also been described. Overall, these studies suggest that the outcome of glial interactions in myelination is affected by the surrounding microenvironment, emphasizing that the activation state of astrocytes likely determines their permissive or inhibitory influence on oligodendrocyte development. Besides the different possibilities of astrocyte phenotypes, it should also be considered the distance of these populations to the lesion site, as relatively small changes in the responsive milieu may have different impacts on oligodendrocyte behavior. It has been hypothesized that while astrocytes more distal to injury are activated cells that contribute in a greater extent to regeneration via the secretion of growth factors and cytokines, astrocytes in closer proximity to the lesion site are more reactive and may hinder the remyelination process (Nash, Ioannidou et al. 2011).

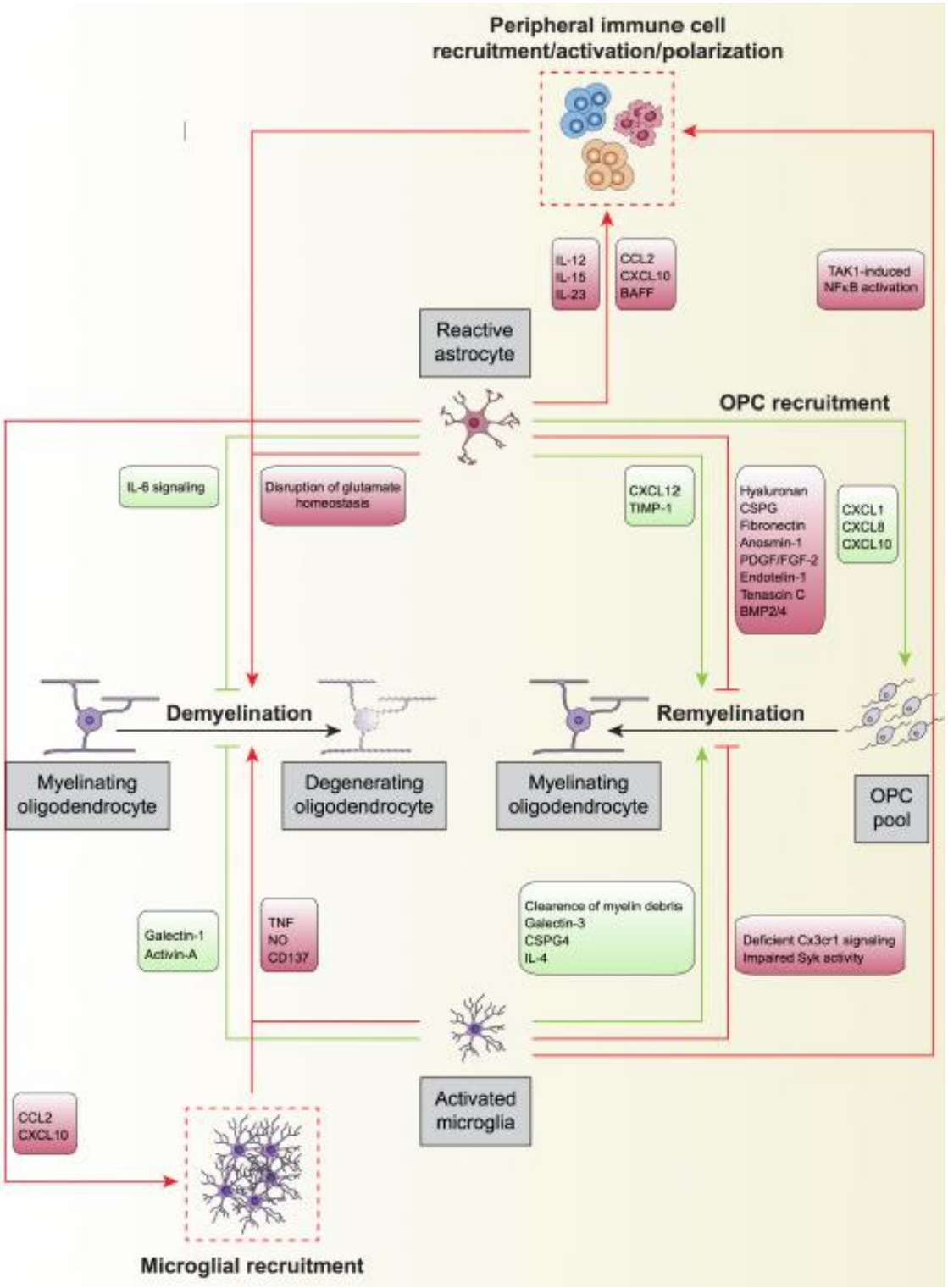

Figure 4. Oligodendrocyte, astrocyte and microglia crosstalk during demyelination and remyelination. Upon an insult to the CNS parenchyma or in neurodegenerative diseases, mature myelinating oligodendrocytes degenerate and eventually die, a processes termed active demyelination. Reactive astrocytes and activated microglia directly participate in this process displaying both detrimental (red) and beneficial (green) roles. Astrocytes may also modulate

the recruitment of peripheral immune cells by secreting different set of cytokines and chemokines, which will further promote the degeneration of myelinating oligodendrocytes. Furthermore, astrocytes secrete the chemokines CCL2 and CXCL10 to recruit overactive microglia, which may further increase oligodendrocyte loss. Microglial TAK1 signaling is also involved in the recruitment of peripheral immune cells to regulate active demyelination. On the other hand, astrocytes and microglia promote remyelination after myelin damage by the generation of oligodendrocytes from the OPC pool in the neuronal parenchyma. During remyelination, and as occurs for active demyelination, reactive astrocytes and activated microglia can promote (green) or impede (red) the process. Astrocyte can further influence remyelination by secreting the chemokines CXCL1, CXCL8 and CXCL10 to recruit OPC to demyelinated zones where they can differentiate into mature oligodendrocytes. Adapted from Prinz & Priller. (Prinz and Priller 2014)

Microglia constitute the myeloid resident population of the CNS, representing around 10% of the total glial cells within the nervous tissue (Soulet and Rivest 2008). Microglia are critically involved in the scavenging of dying cells, pathogens and molecules that engage pattern recognition receptors. As the major component of the immune effector system of the CNS at steady-state conditions, surveillant microglia are usually claimed to act as sensors of pathologic events (Hanisch and Kettenmann 2007). Microglial activation has been described extensively in autoimmune diseases such as MS in humans and in the EAE mouse MS model. In these pathological contexts (Fig. 4), microglia can produce and release neurotoxic (reactive oxygen and nitrogen species and glutamate) or neurotrophic molecules, pro and anti-inflammatory cytokines or chemokines, and present self-antigens to effector immune cells. Pathological evidence indicates that the remyelination onset in fresh lesions of brain and spinal cord of patients with MS occurs in acute, active lesions, which are characterized by a robust inflammatory response (Prineas, Kwon et al. 1989). Following injury, different inflammatory molecules such as cytokines and chemokines are secreted and released by microglia in the surrounding milieu. In this scenario, microglia become activated, expand, migrate and accumulate within the damaged area of the neuronal parenchyma, playing both beneficial and detrimental roles during myelin damage and repair.

Early studies using microglia and oligodendrocyte co-cultures showed that the former stimulate the expression of the myelin-specific proteins MBP and PLP in OLs, suggesting a positive role for microglia in myelination (Hamilton and Rome 1994). In line with this, conditioned medium derived from non-activated microglia enhanced OPC survival and maturation through the increase of PDGFα receptor-signaling pathway and modulation of NF-kB activation (Nicholas, Wing et al. 2001).

The iron status of microglia is also important for OL survival. Increasing the iron load promotes the release of H-ferritin by microglia and incubation of OL cultures with conditioned medium of iron-loaded microglia increases the survival of these cultures (Poliani, Wang et al. 2015).
Conditioned medium of non-activated microglia cultures was compared with that of astrocytes to evaluate their effect in OPC proliferation and differentiation. The results showed that astrocyte-conditioned medium was more efficient in promoting OPC proliferation, while microglia-conditioned medium accelerated oligodendrocyte differentiation more efficiently than that of astrocytes. Analysis of the media composition revealed that astrocyte-conditioned medium had increased levels of PDGFα, FGF2, FGF2 binding protein, CNTF, growth hormone, TIMP-1 and thrombospondin. In contrast, levels of IGF-1, E-selectin, fractalkine (CX3CL1), neuropilin-2, IL-2, IL-5 and vascular endothelial growth factor (VEGF) were significantly higher in microglia-conditioned medium. This distinct pattern of cytokines and growth factors in the conditioned medium of astrocytes and of microglia correlates with differentially activated intracellular signaling pathways in OPC exposed to the two different media (Pang, Fan et al. 2013).
In polarization conditions, such as *in vitro* stimulation with lipopolysaccharide (LPS), the release of cytotoxic effectors by both astrocytes and microglia, produces the opposite effects on OPC (Pang, Cai et al. 2000). LPS-activated microglia hinders OPC differentiation by nitric oxide (NO)-dependent oxidative damage in an early phase and TNF in a later phase (Pang, Campbell et al. 2010). In the presence of astrocytes, LPS-polarized microglia is toxic to differentiating oligodendrocytes via TNF signaling but not via NO-dependent oxidative damage (Li, Ramenaden et al. 2008).
In remyelination, microglia have also been shown to play dual roles. Microglia expressing the CCR5 receptor were identified within early remyelinating lesions in patients at early stages of MS, suggesting a possible role for these cells in initiating remyelination (Trebst, Konig et al. 2008). The phenotype of activated microglia was also shown to influence its beneficial role in efficient remyelination. This process is dependent on microglia changing from an M1- to an M2-dominant response in the lysolecithin-induced demyelination model. Oligodendrocyte differentiation was enhanced with M2 microglia-conditioned medium *in vitro* and impaired *in vivo* following intra-lesional depletion of M2 microglia (Miron, Boyd et al. 2013).
Another important aspect of microglia in remyelination concerns its role in the clearance of myelin debris upon myelin injury. In fact, for the remyelination process to be effective, myelin debris must be cleared from the injury site (Kotter, Li et al. 2006). Myelin clearance by microglia after cuprizone-induced demyelination was found to depend on the expression of microglial triggering receptor expressed on myeloid cells 2 (TREM2), a surface receptor that binds polyanions, such as dextran sulfate and bacterial LPS, and activates downstream signaling cascades through the adapter DAP12 (Poliani, Wang et al. 2015). In the cuprizone model, astrocytes are thought to recruit microglia to the lesion site in order to phagocyte and clear damaged myelin, a process regulated by the chemokine CXCL10. In the absence of astrocytes

and, consequently, microglia recruitment, removal of myelin debris is significantly delayed, inhibiting OPC proliferation and remyelination (Skripuletz, Hackstette et al. 2013).
In conclusion, homeostasis of the CNS myelination depends on the crosstalk between oligodendrocytes, astrocytes and microglia. Understanding the nature and complex dynamics of such interactions, which can play both beneficial and detrimental roles during damage and repair, will increase our knowledge into demyelinating diseases, and may help us to devise novel and more holistic ways to manipulate and improve remyelination.

A.5. Multiple Sclerosis

Multiple sclerosis (MS) is an inflammatory demyelinating disease of the CNS that causes focal destruction of the myelin sheath and astrocytic scar formation (Lucchinetti, Bruck et al. 1996, Lassmann 1998). The pathological hallmark of MS is the white matter "plaque" which is widely scattered throughout the CNS, with a predilection for the optic nerves, brainstem, spinal cord and periventricular white matter. The disease is characterized by a relapsing-remitting (RR) course, or by disability accrual over an extreme variability of time. At diagnosis, about 75% of persons with MS suffer from RRMS, while about 25% of such persons will convert to secondary progressive MS (SPMS) within two to three decades from the onset (Lugaresi, di Ioia et al. 2013). About 10% of patients with MS manifest primary progressive MS (PPMS) at diagnosis, and they show gradual worsening of neurological disability from symptom onset (Lugaresi, di Ioia et al. 2013).
The pathogenesis of MS is characterised by a cascade of pathobiological events, ranging from focal lymphocytic infiltration and microglia activation to demyelination and axonal degeneration (Ciccarelli, Barkhof et al. 2014) (Fig. 5). The long favored hypothesis in MS, referred as "immune initiated disease", implicates that autoreactive T cells generated in the systemic compartment access the CNS, where they persist and induce an inflammatory cascade that results in the injury of previously normal neural tissues (Kawakami, Lassmann et al. 2004, Trapp 2004). A second hypothesis, the so-called "neural initiated disease", implicates that events within the CNS initiate the MS disease process. A frequent speculation is that an acquired acute or persistent infection of neural cells could result in release of tissue antigens that, in turn, would provoke a disease relevant autoimmune response (Antony, van Marle et al. 2004, Rotola, Merlotti et al. 2004).
The licensed MS therapies have shown ability in the management of RRMS forms, but they have not shown efficacy for PMS (D'Amico, Patti et al. 2016). Six agents are approved by regulatory agencies to treat relapsing MS. First line agents include interferon β-1b, intramuscular or subcutaneous interferon β-1a, and glatiramer acetate. Pivotal trials and postmarketing experience support the efficacy, tolerability and safety of these agents. However, all have modest efficacy for patients as a group and are administered by injection. Two agents, mitoxantrone and natalizumab, are more potent and generally well tolerated, but typically are second line because of potential safety concerns (Cohen 2009).

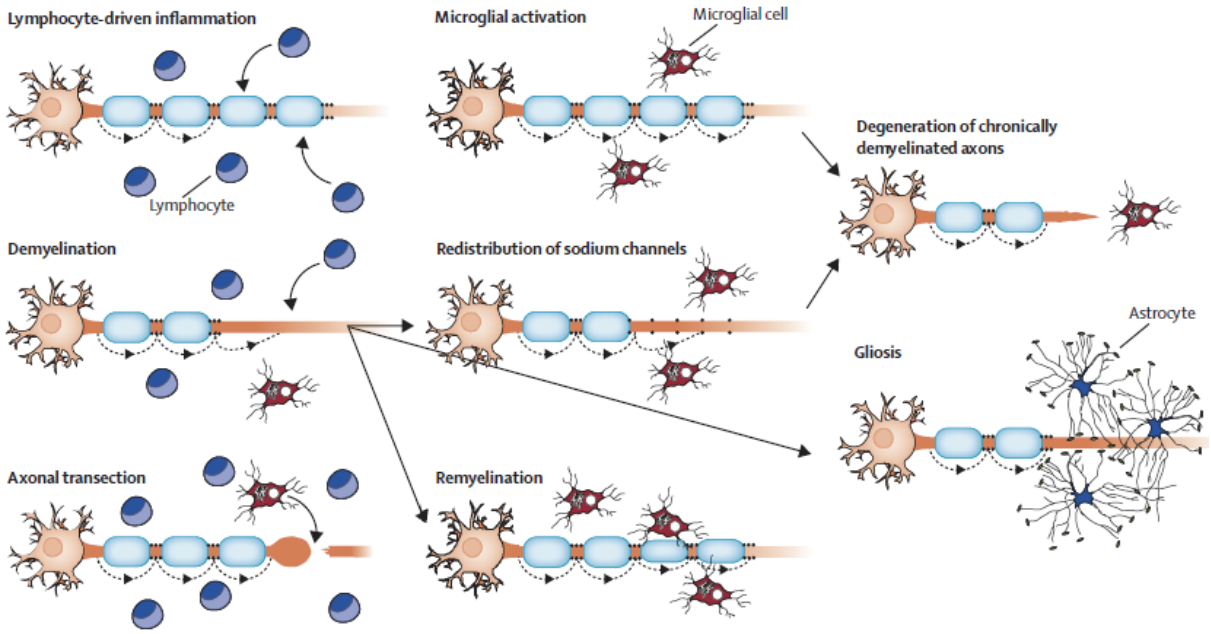

Figure 5. The MS pathogenesis. It is thought that a lymphocyte-driven inflammation induces conduction blocks in structurally intact axons, drives demyelination and induces transection of axons (with consequent conduction block) within acute lesions. Activated microglial cells might contribute to the repair mechanisms that lead to remyelination or to the degeneration of axons. Redistribution of sodium channels along demyelinated axons could restore conduction. Astrocytic activation and proliferation (gliosis) might impede repair. Adapted from Ciccarelli et al. (Ciccarelli, Barkhof et al. 2014).

A.6. Animal models of MS

A.6.1. Experimental allergic encephalomyelitis, virus and toxin induced demyelination models

Despite severe efforts, the exact pathomechanism of MS still remains elusive. It is widely accepted that MS is an inflammatory disease, controlled by T cell mediated autoimmune reaction against the myelin sheet which predominantly affects the white matter. However, this scheme cannot explain the entire spectrum of lesion formation in MS (Barnett and Prineas 2004). Several animal models have been developed to facilitate research into the nature and treatment of MS as well as other myelin disorders. There are three main types of de-/remyelination model: autoimmune, virus-induced and toxin induced (Miller, Asakura et al. 1996). The common autoimmune model is experimental autoimmune encephalomyelitis (EAE). While there are others, the most frequently used virus-induced model is the Theiler's

murine encephalomyelitis virus (TMEV). Toxins commonly used to study myelin disorders are ethidium bromide, lysolecithin and cuprizone (Miller, Asakura et al. 1996).
EAE is one of the most frequently used models that mimics MS pathology and allows a detailed insight into the immunological aspects of this disease. Chronic models of EAE provide histological and behavioural outcomes that mirror some aspects of progressive disease (Amor, Smith et al. 2005, Papadopoulos, Pham-Dinh et al. 2006). EAE is a T-helper (Th) cell-mediated autoimmune disease characterized by T-cell and monocyte infiltration in the CNS, associated with local inflammation (Robinson, Harp et al. 2014). The result is primary demyelination of axonal tracks, impaired axonal conduction in the CNS and progressive hind-limb paralysis. There are currently many pathophysiologic forms of EAE with varying patterns of clinical presentation depending on the animal species and strain, priming protein/peptide, and route of immunization employed. Thus different models have been used to study disease development and specific histopathologic characteristics with relevance to MS, and to dissect mechanisms of potential therapeutic interventions (Robinson, Harp et al. 2014).
TMEV model is based on virus-induced demyelination. Intracranial infection of susceptible mouse strains with TMEV results in biphasic disease of the CNS, consisting of early acute and late chronic demyelinating phase. The late chronic stage of demyelination in the TMEV infection makes this experimental model highly suitable for studying different aspects of the pathomechanism of MS (Oleszak, Chang et al. 2004).
The common feature of the so-called toxin induced demyelination models is that neurotoxic agents are used to induce the loss of myelin sheath in certain areas in the CNS. Experimental models of demyelination based on the use of toxins have provided a remarkable tool for studying the biology of remyelination. The most frequently used demyelinating agents are lysolecithin, ethidium bromide and the copper chelator cuprizone (Blakemore and Franklin 2008).
Injection of lysolecithin very quickly achieves local demyelination, acting in as little as 30 minutes post-injection. The myelin sheath is directly destroyed by this agent, attracting an inflammatory macrophage response. Remyelination is spontaneous and begins when the myelin debris are cleared and finishes in a matter of weeks (Hall 1972). Like lysolecithin, local injection of ethidium bromide causes short-lived demyelination followed by spontaneous remyelination (Yajima and Suzuki 1979).
Because demyelination is not mediated by the immune system in these models, toxins are used to study the glial aspects of demyelination and remyelination without the complicating factors of lymphocytes and a breached BBB (Crang, Franklin et al. 1991).

A.6.2. The cuprizone induced experimental demyelination

The administration of the copper chelator cuprizone (bis-cyclohexanone oxaldihydrazone) to mice induces spatially and temporally well-defined histopathological alterations in the CNS, including copper deficiency and demyelination (Matsushima and Morell 2001). Despite the

experimental use of cuprizone for almost five decades, the underlying mechanism of OL damage is still not completely understood. The copper-chelating property of cuprizone seems to be an obvious explanation. However, the synchronously copper (100 ppm) administration throughout the cuprizone treatment (0.5%) did not reduce the toxic effects (Carlton 1967). When mice were fed 0.2% (w/w) cuprizone and copper supplementation was increased to 130 ppm, the incidence of hydrocephalus declined without any effects on brain edema and spongy degradation (Carlton 1967). These observations pointed to a more complex mode of action that is not only based on the copper-chelating properties but may also regulate other cellular processes.

However, it is generally accepted that cuprizone induces metabolic disturbances in OLs, which lead to apoptosis involving a mitochondrial mechanism. A similar role of the mitochondria has been implicated in OL cell loss in MS as well (Kalman, Laitinen et al. 2007). The massive OL apoptosis is followed by extensive demyelination, which is preceded and accompanied by a down-regulation of myelin-related proteins with varying kinetics. For example, down-regulation of MAG expression can be seen in a few days after the initiation of cuprizone administration, while complete demyelination of the CC is usually observed after six weeks of treatment. While demyelination was thought to affect only particular white matter tracts (i.e. CC and superior cerebellar peduncle) (Komoly 2005), recent studies revealed that other regions, including the hippocampus, putamen, cerebellum and even distinct gray matter areas in the cortex, also undergo demyelination (Kipp, Clarner et al. 2009).

Another prominent pathological feature associated with OL apoptosis is the invasion of demyelinated areas by activated microglial cells. These cells originate from residential microglia, but macrophages immigrating from the blood (Remington, Babcock et al. 2007) also contribute to the marked numbers of phagocytic cells seen most abundantly around the third week of cuprizone treatment. In the acute cuprizone model, activated microglia appear already at the first 2 weeks even before demyelination can be detected by histology and immunohistochemistry (Hiremath, Saito et al. 1998). After 3 weeks activated microglia are numerously present in the CC, cortex and hippocampus. In the next 2-3 weeks highly activated and proliferating microglia clear myelin debris. It has been controversially debated whether microglia play a harmful or beneficial role in the cuprizone model and CNS diseases (Block, Zecca et al. 2007, Hanisch and Kettenmann 2007). Recent data suggest that microglia is fulfilling both roles, and different phenotypes with distinct effector functions are involved in the regulation of de- and regenerative processes. In fact, these cells may further amplify the cuprizone initiated OL cell death by the production and secretion of pro-inflammatory cytokines (Pasquini, Calatayud et al. 2007). Alternatively, microglia may have a beneficial role by stimulating OL precursor cells and promoting remyelination (Komoly 2005). In addition to the microglia activation, a strong astrogliosis, including hypertrophy and hyperplasia of astrocytes, occurs as a response to cuprizone treatment in different white and gray matter structures (Matsushima and Morell 2001, Gudi, Gingele et al. 2014).

One of the best cuprizone feature is that if mice return to a normal diet after six weeks of treatment, demyelination is followed by a complete remyelination, due to the maturation of the OPCs (Lindner, Heine et al. 2008). If the cuprizone challenge is prolonged for 12 weeks, the degree of remyelination may be limited or remyelination may even fail to occur (Lindner, Fokuhl et al. 2009). Moreover, a spontaneous but incomplete remyelination starts at the onset of OPC accumulation and this coincides with the accumulation of microglia and astrocytes following 3 weeks of treatment (Matsushima and Morell 2001, Skripuletz, Gudi et al. 2011).
Histopathological features of the cuprizone-induced demyelination closely resemble those of the type III MS lesions (Lucchinetti, Bruck et al. 2000), including a prominent OL apoptosis and microglial activation in the actively demyelinating lesions (Morell, Barrett et al. 1998). In addition, the cuprizone model shares common features with the earliest phases of MS lesion development, where the apoptosis of OLs occurs in regions with intact myelin (Barnett and Prineas 2004, Henderson, Barnett et al. 2009). As the pathology further evolves, early demyelinating lesions are invaded by scavenging macrophages (innate immune response), which phagocytose and clean up degraded myelin. However, in contrast to either the type III lesions or to the acute (earliest) MS lesions, there are no signs of the involvement of the adaptive immune response in lesions seen in the cuprizone model (Henderson, Barnett et al. 2009).
Considering the above mentioned features, the cuprizone model is suitable for studying basic mechanisms of acute and chronic de- and remyelination, exploring the pathophysiology of OL apoptosis, and testing preclinically new interventions for promoting remyelination and repair in MS lesions.

A.7. Neurotrophins

A.7.1. Neurotrophins: receptors and signaling pathways

Neurotrophins are a family of secreted proteins essential for neuronal development, growth and survival. The first neurotrophin, nerve growth factor (NGF), was discovered during a search for survival factors that could explain the deleterious effects of deletion of target tissues on the subsequent survival of motor and sensory neurons (Levi-Montalcini 1987, Shooter 2001). Its discovery validated the central model of neurotrophic factor action, i.e. that targets of neuronal innervation secrete limiting amounts of survival factors, which function to balance the size of a target tissue with the number of innervating neurons. The discovery of NGF laid the groundwork for the identification of additional factors. The second neurotrophin to be characterized - brain-derived neurotrophic factor (BDNF) - was purified from pig brain as a survival factor for several neuronal populations not responsive to NGF (Barde, Edgar et al. 1982). Conserved features of the sequences of these two proteins made isolation of clones encoding additional members of this family possible. Four neurotrophins are expressed in mammals: NGF, BDNF, neurotrophin-3 (NT-3) and neurotrophin-4 (NT-4). Members of numerous other families of proteins, most notably the glial cell-derived neurotrophic factor

(GDNF) family, also regulate neuronal survival and other aspects of neuronal development and function through activation of receptor tyrosine kinases, but the neurotrophins have continued to be a focus for research (Shooter 2001).

The neurotrophins and their genes share homologies in sequence and structure, and the organization of the genomic segments adjacent to these genes is also similar. Together, these observations provide compelling evidence that the neurotrophin genes have arisen through successive duplications of a portion of the genome derived from an ancestral chordate (Hallbook 1999). The protein product of each gene includes a signal sequence and a prodomain, followed by the mature neurotrophin sequence. Thus, each gene product must be processed by proteolysis to form a mature protein (Hallbook 1999).

The neurotrophins interact with two distinct classes of receptors (Fig. 6). The first receptor to be discovered, named p75 neurotrophin receptor ($p75^{NTR}$), was identified as a low-affinity receptor for NGF, but was subsequently shown to bind each of the neurotrophins with a similar affinity (Rodriguez-Tebar, Dechant et al. 1990, Frade and Barde 1999). $p75^{NTR}$ is a member of the tumour necrosis receptor superfamily with an extracellular domain that comprises four cysteine-rich motifs, a single transmembrane domain and a cytoplasmic domain that includes a 'death' domain similar to those present in other members of this family (He and Garcia 2004). Although this receptor does not contain a catalytic motif, it interacts with several proteins that transmit signals important for regulating neuronal survival and differentiation as well as synaptic plasticity. The three-dimensional structure of the extracellular domain of $p75^{NTR}$ in association with an NGF dimer has demonstrated that each of the four cysteine-rich repeats participates in binding to NGF (He and Garcia 2004). Interestingly, $p75^{NTR}$ binds NGF along the interface between the two NGF monomers and binding results in a conformational change in NGF that alters the monomeric interface on the opposite side of the NGF dimer, eliminating the potential to bind of one NGF dimer to two $p75^{NTR}$ monomers. The results suggest that binding of NGF to $p75^{NTR}$ may result in dissociation of $p75^{NTR}$ multimers, and they are compatible with the possibility that tropomyosin related kinase (Trk) and $p75^{NTR}$ monomers simultaneously bind the same neurotrophin dimer.

Upon neurotrophins binding, $p75^{NTR}$ undergoes oligomerization with other $p75^{NTR}$ or homologous receptors (Anastasia, Barker et al. 2015). The process reinforces the association of the receptor to its signaling molecules, such as Jun kinase, small GTPases, as well as the transcription factor NF-kB (Anastasia, Barker et al. 2015). Oligomerized $p75^{NTR}$ receptors can be cleaved by α- and γ-secretases, with release to the cytoplasm of the peptide p75-intracellular domain (p75-ICD) (Le Moan, Houslay et al. 2011). Upon transfer to the nucleus, p75-ICD participates in the regulated transcription of various genes, such as hypoxia-induced HIF-1α and CycE1. Moreover, another peptide, the p75-extracellular domain (p75-ECD), results from the $p75^{NTR}$ cleavage by surface metalloproteinases (Le Moan, Houslay et al. 2011).

Confirmed by recent evidence in both normal and pathological cells, a key role of $p75^{NTR}$ consists in the inhibition of cellular functions. For example, *in vitro* results in primary cultures of mice neurons, in the rat neural cell line PC12 and *in vivo* experiments in mice, have shown

p75^{NTR} to inhibit processes such as Na^{+} currents, cytosolic Ca^{2+} responses, excitability, persistent firing and neurite outgrowth (Gibon, Buckley et al. 2015, Trigos, Longart et al. 2015). Additional effects, both *in vitro* and *in vivo* in mouse hippocampal neurons, induced by p75^{NTR} associated with sortilin and activated with high affinity by NT precursors (proNTs), result in inhibition and even neuronal death (Yang, Harte-Hargrove et al. 2014).

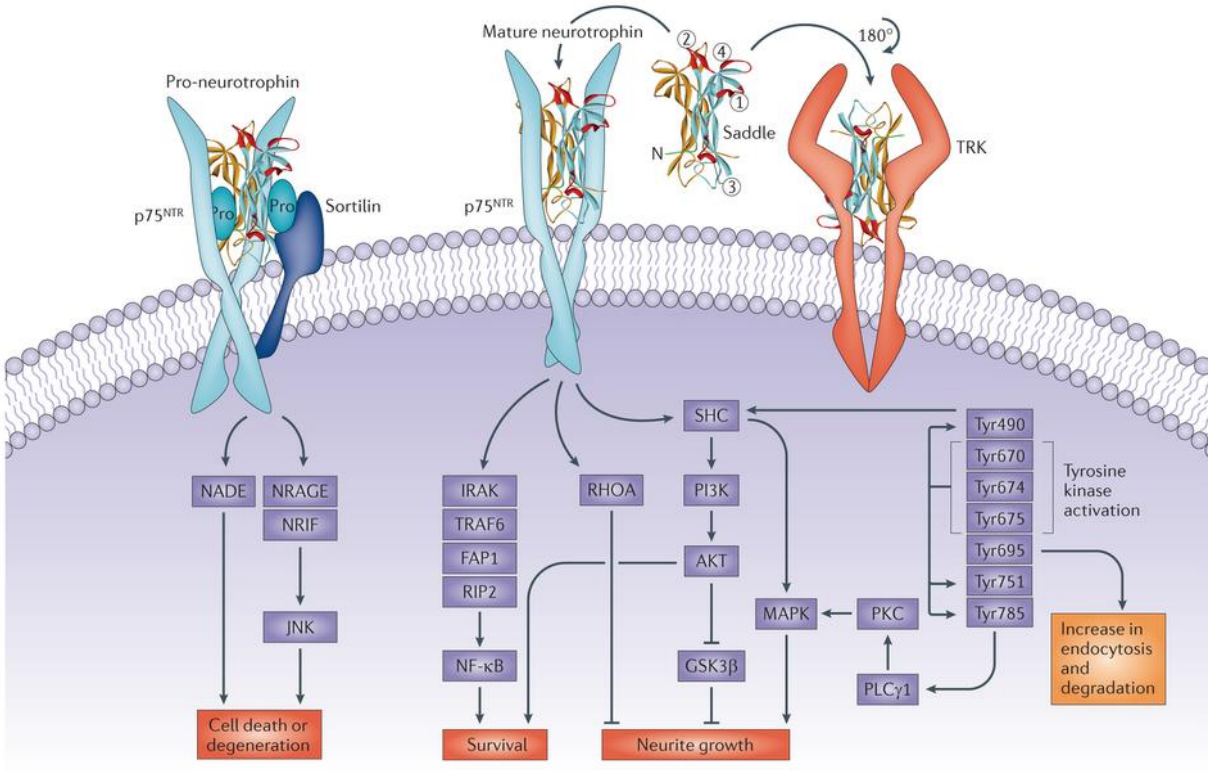

Figure 6. Neurotrophins receptor signaling. In Trk complexes, the neurotrophin apical region containing β-turn loops 1, 2 and 4 is near the membrane, whereas in the p75^{NTR} complex it faces away from the membrane (loops 1-4 and the amino terminus are labelled on the ribbon structure). Pro-neurotrophins are proteolytically processed intra- or extracellularly to remove the pro-region, which is the principal site of interaction with the co-receptor sortilin. Neurotrophin signalling proceeds through preformed or induced receptor dimers, and the binding of p75^{NTR} stimulates extracellular domain shedding and regulated intramembrane proteolysis involving α- and γ-secretases (not shown), which releases intracellular domains that are important for signalling and for interacting with intracellular adaptor proteins. Trk ligand binding by mature neurotrophins results in the phosphorylation of an array of intracellular domain tyrosine residues, which activate kinase activity (Tyr670, Tyr674 and Tyr675 are shown in the activation domain), resulting in further receptor autophosphorylation. Phosphorylation at Tyr490, Tyr785 and possibly Tyr751 (or their equivalent residues in other Trk receptors), forms adaptor binding sites that couple the receptor to mitogen-activated protein kinases (MAPKs),

phosphoinositide 3-kinase (PI3K) and phospholipase Cγ1 (PLCγ1) pathways, which may act locally and/or via signalling endosomes that are transported to the nucleus, to ultimately promote neurite outgrowth, differentiation and cell survival. Mature neurotrophins binding to $p75^{NTR}$, depending on the context, may augment neurotrophin binding to Trk receptors, reinforce Trk signalling through AKT and MAPKs, and further promote survival through the nuclear factor-κB (NF-κB) pathway, or antagonize the actions of Trk through the activation of JUN N-terminal kinase (JNK) and RHOA pathways. Pro-neurotrophin binding in complex with sortilin selectively activates cell-death-related pathways. Adapted from Longo & Massa (Longo and Massa 2013).

In mammals, the three members of the Trk subfamily of receptor tyrosine kinases constitute the second major class of neurotrophin receptors (Chao 2003, Huang and Reichardt 2003) (Fig. 6). The Trk receptors are typical receptor tyrosine kinases whose activation is stimulated by neurotrophin-mediated dimerisation and transphosphorylation of activation loop kinases (Huang and Reichardt 2003). Trk receptors are activated specifically by the mature and not the pro-forms of the neurotrophin gene products (Lee, Kermani et al. 2001). Thus, the proteases that control processing of proneurotrophins control Trk receptor responsiveness. The cytoplasmic domains of the Trk receptors contain several additional tyrosines that are also substrates for phosphorylation by each receptor's tyrosine kinase. When phosphorylated, these residues form the cores of binding sites that serve as a scaffolding for the recruitment of a variety of adaptor proteins and enzymes that ultimately propagate the neurotrophin signal (Longo and Massa 2013).

The extracellular domain of each of the Trk receptors consists of a cysteine-rich cluster followed by three leucine-rich repeats, another cysteine-rich cluster and two Ig-like domains. Each receptor spans the membrane once and is terminated with a cytoplasmic domain consisting of a tyrosine kinase domain surrounded by several tyrosines that serve as phosphorylation-dependent docking sites for cytoplasmic adaptors and enzymes. Within the activated Trk molecule the phosphotyrosines and their surrounding amino acid residues create binding sites for proteins containing phosphotyrosine-binding (PTB) or Src homology 2 (SH2) domains. In addition, endocytosis and transfer of Trk receptors to different membrane compartments control the efficiency and duration of Trk-mediated signalling, in part because many adaptor proteins are localised to specific membrane compartments (Longo and Massa 2013).

In contrast to interactions with $p75^{NTR}$, the neurotrophins dimerize the Trk receptors, resulting in activation through trans-phosphorylation of the kinases present in their cytoplasmic domains. The four neurotrophins exhibit specificity in their interactions with the three members of this receptor family with NGF activating TrkA, BDNF and NT-4 activating TrkB, and NT-3 activating TrkC. In addition, NT-3 can activate the other Trk receptors with less efficiency. The major site at which neurotrophins interact with these receptors is in the membrane-proximal Ig-

like domain. The three-dimensional structures of this domain in each of the Trk receptors have been solved (Ultsch, Wiesmann et al. 1999). Expression of a specific Trk receptor confers responsiveness to the neurotrophins to which it binds. Splicing, however, introduces some limitations to this generalization. For example, differential splicing affects ligand interactions of each of the Trk receptors through insertions of short amino acid sequences into the juxtamembrane regions of the extracellular domains of TrkA, TrkB and TrkC (Strohmaier, Carter et al. 1996). For both TrkA and TrkB, the insertion of the sequence encoded by a small exon enhances the binding of the receptor to non-preferred ligands. TrkA and TrkB isoforms that lack these inserts are activated strongly only by NGF and BDNF, respectively. The isoform of TrkA including an insert is also activated by NT-3 in addition to NGF (Clary and Reichardt 1994), while the similar isoform of TrkB is activated by NT-3 and NT-4 in addition to BDNF (Strohmaier, Carter et al. 1996). Differential splicing of exons encoding portions of the intracellular domains of Trk receptors also regulates the signalling initiated by neurotrophin binding. Splicing generates isoforms of TrkB and TrkC that include comparatively short cytoplasmic motifs without a tyrosine kinase domain. Expression of a non-kinase-containing isoform has been shown to inhibit productive dimerization of kinase-containing Trk receptors, thereby inhibiting responses to neurotrophins, such as activation of phospholipase C-g1 (PLC-g1) (Eide, Vining et al. 1996). For many years, it appeared that these truncated receptors did not directly signal, but instead functioned to restrict the diffusion of neurotrophins and possibly participate in their presentation to signal-transducing receptors. Rose and colleagues, however, have demonstrated that the BDNF-mediated activation of the truncated T1 isoform of TrkB controls release of Ca_2C from intracellular stores through a G protein and IP3-dependent pathway (Rose, Blum et al. 2003).

Differential splicing of the Trk receptor mRNAs is not the only influence that modulates neurotrophin binding and action. In some CNS neurons, many Trk receptors are localized in intracellular vesicles. Second signals, such as cAMP or Ca_2C, promote insertion of the receptors into the surface membrane, where they are accessible to neurotrophins (Du, Feng et al. 2000). In these cells, responsiveness to neurotrophins may require incorporation of neurons into signalling networks that result in the production of these second messengers. TrkB has also been shown to be recruited to cholesterol-rich rafts following ligand engagement in a Trk-kinase-dependent manner (Du, Feng et al. 2003). Some of the signalling consequences of TrkB activation are not observed when these rafts are disrupted. Finally and not surprisingly, Trk receptor endocytosis is also stimulated by ligand engagement as well as cytoplasmic Ca_2C (Du, Feng et al. 2003).

Upon binding their specific neurotrophins, Trks dimerize and undergo auto-phosphorylation (Colombo, Racchetti et al. 2014). The effects of their activation, including neuronal survival, proliferation and differentiation, are lasting longer than the effects of growth factor receptors (Chao, Rajagopal et al. 2006). These effects are potentiated when the receptors are internalized and undergo intracellular trafficking (Chao, Rajagopal et al. 2006, Philippidou, Valdez et al. 2011). Signaling of all Trks include activation of ERK, AKT and PLCγ signaling cascades

(Chen, Lin et al. 2012) which can, however, trigger differential effects in various neurons. For instance, in mice Purkinje neurons, neurite outgrowth and spine density depend primarily on TrkC (Joo, Hippenmeyer et al. 2014), whereas in pyramidal CA1 hippocampal neurons they depend on TrkB (Wang, Chang et al. 2015). In hippocampal and other neuron synapses, TrkB regulates also the prolonged reinforcement of synaptic activity (long-term potentiation, LTP) (Guo, Ji et al. 2014). However, at layer 2/3 cortical synapses, the activation of TrkB does not result on synaptic reinforcement but rather on prolonged weakening (long-term depression, LTD) (Zhao, Yeh et al. 2015).

In conclusion, the two types of NT receptors have complex, often opposite roles in a variety of brain functions. In these functions the receptors play defined, but not unique roles. Because of their multiple functions, the relevance of the two type NT receptors in several diseases is highly relevant.

A.7.2. Neurotrophins and MS

Although current MS treatments reduce severity and slow disease progression, they do not directly repair damaged myelin. As a result, MS research has recognized the importance of neurotrophins, such as NGF, as a potential novel therapeutic strategy to facilitate re-myelination of MS-induced lesions.

In the CNS, neurotrophins-regulated processes include neuronal differentiation, survival and death, axonal outgrowth, synapse generation and plasticity (Longo and Massa 2013). Specifically, NGF has been shown to possess neuro-protective (Martinez-Serrano and Bjorklund 1996), immunosuppressive and immunomodulatory functions (Villoslada, Hauser et al. 2000). The results of various studies using the EAE model have shown that exogenous administration of NGF delayed the onset of clinical EAE and, pathologically, prevented the full development of EAE lesions (Villoslada, Hauser et al. 2000, Kuno, Yoshida et al. 2006), while administration of NGF antibodies exacerbated neuropathological signs of EAE (Micera, Properzi et al. 2000). Human MS studies also support the beneficial role of NGF. For example, cerebral spinal fluid of MS patients show increased NGF levels during acute attacks that significantly decrease during remission (Laudiero, Aloe et al. 1992). These results suggest that NGF levels increase in response to the immune system insult on myelin in order to facilitate neurological recovery. Once myelin is repaired, as evident by complete neurological recovery, NGF levels subside back to baseline values required for normal myelin maintenance. The beneficial effects by which NGF promotes neurological recovery is thought to occur *via* its ability to enhance axonal regeneration (Oudega and Hagg 1996) and remyelinate axons *via* its protective and survival effects on OPCs and OLs (Takano, Hisahara et al. 2000). This suggests NGF may act to induce remyelination through its activity on innate OLs (Laudiero, Aloe et al. 1992). In addition, the immunomodulatory effects of NGF become evident by the fact that neurons of the CNS, microglia, astrocytes, OLs, immune cells, such as T cells, B cells, and mast cells have all been identified as cellular sources and targets of NGF (Ehrhard, Erb et al. 1993,

Leon, Buriani et al. 1994, Santambrogio, Benedetti et al. 1994, Micera, De Simone et al. 1995, Frade and Barde 1998). Thus, there are populations of several cell types that are sources of and can respond to NGF under normal and pathological conditions. The beneficial biological effects of NGF identified in both animal and human studies, taken together with its direct effects on the various cell types involved in myelination, poise NGF as a key mediator that regulates myelin formation and repair.

A.8. Neurosteroids

A.8.1. Biosynthesis

The term neurosteroids was first introduced in the 1981 by the French endocrinologist Étienne-Émile Baulieu to describe steroids produced *de novo* in the brain from cholesterol (Corpechot, Robel et al. 1981); it was later expanded to include those derived from the local metabolism of peripherally derived steroid precursors such as progesterone and corticosterone (Baulieu and Robel 1990). Neurosteroids are modulators of aminobutyric acid type A receptors ($GABA_AR$) and can induce analgesic, anxiolytic, sedative, anesthetic and anticonvulsant effects (Belelli, Harrison et al. 2009).

There are three main classes of neurosteroids (Fig. 7): the pregnane (e.g., allopregnanolone), the sulfated (e.g., dehydroepiandrosterone sulfate, or DHEAS), and the androstane (e.g., androstanediol), which are classified according to their structural homology (Reddy 2010). Allopregnanolone and THDOC can be synthesized from cholesterol by a series of steroidogenic enzymes (Belelli and Lambert 2005). Briefly, the cholesterol is transported into the inner mitochondrial membrane *via* the steroidogenic acute regulatory protein (StAR) and translocator protein 18 kDa (TSPO), also known as the peripheral benzodiazepine receptor (Papadopoulos, Baraldi et al. 2006). Here, mitochondrial cholesterol side-chain cleavage enzyme (cytochrome P450scc) catalyzes a side chain cleavage to convert cholesterol into pregnenolone, an important rate-limiting step for the production of allopregnanolone and THDOC. Pregnenolone is then converted by 3β-hydroxysteroid dehydrogenase (3β-HSD) into progesterone, with further metabolism of progesterone by 21 hydroxylase (p450c21), yielding deoxycorticosterone. Finally, progesterone and deoxycorticosterone are metabolized by 5α-reductase followed by 3α-hydroxysteroid dehydrogenase (3α-HSD), to yield allopregnanolone and THDOC, respectively.

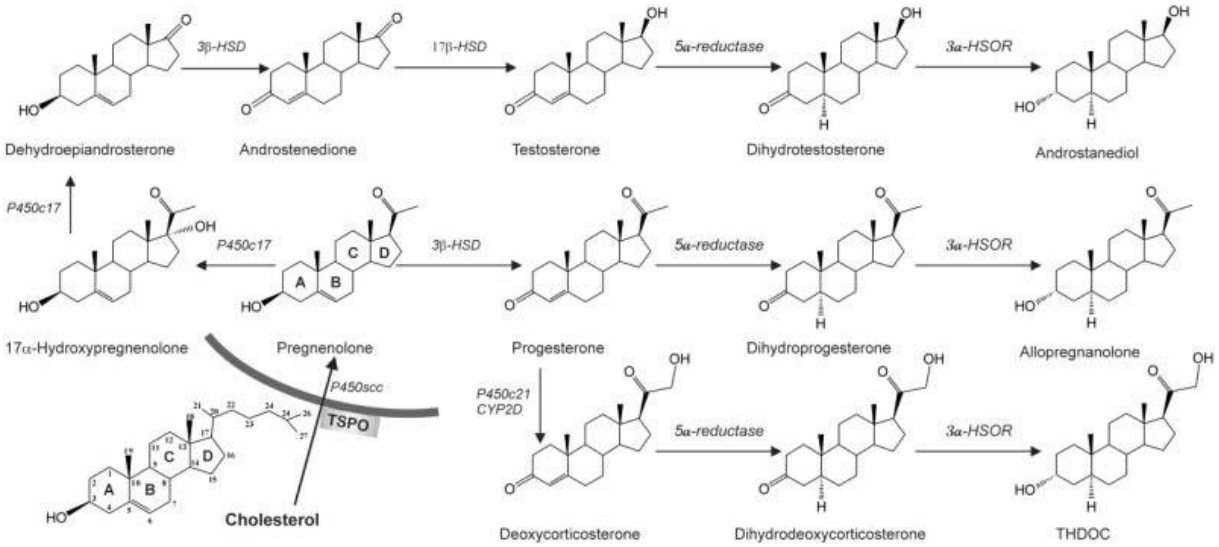

Figure 7. The biosynthesis of neurosteroids. Cholesterol is converted to pregnenolone by P450scc in the inner mitochondrial membrane. Pregnenolone is the precursor for progesterone and other neurosteroids. Progesterone, deoxycorticosterone and testosterone undergo two sequential A-ring reduction steps catalyzed by 5α-reductase and 3α-HSOR to form the 5α, 3α-reduced neurosteroids. The conversion of progesterone, deoxycorticosterone or testosterone into neurosteroids occurs in several regions within the brain. The 5α-reductase, 3α-HSOR and other enzymes are present in the brain. Adapted from Papadopoulos et al. (Papadopoulos, Baraldi et al. 2006)

A.8.2. Dehydroepiandrosterone

The neurosteroid dehydroepiandrosterone (DHEA), a C19 adrenal steroid produced by neurons and glia (astrocytes and oligodendrocytes), was first isolated in 1934 from male urine and in 1954 from human plasma (Orentreich, Brind et al. 1992, Baulieu and Robel 1998, Zwain and Yen 1999). Dehydroepiandrosterone sulfate (DHEAS), a sulfated form of DHEA, was obtained in 1944 (Lieberman 1995). Dehydroepiandrosterone (DHEA) and its sulfate ester DHEAS, together represent the most abundant steroid hormones in the human body (Maninger, Wolkowitz et al. 2009).

During human gestation, high concentrations of DHEA(S) are secreted by the fetal zone of the adrenal gland (Mesiano and Jaffe 1997). After birth, DHEA(S) concentrations decline over the first six months and remain low until adrenarche starts at six to eight years in both boys and girls, at which point DHEA(S) is synthesized and secreted from the zona reticularis layer of the adrenal cortex and circulating concentrations begin to rise (Havelock, Auchus et al. 2004). Adult humans secrete both DHEA and DHEAS from the zona reticularis of the adrenal cortex

and also DHEA from the ovary and testis (Havelock, Auchus et al. 2004). Circulating concentrations (in both plasma and cerebrospinal fluid) peak in the mid-20's and then progressively decline with age in both men and women, approaching a nadir (20% of peak concentrations) at approximately 65 to 70 years, the age at which the incidence of many age-related illnesses steeply increases (Regelson and Kalimi 1994).

A.8.3. DHEA interacts with the NGF receptors

DHAE binds with high affinity to all neurotrophin receptors (TrkA, TrkB, TrkC and $p75^{NTR}$) (Lazaridis, Charalampopoulos et al. 2011, Pediaditakis, Iliopoulos et al. 2015). It exerts strong neuroprotective effects, inducing pro-survival signaling by enhancing ERK1/2 and Akt activity, increasing the expression of anti-apoptotic Bcl-2 proteins and activating NFkB and CREB transcriptional machinery (Charalampopoulos, Tsatsanis et al. 2004, Charalampopoulos, Margioris et al. 2008). It is of note that DHEA and some of its steroid derivatives (such as the 5-androsten-3b, 17b-diol or ADIOL), have been shown to inhibit relapsing-remitting EAE in mice by restricting the production of autoimmune T cells or by suppressing T17 cells via ERβ signaling (Du, Khalil et al. 2001, Offner, Zamora et al. 2002, Saijo, Collier et al. 2011, Aggelakopoulou, Kourepini et al. 2016).

A.8.4. BNN27

DHEA is metabolized to androgens and estrogens and its levels are associated to higher risk for hormone-dependent tumors, particularly in genetically predisposed patients (Charalampopoulos et al, 2008; Furkala et al, 2012), limiting its long-term clinical use (Compagnone and Mellon 2000, Calogeropoulou, Avlonitis et al. 2009). To overcome this problem, a new family of synthetic C17-spiro derivatives of DHEA, called microneurotrophins (MNT) due to their small size and agonistic effects through Trks and $p75^{NTR}$ receptors, has been synthesized (Calogeropoulou, Avlonitis et al. 2009). One of these derivatives, named BNN27, does not interact with the classical steroid receptors or with TrkB and TrkC (Pediaditakis, Efstathopoulos et al. 2016). In particular, BNN27 specifically activates the NGF receptors, TrkA and $p75^{NTR}$, inducing TrkA tyrosine phosphorylation and downstream neuron survival signaling (Pediaditakis, Efstathopoulos et al. 2016, Pediaditakis, Kourgiantaki et al. 2016). Furthermore, BNN27 effectively rescues from apoptosis TrkA-positive sympathetic sensory neurons and $p75^{NTR}$-expressing, TrkA-negative cerebellar granule neurons, while being deprived of the hyperalgesic properties described for NGF (Pediaditakis, Efstathopoulos et al. 2016, Pediaditakis, Kourgiantaki et al. 2016). In addition to its effect on neuronal cells, we have recently reported that BNN27 induces the TrkA phosphorylation (at Y490) of TrkA-positive BV2 mouse glial cells in culture (an immortalized rodent cell line used as primary microglia substitute) (Blasi, Barluzzi et al. 1990, Henn, Lund et al. 2009), decreasing the levels of intereleukin (IL) 6 mRNA (Pediaditakis, Efstathopoulos et al. 2016).

B. INTRODUCTION II

B.1. Molecular organization of the axonal domains of myelinated fibers

During the myelination process the heminodes, structures enriched in voltage-gated Na^+ (Na_v) channels and placed at the border of the myelinated segments (Vabnick, Novakovic et al. 1996), fuse into a node of Ranvier as the myelin segments grow and approach each other. At both sides of the node, the myelin spirals around the axon forming paranodal loops, which have been shown to constitute septate-like junctions with the axon (Einheber, Zanazzi et al. 1997). These junctions may preclude current leakage across the paranodes and favor rapid propagation, while also promoting the sequestration of the K_v channels Kv1.1/Kv1.2 in the juxtaparanodal area (Vabnick, Trimmer et al. 1999). The localization of the Na_v and K_v channels is strongly dependent on cell adhesion molecules (CAMs) at nodes, paranodes and juxtaparanodes (Fig. 8). More specifically, a heteromeric complex of TAG-1/Contactin-2 and Caspr2 is implicated in the formation of juxtaparanodes in both CNS and PNS nervous system (Poliak, Salomon et al. 2003, Traka, Goutebroze et al. 2003).

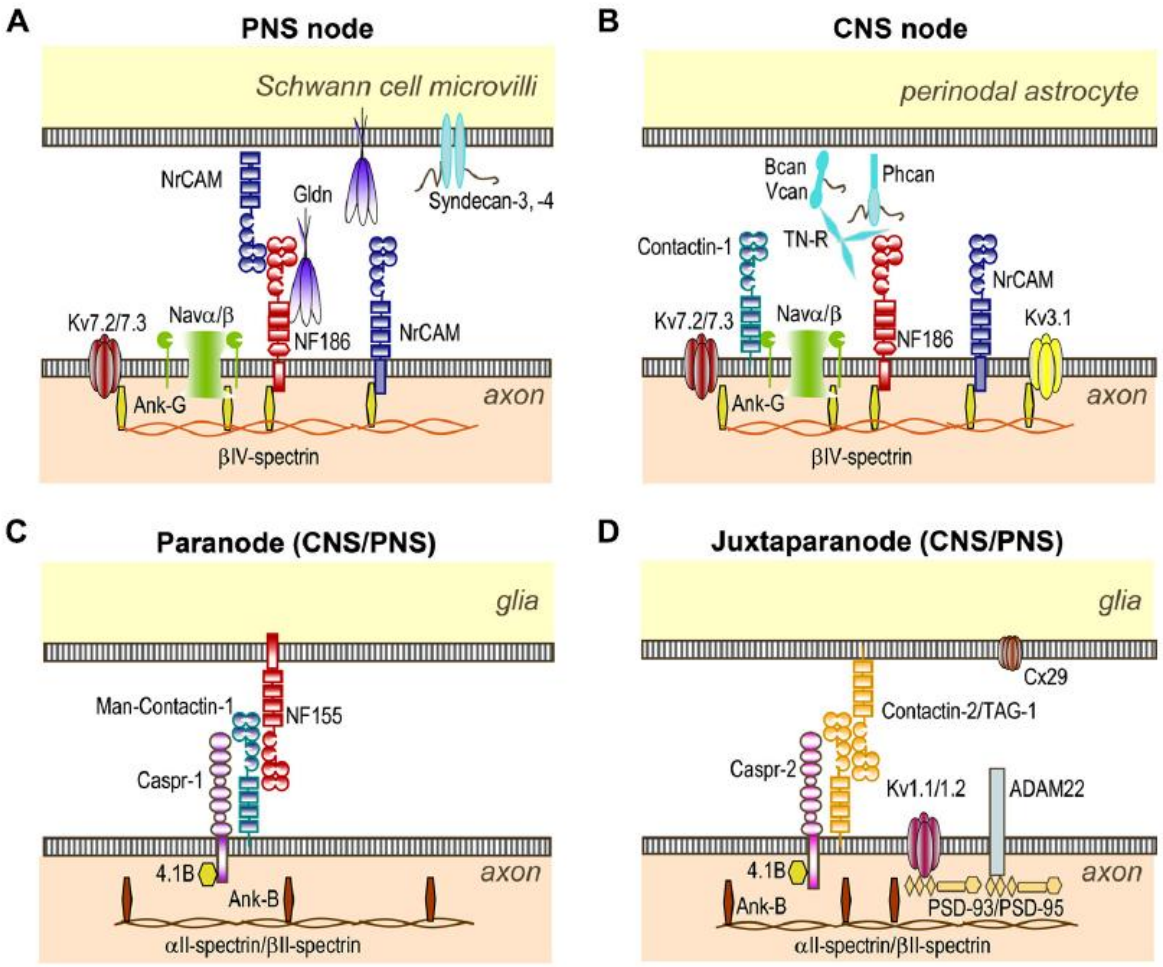

Figure 8. Organization of CNS and PNS axonal domains. (A) At PNS nodes, Neurofascin (NF) 186 binds Gliomedin (Gldn) and NrCAM which are secreted by Schwann cells in the nodal gap lumen. The cytoplasmic region of axonal NF186 and NrCAM bind ankyrin-G, which anchors the nodal complex to βIV-spectrin and to the actin cytoskeleton. Ankyrin-G enables the clustering of Nav and Kv7.2/7.3 channels at nodes. (B) In the CNS, Tenascin-R (TNR), Brevican (Bcan), Versican (Vcan), and Phosphacan (Phcan) are enriched in the extracellular rmatrix surrounding the nodes, and stabilize the nodal complex. These molecules bind NF186, NrCAM, and Contactin-1 which are expressed at CNS nodes. (C) The complex Contactin-1/Caspr-1/NF155 forms the septate-like junctions at both PNS and CNS paranodes. This complex is stabilized by the cytosolic protein 4.1B which co-localizes with ankyrin-B, αII-and βII-spectrin at both paranodes and juxtaparanodes. (D) The complex TAG-1/Caspr-2 enables the sequestration of Kv1.1/Kv1.2/Kv1.6 channels at juxtaparanodes, but also of PSD-93 and PSD-95. ADAM22 and Connexin-29 (Cx29) are also enriched at juxtaparanodes. Adapted from Faivre-Sarrailh & Devaux. (Faivre-Sarrailh and Devaux 2013)

TAG-1 is a GPI anchored adhesion molecule of the immunoglobulin superfamily (IgSF), expressed both by neurons and myelinating glia in the CNS and the PNS (Poliak, Salomon et al. 2003, Traka, Goutebroze et al. 2003). During development, TAG-1 is implicated in neurite outgrowth and extension, axon fasciculation and migration, while in adulthood it plays a role in the molecular organization of juxtaparanodal regions in myelinated fibers (Traka, Dupree et al. 2002, Traka, Goutebroze et al. 2003). As mentioned before, in the juxtaparanodes TAG-1 forms a tripartite complex with a member of the neurexin family of proteins, Caspr2 (Contactin associated protein-2), and the Shaker-type voltage-gated potassium channels (VGKCs) (Traka, Goutebroze et al. 2003, Tzimourakas, Giasemi et al. 2007). Absence of either TAG-1 or Caspr2 in knockout mice results in the disruption of the juxtaparanodal complex and diffusion of the VGKCs towards the internodal area (Poliak, Salomon et al. 2003, Traka, Goutebroze et al. 2003, Savvaki, Panagiotaropoulos et al. 2008). Furthermore, *Tag-1*$^{-/-}$ mice display severe behavioral defects in learning and memory abilities as well as in motor coordination and balance (Savvaki, Panagiotaropoulos et al. 2008). It has been shown that the glial expression of TAG-1 alone is able to rescue the phenotype of the *Tag-1*$^{-/-}$ mice, restoring the tripartite complex via an in trans-interaction with axonal counterparts, leading also to the full recovery of behavioral deficits, suggesting a crucial role of the glial TAG-1 in these processes (Savvaki, Theodorakis et al. 2010). Moreover, TAG-1 was identified as an autoantigen in a proportion of patients with MS (Derfuss, Parikh et al. 2009).

Although some of the cellular/molecular mechanisms underlying axoglial interactions in the node and paranode have been revealed in the last few years, the interactions and the molecular composition of juxtaparanodes have only started being deciphered.

B.2. Microtubule-associated protein 1B

Microtubule-associated protein 1B (MAP1B) is a high-molecular-weight protein. The precursor polypeptide undergoes proteolytic processing to generate the C-terminal-derived light chain and the N-terminal-derived heavy chain. The C-terminal product is a small protein, called MAP1B light chain 1 (Mei, Sweatt et al. 2000), which contains a microtubule and actin binding domain and can regulate interactions between microtubules and microfilaments (Noiges, Eichinger et al. 2002). The MAP1B heavy chain contains a microtubule-binding domain and mediates binding of MAP1B light chain 1 to microtubules. The MAP1B heavy chain binds actin and regulates interactions between microtubules and actin (Cueille, Blanc et al. 2007). This indicates that MAP1B can regulate microtubule stability, interactions between microtubules and actin, and axonal extension (Cueille, Blanc et al. 2007). MAP1B heavy chain is mainly involved in axonal longitudinal growth, microtubule stability and local actin dynamics, while MAP1B light chain 1 may enhance growth cone dynamics by providing nodes for F-actin assembly (Cueille, Blanc et al. 2007).

MAP1B is the first MAP expressed during embryonic development of the nervous system (Schoenfeld, McKerracher et al. 1989). Subsequently, its expression is developmentally down-regulated until it almost disappears from the axon during the formation of synaptic contacts between neurons in the CNS. Consistent with its early expression, MAP1B plays critical roles in neurite growth and synapse development (Gonzalez-Billault, Jimenez-Mateos et al. 2004). It is required for both axon growth (Tymanskyj, Scales et al. 2012) and spine maturation (Tortosa, Montenegro-Venegas et al. 2011) in developing neurons, and these functions are probably due to the capacity of MAP1B to modulate the activity of the small GTPases Rho and Rac1 via its interaction with specific guanosine nucleotide exchange factors (GEFs), such as GEF-H1 and Tiam (Tortosa, Montenegro-Venegas et al. 2011, Henriquez, Bodaleo et al. 2012).

MAP1B has also been described in the post-synaptic compartment (Kawakami, Muramoto et al. 2003), a scaffolding specialization of the neuronal synapses at the tip of the dendritic spine. Dendritic spines are actin-rich membrane protrusions that extend from the dendritic shaft with a globular head and thin neck. MAP1B plays an important role in dendritic spine formation and synaptic maturation by regulating of actin cytoskeleton (Kawakami, Muramoto et al. 2003).

Overall, MAP1B and phosphorylated MAP1B maintain dynamic balance in CNS neurons and axons. They regulate microtubule stability and dynamics, maintain balance between microtubules and actin, and control their interaction to promote axonal growth, connectivity, and regeneration post-injury.

B.3. Microtubule-associated protein 2

Mammalian microtubule-associated protein 2 (MAP2) is expressed mainly in neurons, but immunoreactivity is also detected in some non-neuronal cells such as oligodendrocytes. MAP2c is the juvenile isoform and is downregulated after the early stages of neuronal development,

whereas MAP2b is expressed both during development and adulthood. MAP2a becomes expressed when MAP2c levels are falling and is not detected uniformly in all mature neurons (Garner, Farmer et al. 1988). Shortly after axonogenesis in developing cortical and hippocampal neuronal cultures, MAP2 segregates into the nascent dendrites (at this stage dendrite precursors are called 'minor neurites') (Matus 1990). It is believed that a combination of protein stability, differential protein sorting and dendrite-specific transport of MAP2 mRNA, are responsible for this spatial segregation of this protein (Hirokawa, Funakoshi et al. 1996).

MAP2 family was originally discovered for and characterized by their ability to bind and stabilize microtubules. Microtubules exhibit dynamic instability, an intrinsic behavior characterized by alternating phases of growth, shortening and pausing. The switch from growth to shortening and the switch from shortening to growth are called ‘catastrophes’ and ‘rescues’, respectively. Specifically, MAP2 can bind both microtubules and F-actin, and both activities have been mapped to its microtubule-binding-repeat domain. MAP2c by itself can induce neurites in Neuro-2a neuroblastoma cells; its microtubule-stabilizing activity is necessary for this effect but is not sufficient, and F-actin dynamics also need to be altered (Dehmelt, Smart et al. 2003). MAP2 ability to interact with F-actin appears to be key to this specific biological function. MAP2 proteins bind along the length of microtubules and stabilize microtubules by altering this dynamic behavior (Panda, Samuel et al. 2003). The small isoform MAP2c stabilizes microtubules primarily by reducing the frequency and duration of catastrophes (Gamblin, Nachmanoff et al. 1996). Under conditions where its concentration is non-saturating, MAP2 can also form clusters on microtubules, and microtubule catastrophes stop at such clusters (Ichihara, Kitazawa et al. 2001). In cells, microtubules still exhibit dynamic behavior even when stabilizing MAPs are highly expressed, perhaps because their binding is regulated by phosphorylation and other factors (Ichihara, Kitazawa et al. 2001).

MAP2 family has also been shown to interact with numerous proteins. For instance, the binding of MAP2 to the RII regulatory subunit of protein kinase A (PKA) is one of the best-characterized examples of a classical MAP functioning as an adaptor protein. Knockout mice show that MAP2 is essential for linking PKA to microtubules in various brain regions (Dehmelt, Smart et al. 2003). Interestingly, the absence of MAP2 affects the phosphorylation of cAMP-responsive element binding protein (CREB), suggesting a role for the MAP2-PKA interaction in CREB-mediated signal transduction. Deletion of the PKA-binding site in MAP2c reduces its ability to induce neurites in neuroblastoma cells (Dehmelt, Smart et al. 2003).

B.4. Reelin

Reelin is an extracellular glycoprotein that controls diverse aspects of mammalian brain development and function (Lee and D'Arcangelo 2016). The gene for Reelin (RELN) in humans is located on chromosome seven (DeSilva, D'Arcangelo et al. 1997), and its protein product is a secreted ECM protein (de Bergeyck, Naerhuyzen et al. 1998).

Reelin contains a signal peptide, followed by an N-terminal sequence and hinge region, eight

Reelin repeats of 350–390 amino acids, and ends with a highly basic C-terminus (de Bergeyck, Naerhuyzen et al. 1998). Reelin is cleaved during processing at two locations: between repeats 2 and 3 (site N-t), and between repeats 6 and 7 (site C-t) (Jossin, Ignatova et al. 2004). Little is known about the enzymes responsible for the proteolytic cleavage of Reelin beyond that it is likely one or more metalloproteinase (Jossin, Ignatova et al. 2004, Kohno, Nakano et al. 2009). Recent work has shown that cleavage at the N-t site reduces Reelin's signaling ability by 100 fold, as measured by the ability to induce disabled 1 (Dab1) phosphorylation (Kohno, Nakano et al. 2009).

The most prominent activity of Reelin is the control of neuronal migration and cellular layer formation in the developing brain (Lee and D'Arcangelo 2016). It is secreted by Cajal-Retzius cells in the marginal zone (MZ) (Hevner, Neogi et al. 2003) and orchestrates the arrangement of postmitotic cortical neurons in an 'inside-out' manner, meaning that younger neurons are located more superficially than the earlier-born ones (Rice and Curran 2001). This process is severely disturbed in the spontaneous mouse mutant *reeler*, where disruption of the gene encoding Reelin leads to an approximate inversion of the cortical layering (Jossin, Ogawa et al. 2003). Other laminated brain structures are affected as well, resulting in a typical "*reeler* phenotype", which includes the eponymous reeling gait as a consequence of cerebellar hypoplasia (Jossin, Ogawa et al. 2003). Characteristic positioning defects of pyramidal and granule neurons in the hippocampus are found as well (Tissir and Goffinet 2003).

In addition to regulating layer formation in the neocortex and other laminated brain structures, Reelin functions in the developing and adult brain, where it is highly expressed by GABAergic interneurons in the forebrain and by cerebellar granule neurons (Pohlkamp, David et al. 2014). Its functions include the regulation of filopodia formation, dendrite outgrowth, spine formation and synaptogenesis, as well as modulation of synaptic plasticity and neurotransmitter release (Forster, Bock et al. 2010).

B.5. Tenascin-R

Tenascins are a family of large ECM glycoproteins composed of repeated epidermal growth factor (EGF)-like domains, fibronectin-type III (FNIII) domains and a C-terminal fibrinogen related domain (FReD). Near the N-terminus is a region that forms a coiled-coil, and most tenascins are believed to exist as trimers or as hexamers formed from 2 trimers held together with disulfide bonds (Tucker, Drabikowski et al. 2006). In tetrapods (amphibians, reptiles, birds and mammals) there are 4 tenascin genes: tenascin-C, tenascin-R, tenascin-W and tenascin-X. Tenascin-C (TNC), the first tenascins described, is expressed by motile cells such as the neural crest, at sites of connective tissue differentiation and in the adult in numerous stem cell niches; it also reappears during inflammation, at the margins of healing wounds and in the stroma of solid tumors (Chiquet-Ehrismann and Tucker 2011). Tenascin-R (TNR), the second tenascin to be discovered, is restricted in its expression to the nervous system, but transiently appears also in Schwann cells during peripheral nerve development, and tenascin-R knockout mice also

display abnormal behavior (Rathjen, Wolff et al. 1991). Tenascin-W (TNW) is often co-expressed with tenascin-C both in development and in stem cell niches (Scherberich, Tucker et al. 2004). Finally, tenascin-X (TNX) is widely expressed in loose connective tissue both in the adult and during development. Knock-out of the tenascin-X gene in the mouse results in Ehlers-Danlos Syndrome (i.e., loose skin and hypermobile joints) (Mao, Taylor et al. 2002).

TNR is an ECM molecule expressed by oligodendrocytes and subpopulations of neurons in the adult CNS of vertebrates (Dityatev and Schachner 2003). This protein is accumulated around nodes of Ranvier and in perineuronal nets surrounding motoneurons and subpopulations of interneurons. TNR regulates inhibitory perisomatic inhibition via interactions of its HNK-1 (human natural killer cell) carbohydrate epitope with $GABA_B$ receptors and thus influences synaptic transmission and plasticity in the hippocampus (Brenneke, Bukalo et al. 2004). In myelinated CNS axons, TNR is a functional modulator of the β-subunit of Na_v channels (Xiao, Ragsdale et al. 1999), while *in vitro* experiments have shown that neurites of retinal and dorsal root ganglion cells, as well as cerebellar neurons, are repelled by a substrate border of TNR (Becker, Anliker et al. 2000). TNR also has inhibitory functions in the outgrowth and guidance of optic axons *in vivo* (Becker, Schweitzer et al. 2004). Furthermore, it has been observed that it influences a variety of microglial functions, such as cell adhesion, migration and secretion of cytokines and growth factors (Liao, Bu et al. 2005). All of these findings indicate that TNR is an important modulator of plasticity and repair processes in the CNS.

C. GOALS OF THE STUDY

In the first part of the study we wanted to elucidate the exact role of specific 17-spiro steroid derivative BNN27 in de- and remyelination, taking advantage of the cuprizone demyelinating model, where the these processes can be studied without the direct involvement of the adaptive immune system. We focused on the effects of BNN27 in the glial population that is under attack in the cuprizone model, and comprises the main target in patients with MS. In addition, complete remyelination is allowed in this model, thus permitting the analysis of the mechanisms underlying this process, which is an essential step for the restoration of myelin in demyelinating pathologies.

The questions we aimed to answer were:

- Does BNN27 promote the survival of the mature oligodendrocytes (OLs)?
- Does BNN27 enhance the recruitment of the oligodendrocyte precursors (OPCs)?
- Does BNN27 enhance the remyelination?
- Through which mechanism(s) is it acting?

The available treatments for MS can only ameliorate or prevent specific aspects of the disease while they fail to promote myelin restoration and neuroprotection. Developing therapeutic agents that could improve remyelination is a challenge for neuroscientists.

In the second part of the study, we pursued the identification of novel partners of the GPI anchored adhesion molecule TAG-1. To do that, we took advantage of a new computational tool, called UniReD, developed by our collaborator Dr Ioannis Iliopoulos and his team: this software not only identifies known protein-protein interactions (PPIs) described in biomedical literature, but also predicts new interactions not yet documented. Apart from the known molecules that interact with TAG-1, several other putative interactors were identified by the UniReD software, and four of them (MAP1B, MAP2, Reelin and Tenascin-R) were validated by using proteomics approaches, including immunoprecipitation of TAG-1-containing protein complexes.

D. MATERIALS AND METHODS I

D.1. Animals

All research activities strictly adhered to the EU adopted Directive 2010/63/EU on the protection of animals used for scientific purposes. Animals were kept in the Animal House of the Institute of Molecular Biology and Biotechnology (IMBB-FoRTH, Heraklion, Greece), in a temperature-controlled facility on a 12 h light/dark cycle. In the study, the following animals were used:

1. C57B110/CBA background (for the *in vivo* cuprizone demyelinating model)

2. C57BL/6 background: $p75^{NTR\ -/-}$ mice (B6.129S4-*Ngfr*^{tm1Jae}/J or $p75^{NGFR}$, for the *in vitro* experiments)

$p75^{NTR}$ heterozygous mice were obtained from the Jackson Laboratory and maintained on C57BL/6 background. The $p75^{NTR}$ knockout mice lacked the 3rd exon, which encodes for three of the four extracellular Ig-like domains (Lee, Li et al. 1992). Mice heterozygous for the $p75^{NTR}$ gene disruption were interbred to obtain mice homozygous for the disrupted gene.

D.2. Genotyping

Animals from breedings were handled at an early age (postnatal days 5-10) and a small piece of tail was collected after they were marked according to their fingers.

D.2.1. Genomic DNA extraction

1. Lysis of the tail by addition of 400 μL Tail Lysis Buffer (see recipe below), 5 μL of protease K (stock: 20 mg/mL) and incubation at 55°C overnight.

2. Addition of 1 μL RNase (stock: 10 mg/mL) and incubation at 37°C for 10 min.

3. Addition of 1 volume (V) of phenol and moderate mixing for 10 min at RT.

4. Addition of 1 V of chloroform and moderate mixing for 10 min at RT.

5. Centrifuge at 13000 g, 5 min, RT and transfer supernatant to a new eppendorf tube.

6. Addition of 1 V of chloroform and moderate mixing for 10 min at RT.

7. Centrifuge at 13000 g, 5 min, RT and transfer supernatant to a new eppendorf tube.

8. DNA precipitation: addition of ½ V ammonium acetate 10M and 2 V ice cold 100% EtOH and mixing by vigorous shaking or vortex.

9. Centrifuge at 13000 g, 15-20 min, 4°C.

10. Discard the supernatant and air-dry the pellet.

11. Resuspend in 100-150 µL sterile dH2O

Tail Lysis Buffer
100 mM NaCl 10 mM Tris HCl, pH 8.0 25 mM EDTA, pH 8.0 0.5% w/v SDS

D.2.2. PCR

The following primers were used to identify the genotype of the animals used in the study:

Primer	**Sequence 5' --> 3'**
oIMR7617	GCT CAG GAC TCG TGT TCT CC
oIMR7618	CCA AAG AAG GAA TTG GTG GA
oIMR8162	TGG ATG TGG AAT GTG TGC GAG

The setup of the reaction and the PCR program used are shown below:

PCR Reaction (V_{tot}=50 µL)			PCR Program		
Reaction Component	**Final Concentration**	**Unit**	**Step #**	**Temp °C**	**Time**
ddH2O	up to final volume		1	95	5 min
Coral Red buffer	1.3	X	2 (35x)	95 55 72	30 sec 30 sec 30 sec
$MgCl_2$	2.6	mM	3	72	5 min
dNTPs	0.26	mM	4	4	∞
oIMR7617	0.5	µM			
oIMR7618	0.5	µM			
oIMR8162	0.5	uM			
Hot Star Taq polymerase	0.03	U/µl			
DNA	50-200	ng			

D.2.3. Agarose gel electrophoresis

Following PCR run, reactions were loaded on a 1% agarose gel containing 0.25 mg ethidium bromide per mL and separated by electrophoresis in a tank filled with 1xTAE Buffer (see recipe below), to detect PCR products. DNA fragments were detected under UV irradiation.

50x TAE Buffer
40 mM Tris-acetate 500 mM EDTA pH 8.0 Adjust pH to 8.5

D.3. *In vitro* studies

D.3.1. Oligodendrocyte and microglia primary cultures

Primary mixed glial cell cultures were prepared from the cortices of new born mouse pups (postnatal day 2), as previously described (McCarthy and de Vellis 1980), with minor modifications (Tamashiro, Dalgard et al. 2012). After the removal of the meninges, the cortices were chopped into small pieces and subsequently mechanically dissociated. Cells were plated onto poly-L-lysine (PLL, Sigma-Aldrich, 100 µg/ml)-coated 75 cm^2 culture flasks and cultured in DMEM (+Glutamax^{TM}, +4,5 g/L D-Glucose, -Pyruvate), supplemented with 10% FBS (Biosera) and 2% penicillin/streptomycin (P/S), until a clear layer of glial cells was formed. The culture medium was replenished twice a week. Once the mixed glial cell cultures achieved 90% confluence (after 10-14 days), the microglia cells were isolated using an orbital shaker at 200 rpm for 1 h, 37°C. Medium was subsequently removed, microglia pelleted via centrifugation (300 g for 10 min) and, following resuspension, maintained in DMEM supplemented with 10% FBS and 2% P/S, at a concentration of 2 x 10^5 cells per coverslip (13 mm diameter) in PLL-coated 12-well culture plates. Non-adherent cells were removed after 60 min and then adherent microglia were incubated for 24 h in culture medium before being serum-starved for 4 h prior to the beginning of experiments. Culture purity was verified by immunostaining using cell type specific antibodies against ionized calcium-binding adapter molecule 1 (IBA-1; microglia), glial fibrillary acidic protein (GFAP; astrocytes) and neuronal nuclear antigen (NeuN; neurons), and revealed a > 99% purity of microglia. After microglia detaching, the oligodendrocyte precursor cell (OPC) population was separated from the underlying astrocytic cell layer by vigorous shaking (16 h at 240 rpm, 37°C) and plated onto PLL-coated coverslips (13 mm diameter) at 7 × 10^4 cells per coverslip. The cells were cultured in DMEM (+GlutamaxTM, +4,5 g/L D-Glucose, –Pyruvate) supplemented with 1% N2, 1 µM biotin, 1% BSA-FFa (Sigma-Aldrich), 60 µg/ml cysteine (Sigma-Aldrich), 1% P/S, 10 ng/ml FGF-2 (Peprotech) and 10 ng/ml PDGF-AA (Peprotech), the last two being essential growth factors for OPC proliferation. After 2 days of expansion period, the cells were cultured for other 10 days in the same medium as before, without FGF-2 and PDGF-AA, but with triiodothyronine (T3, Sigma-Aldrich, 40 ng/ml), an essential growth factor for OPC differentiation. The medium was replenished every other day. The cultures were named d1 to d12 with respect to the number of days cultured under proliferating or differentiating conditions. Using this culture paradigm, the cells differentiated to post-mitotic oligodendrocytes (mature oligodendrocytes, OLs) by d6, and about 60% of the cells expressed the myelin marker MBP (myelin basic protein) by d10, when the different treatments were applied. More than 90% of total cell number stained for oligodendroglial marker Olig2 (oligodendrocyte transcription factor 2), indicating a high purity of the cultures. Unless specified, all culture reagents were purchased from Gibco.

D.3.2. Cuprizone, NGF and BNN27 administration *in vitro*

Cuprizone powder (bis-cyclohexanone oxaldihydrazone; Sigma-Aldrich) was dissolved in 50% ethanol at a concentration of 10 mM under shaking at 225 rpm at 37 °C for 20 min, until complete dissolution. To obtain the required final concentration (100 μM, established after preliminary studies), this stock solution was diluted in the respective medium for each experiment. For all the performed assays the cuprizone solution was freshly prepared. NGF and BNN27 were dissolved in the appropriate medium at a respectively concentration of 10 ng/ml and 100 nM. At d10 OLs were treated for 48 h with cuprizone alone or in combination with NGF or BNN27, while control cultures were kept in medium containing T3. To analyze the effect of NGF and BNN27 in the absence of cuprizone, they were added in the cultures at a respectively concentration of 10 ng/ml and 100 nM for 48 hours. To block the action of BNN27 on the TrkA receptor, a specific TrkA inhibitor (CAS 388626-12-8, Calbiochem, 10 nM) was applied for 1 hour to d10 OL cultures prior the addition of cuprizone, NGF or BNN27, and then maintained for 48 hours. After the isolation from the mixed glial cultures, microglia cells were cultured for 24 hours, the medium was then discarded, the cells washed in phosphate-buffered saline (PBS) and incubated with 100 μg/ml of LPS (Sigma-Aldrich, concentration established after preliminary studies) in the culture medium for 24 or 48 hours. Control cultures were maintained in culture medium in the absence of serum (NO SERUM group). In all experiments, cells were serum starved for 4 h prior the addition of LPS, BNN27 (100 nM) or cuprizone (100 μM).

D.3.3. Immunocytochemistry

After the different treatments, OLs and microglia were immunostained as described below:

1. Cells were post-fixed in 4% ice-cold paraformaldehyde (PFA) at RT for 10 min.

2. Rinsed (3x) in 1x PBS.

3. Cells were permeabilized with 0.1% Triton X-100 at RT for 10 min.

4. Rinsed (3x) in 1x PBS.

5. Cells were incubated in Blocking Solution of 5% bovine serum albumin (fraction V, BSA) in 1x PBS for 30 min, RT.

6. Incubation with the appropriate primary antibodies (Table 1, appendix) diluted in Blocking Solution for 1 h at RT.

7. Rinsed (3x) in 1x PBS.

6. Incubation with the appropriate secondary fluorescently labeled antibodies (Table 2, Appendix) in Blocking Solution for 30 min, RT.

8. Nuclear counterstaing with DAPI (0.1µg/mL in dH2O, Sigma-Aldrich) for 3 min, RT.

9. Rinsed (3x) in 1x PBS.

9. Mount using mounting medium containing MOWIOL® 4-88 Reagent (Cat. No. 475904, Calbiochem, EMD Chemicals, Merck KGaA).

10. Coverslips storage at 4°C until imaging take place and for long term storage after it is completed.

10x PBS (Vfinal=1 L)
70,1 g NaCl
12,8 g Na2HPO4
4,4 g NaH2PO4
2 g KCl
Fill up to a final volume of 1 L with dH20

Mounting Medium for ICC
2.6 g MOWIOL® 4-88 Reagent
6 g glycerol
12 mL Tris 0.2 M pH 8.5
6 mL dH2O

D.3.4. Measurement of OL apoptosis and cell viability

Apoptosis in OLs was studied using two different approaches: the analysis of the activated (cleaved) Caspase-3 staining (aCaspase3), and the determination of apoptotic bodies by DAPI (4',6-diamidino-2-phenylindole dihydrochloride) nuclear staining. aCaspase-3 staining was quantified by counting the percentage of MBP^+ cells (OLs) showing Caspase-3 cleavage ($aCaspase3^+$ - MBP^+), over the total number of MBP^+ cells. For the DAPI analysis, apoptotic cells were recognized and determined based on characteristic observations, including the presence of condensed, fragmented and degraded nuclei. In both cases, OLs in at least ten visual fields per coverslip were counted. Data were normalized to the control group. Duplicate measurements were averaged in three independent experiments. Cell viability was determined using the MTT (3-(4, 5-Dimethylthiazol-2-yl) -2, 5-diphenyltetrazolium bromide) assay protocol (Molecular Probes, Vybrant MTT Cell Proliferation Assay Kit), which assesses the ability of metabolically active cells to reduce the tetrazole-dye to purple-colored formazan compounds (Bruck, Pfortner et al. 2012, Wang, Liu et al. 2015). Cells were incubated with cuprizone, with or without NGF or BNN27 for 48 h, as previously described. After the treatment, cells were washed twice with PBS and medium containing 10% MTT was added, followed by incubation for 2 h at 37°C. Cells were then lysed using 0.04 N HCl in isopropanol. The absorbance of cell supernatants was measured at 570 nm using a multimode microplate reader (Tecan, Research Triangle Park, NC, USA). The analysis was conducted in triplicate. Cell viabilities were defined relative to control cells (considered to be 100%).

D.3.5. Analysis of OL morphology

OLs identified by the stage-specific marker MBP were analyzed and a minimum of 150 cells (quantification of OL complexity) and 30 cells (quantification of myelin-like membrane sheets) per experimental condition were randomly chosen and measured (n=3 independent experiments). Image acquisition and analysis were performed by the high content screening system Operetta (Perkin Elmer), using the software Harmony 4.1. OL complexity was defined according to branching and to the degree of myelin membrane formation (see Fig. 12D): briefly, type A were considered cells with MBP^+ primary and secondary processes and with low ramification branching, type B were recognized as cells with MBP^+ primary, secondary and tertiary processes with an increased branching level but lack of visible myelin membrane, whereas type C cells displayed an incremented level of complexity and myelin membrane. The quantification of MBP^+ membrane sheets was performed by analyzing only type C cells. Random fields were chosen and converted to 8-bit images, then all MBP^+ cells were individually selected by outlining and creating regions of interest corresponding to each individual cell. For each cell, the signal was determined by adjusting the threshold in order to select the whole cell. Membrane-sheets area was quantified by tracing the MBP^+ myelin-like membrane sheets (see Fig. 12E) and the surface area was reported in arbitrary units, then converted in percentage relative to control cells (considered to be 100%).

D.3.6. Analysis of microglia proliferation and morphology

Microglia proliferation was assessed by counting the number of $Ki67^+$ cells in control cultures and cultures treated with LPS alone or in combination with BNN27, for 24 or 48 h. To determine if BNN27 and/or cuprizone have a direct effect on microglia cells *per se*, these two molecules were applied in cultures in the absence of LPS. The percentage of $Ki67^+$ cells was evaluated in ten random fields for each experimental condition in three independent experiments. To verify the presence of morphology changes, $IBA\text{-}1^+$ cells were categorized in two groups: ramified and amoeboid (see Fig. 23L). Ramified (resting) microglia were defined as having a small circular body with ramified processes. In response to LPS administration, ramified microglia transformed into activated cells, characterized by the swelling of the cell body, a thickening of the proximal processes and an amoeboid shape. The percentage of each cell type (ramified and amoeboid), over the total number of $IBA\text{-}1^+$ cells, was calculated within ten random fields for each experimental group, in triplicates. Also in this experiment, BNN27 and cuprizone were administered to cell cultures in the absence of LPS.

D.4. The cuprizone model of demyelination

D.4.1. Cuprizone and BNN27 administration

For the *in vivo* study, eight-week-old male mice were fed for 3 (n=16), 5 (n=16) or 6 (n=20) weeks with 0.2% cuprizone (w⁄w), mixed into the ground standard rodent chow. Food was freshly prepared daily. Age-matched control mice (3 weeks, n=8; 5 weeks, n=8; 6 weeks, n=10) were fed with the regular standard ground chow. Body weight of mice was monitored over the whole experimental time. BNN27 was administered using a specific pellet (Innovative Research of America, Sarasota, FL) with a biodegradable matrix that effectively, stably and continuously releases the active product in the animals (21-day release, 2,86 mg/day, 60 mg in total), which was implanted subcutaneously in the back of the mice at the beginning of the second (day 8) and the fifth (day 29) week of cuprizone administration (see Fig. 18A). Pellets contained BNN27 (BNN27 group) or were devoid of any substance (CUPRIZONE group). For the remyelination study, eight-week-old male mice (C57B110/CBA) (n=10) were fed for 6 weeks with 0.2% cuprizone (w⁄w), mixed into the ground standard rodent chow, while age-matched control mice (n=5) were fed with the regular standard ground chow. BNN27 was administered through pellets (as described above), implanted after the demyelinating period (i.e. after 6 weeks of cuprizone administration), and remyelination was allowed to proceed for 3 weeks, by removing the cuprizone from the chow (see Fig. 22A).

D.4.2. Areas of study

As previously described, the administration of cuprizone causes cell death of the OLs, which leads to subsequent demyelination in several areas, most notably the corpus callosum (CC) (Matsushima and Morell 2001), while toxin removal from the chow allows remyelination to occur. Two ROIs (regions of interest) within the caudal region (including all sections of bregma -0,9 to -1,70), of the CC were defined. The central (arrow) and the lateral part (asterisk) were analized (Figure).

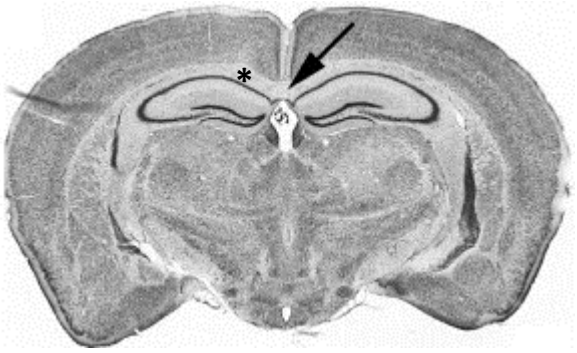

Figure 9. Illustration of the area of the corpus callosum used for the quantification analysis.

D.5. CNS tissue collection, preparation and histological methods

D.5.1. Tissue fixation, dissection and isolation

Adult mice received an intra-peritoneal injection of anesthesia (per g of body weight: 200 μg of ketamine (Vetoquinol) and 30 μg of xylazine (Vetoquinol), diluted in sterile dH2O in a final volume of 10 μL). Responsiveness to painful stimuli was checked by pinching of the tail or hind limb. After lack of response was ensured, incisures were made to expose the sternum and internal organs, the diaphragm and ribcage was cut to expose the heart. A peristaltic pump was used to circulate 20-25 mL 1x PBS through the vasculature by inserting a needle in the lower wall of the left ventricle and releasing extra pressure by an opening a small hole at the right atrium. Following clearance of the blood 50-60 mL of cold 4% PFA in 1x PBS were circulated to fix the tissues. The brain was carefully dissected and post-fixed in 4% PFA in 1x PBS on ice, for 20-30 min.

D.5.2. Embedding, freezing and cryosectioning

Following post-fixation, samples were washed 3 times in 1xPBS and submerged in 10 volumes of 30% sucrose, 0.1% NaN3 in 1xPBS. Samples were kept at 4°C until the sucrose completely replaces the intracellular water, so that the samples sank at the bottom of the container. After cryoprotection, samples were embedded in a gel containing 15% w/v sucrose, 7.5% gelatin from porcine skin (Cat. No. G-2500, Sigma) in 1xPBS. To ensure uniform freezing, samples were submerged in methylbutane and frozen at -35 to -40°C. Tissue blocks were then stored at -80°C before proceeding to cryosectioning (Leica). 10-μm-thick sections were collected on glass slides and stored in cryoboxes at -20°C until further processing.

D.5.3. Immunohistochemistry

Cryosections derived from the brain of adult mice were immunostained as described below:

1. Cryosections were removed from -20°C, encircled in Dako Pen (Cat. No. S200230, Dako, Agilent Technologies) and post-fixed in ice-cold acetone at -20°C for 10 min.

2. Washes (3x) in 1x PBS, 5 min each.

3. Incubation in Blocking Solution of 5% bovine serum albumin (fraction V, BSA) in 0.5% Triton X-100 in 1x PBS for 1 h, RT.

4. Incubation with the appropriate primary antibodies (Table 1, Appendix) diluted in Blocking Solution at 4°C, overnight.
5. Washes (3x) in 1x PBS, 5 min each.

6. Incubation with the appropriate secondary fluorescently labeled antibodies (Table 2, Appendix) in Blocking Solution for 1.5 h, RT.

7. Nuclear counterstaing with DAPI (0.1μg/mL in dH2O, Sigma-Aldrich), for 5 min, RT or with TO-PRO®3 iodide (500 nM in 1x PBS, Molecular Probes, Thermo Fisher Scientific) for 3 min, RT.

8. Washes (3x) in 1x PBS, 5 min each.

9. Mount using mounting medium containing MOWIOL® 4-88 Reagent (Cat. No. 475904, Calbiochem, EMD Chemicals, Merck KGaA).

10. Slide storage at 4°C until imaging take place and for long term storage after it is completed.

D.5.4. Morphological stainings

Ten micron cryosections were stained using Luxol Fast Blue staining (LFB, Alfa Aesar) with Cresyl violet (Sigma-Aldrich). To evaluate demyelination, three independent blinded readers scored LFB/cresyl violet-stained sections (central and lateral part of the CC), between zero and three. A score of three is equivalent to the myelin status of an untreated mouse, whereas zero is equivalent to totally demyelinated CC. Eight animals of each group were included in the study.

1. Hydrate to 95% alcohol.

2. Luxol fast blue solution, overnight, 60°C.

3. Rinse in 95% alcohol.

4. Rinse in distilled water.

5. Lithium carbonate solution, 5 seconds.

6. 70% alcohol, two changes, 10 seconds each.

7. Wash in distilled water.

8. Repeat steps 5-7 until there is a sharp contrast between the blue of the white-matter and the colorless gray-matter.
9. Rinse in 70% alcohol.

12. Cresyl violet, 1 minute.

13. Rinse in distilled water.

14. Dehydrate through 95% and 100% alcohol, clear in xylene and mount using xylol (Sigma Aldrich).

Luxol Fast Blue Solution	0.05% Lithium Carbonate	0.25% Cresyl Echt Violet
Luxol fast blue 1 g 95% alcohol 100 ml 10% acetic acid 5 ml	Lithium carbonate 0.5 g Distilled water 1000 ml	Cresyl Echt violet 0.25 g Distilled water 100 ml 10% Acetic acid 1 ml

D.5.5. Scoring and quantification of demyelination

Demyelination was evaluated in 10 μm cryosections at different levels of the caudal region of the CC using Luxol fast blue (LFB) staining with Cresyl violet. Three independent blinded readers scored LFB/cresyl violet-stained sections between zero and three. A score of three is equivalent to the myelin status of a mouse not treated with cuprizone, whereas zero is equivalent to totally demyelinated CC. A score of one or two corresponds to one-third or two-third fiber myelination of the CC, respectively. Ten animals of each group were included in the study. In addition, densitometric measures of the CC stained for the myelin marker MBP were performed on binary converted pictures using the freely available Image J software (National Institute of Health, USA).

D.5.6. Quantification of mature oligodendrocytes, oligodendrocyte precursor cells, astrocytes and microglia

The density of mature oligodendrocytes (OLs), oligodendrocyte precursor cells (OPCs), astrocytes and microglia cells was quantified in the CC of untreated, cuprizone-treated and BNN27-treated animals at the various time points analyzed in a minimum of 3 sections per animal. Coronal cryosections of the forebrain immunostained against the OLs marker CC-1, the OPC marker PDGFRα, the astrocytic marker GFAP and the microglial marker IBA-1 were imaged with a 40x lens and further processed and analyzed in ImageJ software. Cells were counted manually at the CC area and expressed as number of positive cells per 10000 μm^2.

D.6. Statistical analysis

Image processing, analysis and measurements were carried out using Photoshop 9.0-CS2 and NIH Image J software. Data are depicted as means ± standard deviation of the mean. For each assay, normality distribution and equality of variances of data were tested with the D'Agostino-Pearson normality test. For all the quantifications (except the quantification of OL complexity, the evaluation of the microglia morphology and the quantification of LFB scoring), one-way analysis of variance (ANOVA), followed by Tukey post-hoc test for pairwise multiple comparison procedures, was performed. For the quantification of OL complexity and the evaluation of the microglia morphology, two-way analysis of variance (ANOVA), followed by Tukey post-hoc test for pairwise multiple comparison procedures, was used. In case of normality and/or equality variance failing (quantification of LFB scoring), the Friedman ANOVA on ranks as a non-parametric test, followed by the Tukey post-hoc test for pairwise multiple comparison procedures, was performed. Differences were considered significant at values of $p < 0.05$ or lower.

D.7. Immunoblot analysis

D.7.1. Sample preparation

Cultured OPCs (d2), OLs (d10) and CC of mice after 6 weeks of treatment (25 mg of the tissue) were homogenized in ice-cold RIPA buffer (see recipe below) with an addition of protease inhibitor cocktail (Roche), followed by a brief sonication on ice. The total protein concentration in each sample was quantified with the Bradford kit (Bio-Rad Laboratories). The samples were prepared with 50 µg of total protein with the addition of the appropriate amount of 2x or 4x Laemmli Sample Buffer (see recipe below). After mixing, samples were incubated for 5 min at 100°C and subsequently cooled on ice.

RIPA Buffer	**2x Laemmli Sample Buffer**
10 mM Sodium phosphate pH 7.0 150 mM NaCl 2 mM EDTA 50 mM Sodium fluoride 1% w/v NP-40 1% Sodium deoxycholate 0.1% SDS	125 mM Tris-base 4% sodium dodecyl sulfate (SDS) 20% glycerol 100 mM dithiothreitol (DTT) Bromophenol blue

After blocking (5% powdered skim milk and 0.1% Tween-20 in PBS) for 1 h, the membrane was incubated overnight at 4°C with the appropriate primary antibody (Table 1, Appendix). After washing 3 times for 10 min in 0.1% Tween-20 in PBS, samples were incubated for 1 h at

room temperature with horseradish peroxidase-coupled secondary antibodies (Table 2, Appendix) and proteins were visualized by enhanced chemiluminescence (ECL Plus, GE Healthcare Bio-Sciences).

D.7.2. SDS-polyacrylamide gel electrophoresis (SDS-PAGE)

Samples (equal amount of total protein/lane) were resolved by a SDS-polyacrylamide gel of appropriate acrylamide percentage (see tables below).
The gel was placed in the wet electrophoresis tank (Bio-Rad Laboratories) according to manufacturer's instructions and covered with 1 L 1x SDS-PAGE Running Buffer (see section below). Samples were loaded in the buffer-submerged wells, next to a commercial protein ladder. The electrophoresis device was set to 60 V during the packing of the samples in the stacking gel and then to 100-120 V until the bromophenol blue exits the gel.

Stacking gel (1 minigel 1.5 mm-thick)
1 mL 30% acrylamide
0.75 mL Tris-HCl 1M, pH 6.8 + 0.4% SDS
60 µL 10% ammonium persulfate (APS)
6 µL N,N,N',N'- tetramethylethylenediamine (TEMED, Merck)
4.1 mL dH2O

Separating gel (For 1 minigel 1.5 mm-thick)		
8% acrylamide	**12% acrylamide**	
2.67 mL	4 mL	30% acrylamide
2.5 mL	2.5 mL	Tris-HCl 1.5M, pH 8.8 + 0.4% SDS
100 µL	100 µL	10% APS
8 µL	8 µL	TEMED
4.63 mL	3.3 mL	dH2O

D.7.3. Western Blotting

The gel was removed from the device and proteins were transferred to a 0.45 μM Protran nitrocellulose transfer membrane (Schleicher & Schuel, Biosience) in the following way:

1. The stacking gel is removed and the rest of the gel is placed on top of a presoaked (in 1x Transfer Buffer) Protran nitrocellulose membrane of equal size between two pieces of presoaked Whatman paper (Whatman, GE Healthcare) on each side, flanked by two sponges, inside the plastic tray.

2. The whole plastic tray is closed carefully to avoid bubbles and placed in the transfer tank, with the black side towards the black side of the tank.

3. The tank is filled with freshly made cold 1x Transfer Buffer until the plastic tray is completely submerged in the buffer and the accompanying ice container is also placed in the tank (this helps maintain the temperature as low as possible).

4. The whole tank is placed in a container filled with ice and then the device is set to 310 mA for 1h to ensure the transfer of the proteins from the gel to the membrane.

10x Running/Transfer Buffer (RTB) (Vfinal=5 L)	**1x SDS-PAGE Running Buffer**	**1x Transfer Buffer**
50 g sodium dodecyl sulfate (SDS)	10% v/v 10xRTB in dH20	10% v/v 10xRTB
720 g glycine		20% v/v methanol in dH20
150 g Tris-base		
Fill up to a final volume of 5 L with dH20		

D.7.4. Immunoblotting

1. The membrane is carefully removed from the apparatus and briefly washed in 1xPBS-T.

2. Blocking with 5% BSA in 1xPBS-T for 1 h at RT.

3. Incubation with the appropriate antibodies follows (see Table 1, Appendix) in 5% BSA in 1x PBS-T at 4°C overnight.

4. Washes (3x) with 1x PBS-T, 15 min each.

5. Incubation of the membrane with the appropriate horseradish-conjugated secondary antibodies (see Table 2, Appendix).

6. Washes (3x) with 1x PBS-T, 15 min each.

7. Visualization of signal with enhanced chemiluminescence (ECL Plus, Amersham, GE Healthcare Bio-Sciences).

D.7.5. Western blot quantification and statistical analysis

In the case of the CC, band intensity of comparable animal groups (n = 3 from each group) was quantified with Tinascan version 2.07d and normalized with the respective Tubulin intensity levels as loading control. Expression values are shown as percentage considering control animal values as 100%. Data are expressed as mean ± standard deviation of the mean and statistical analysis was performed GraphPad Prism version 5.00 for Windows (GraphPad Software). Normalized protein levels were compared using unpaired t test and differences were considered as significant when $P<0.05$.

E. MATERIALS AND METHODS II

E.1. Animals

In the study, the following animals were used:

1. C57B110/CBA background
   - *Tag-1*$^{+/+}$ mice

E.2. Tissue lysate preparation, Co-immunoprecipitation and Western Blot analysis

Adult and embryonic (E15.5) mice cortices were carefully dissected and homogenized in ice-cold 85 mM Tris, pH 7.5, 30 mM NaCl, 1 mM EDTA, 120 mM glucose, 1% Triton X-100, 60 mM octyl Q-D glucopyranoside (Sigma-Aldrich), protease inhibitor mixture diluted 1:1000 (Sigma-Aldrich) and phosphatase inhibitor mixture (1:500), followed by a brief sonication on ice. The total protein concentration in each sample was quantified with the Bradford kit (Bio-Rad Laboratories).

Co-immunoprecipitation was performed as described below:

<u>First Day</u>

1. Add 30 µl of Protein A stock beads to each lysate and incubate for 2 h at 4°C, shacking in the circular rotator (pre-clearing phase).

2. Centrifuge for 5 minutes at 2000 rpm at 4°C and transfer the supernatant (pre-cleared protein extract) to a new tube.

3. Keep the remaining beads, wash them for 3 times with wash buffer (see recipe below), and store them at -20°C (PRE-CLEARING).

4. Add 1-5 µl Ab to the pre-cleared protein extracts (2 µg for 200 µg of proteins), and leave O/N at 4°C, shacking in the circular rotator.

<u>Second Day</u>

1. Add 30 µl of Protein A stock beads to each sample and incubate for 2 h at 4°C, shacking in the circular rotator.

2. Centrifuge for 5 minutes at 2000 rpm at 4°C and separate the supernatant from the beads (IP).

3. Add 10X the bead's volume of wash buffer (700 µl-1 ml). Mix by hand-shaking and place in the circular rotator at 4°C for 10 minutes.

4. Centrifuge for 5 minutes at 2000 rpm at 4°C. Discard the supernatant and wash the beads 2x with wash buffer.

Immunoprecipitates were analyzed on a SDS-polyacrylamide gel of appropriate acrylamide percentage and transferred to a 0.45 µM Protran nitrocellulose transfer membrane (GE Healthcare LifeSciences), over 1 h using a wet transfer unit (Bio-Rad Laboratories). After blocking (5% powdered BSA and 0.1% Tween-20 in PBS) for 1 h, the membrane was incubated overnight at 4 °C with the primary antibodies (Table 1, Appendix). After washing three times for 15 min in 0.1% Tween-20 in PBS, samples were incubated for 1 h at room temperature with horseradish peroxidase–coupled secondary antibodies (Table 2, Appendix), and proteins were visualized by enhanced chemiluminescence (Luminata Classico HRP Substrate, Millipore).

Wash buffer
10 mM Tris (adjust to pH 7.4)
1 mM EDTA
1 mM EGTA (pH 8.0)
150 mM NaCl
1% Triton X-100
0.2 mM sodium orthovanadate

E.3. Production of recombinant Reelin and Western Blot analysis

Stably transfected HEK 293-cells expressing either full-length Reelin or control cells transfected with a control vector (MOCK) were grown in Dulbecco's modified eagle medium (DMEM, low glucose, Invitrogen) with 10% fetal bovine serum, low glucose (Invitrogen), 100 U/mL penicillin, and 100 µg/mL streptomycin (Invitrogen), and 0.9 g/L G418 (Invitrogen) for 2 days to reach full confluence. The medium was then replaced by serum-free DMEM, and the cells were incubated for 2 days at 37°C in 5% CO_2. Conditioned medium was collected and centrifuged. The supernatant was concentrated 10-fold using 100-kDa cut-off centrifugal filters (Millipore), sterile filtered, and stored at -80°C until used.
One microliter recombinant reelin supernatant, 1 ml control supernatant and 1 ml each of the different media were diluted with sample buffer and boiled for 5 minutes. Proteins were separated by 3-8% gradient Tris-Acetate gel electrophoresis (SDS-PAGE, Invitrogen, Karlsruhe, Germany) and transferred electrophoretically to polyvinylidene fluoride (PVDF) membranes. A monoclonal antibody against reelin (E4) was used as primary antibody (Table

1, Appendix), followed by an alkaline phosphatase-conjugated secondary antibody (Table 2, Appendix).

F. RESULTS I

F.1. Establishment of primary oligodendrocyte and microglia cultures

To test the putative involvement of BNN27 in OL survival and maturation, we generated primary oligodendrocyte and microglia cultures from P2 mice, referring to the protocol of McCarthy and de Vellis (McCarthy and de Vellis 1980), with minor modifications (Tamashiro, Dalgard et al. 2012). After the plating on coverslips (where the majority of the cells were PDGFRα$^+$, i.e. precursors, Fig. 10A), the oligodendrocyte cultures were named d1 to d12 with respect to the number of days cultured under proliferating or differentiating conditions. Using this culture paradigm, the cells differentiated to post-mitotic oligodendrocytes (mature oligodendrocytes, OLs) by d4 (Fig. 10B-C), and about 60% of the cells expressed the myelin marker MBP (myelin basic protein) by d10 (Fig. 10D), when the different treatments were applied. More than 90% of total cells stained for oligodendroglial marker Olig2 (oligodendrocyte transcription factor 2), indicating a high purity of the cultures.
For the microglia cultures, the purity was verified by immunostaining using cell type specific antibodies against ionized calcium-binding adapter molecule 1 (IBA-1; microglia), glial fibrillary acidic protein (GFAP; astrocytes) and neuronal nuclear antigen (NeuN; neurons), and revealed a > 99% purity of microglia.

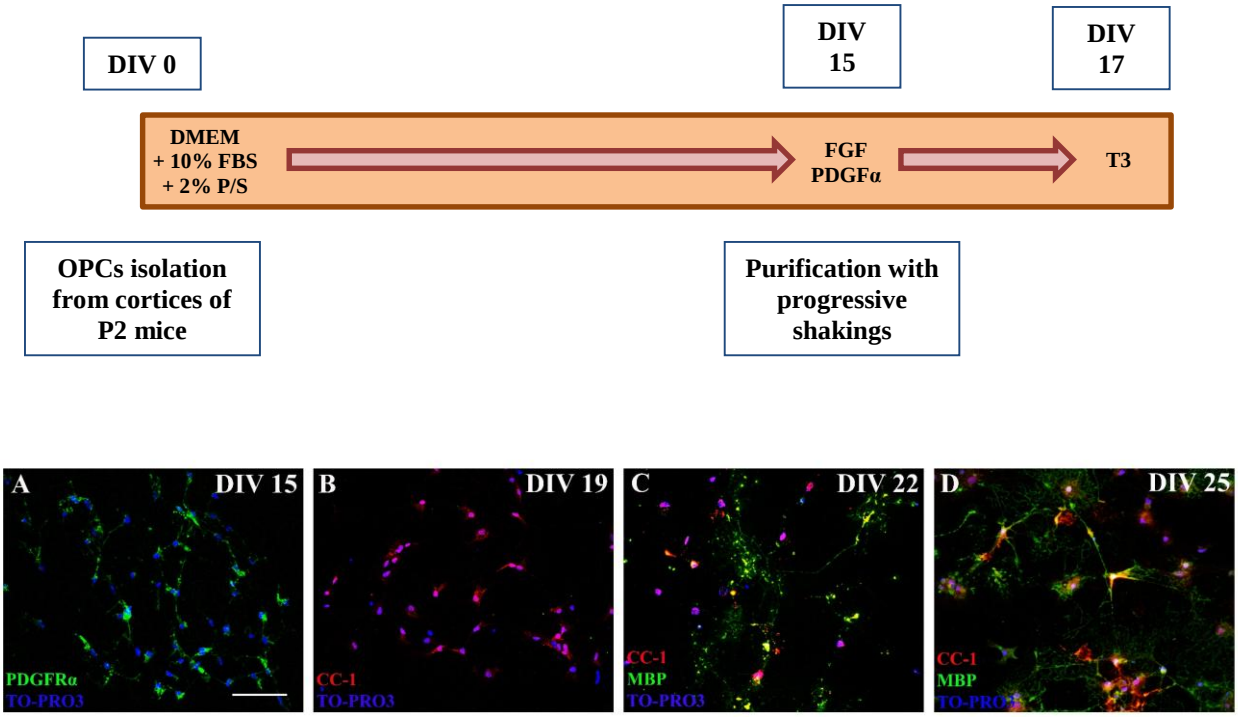

Figure 10. Oligodendrocyte primary cultures. Oligodendrocytes were obtained from cortices of newborn mouse pups (P2). Oligodendrocyte precursor cells (OPC) were purified with

progressive shakings and further treated with specialized culture media including growth factors for OPC proliferation (FGF and PDGFα), or OPC differentiation (T3) (see scheme).

F.2. Mature oligodendrocytes express the NGF receptors, TrkA and p75^{NTR}

Although NGF plays an essential role in the regulation of OL survival (Cohen, Marmur et al. 1996, Takano, Hisahara et al. 2000), the expression of its receptors on this specific cell type has not been fully defined (Casaccia-Bonnefil, Carter et al. 1996, Cohen, Marmur et al. 1996). To clarify this point, we performed immunostaining for TrkA and p75^{NTR}, both in OL primary cultures and on cryosections of the CC, one of the main regions affected by demyelination in the cuprizone model.

OLs were differentiated for 10 days and then immunostained for TrkA: OLs *in vitro*, recognized by the stage-specific marker MBP, were positive for the TrkA receptor (Fig. 11A-C and inserts). We also identified positive OLs for p75^{NTR}, with prominent staining on the cell body and extension into some of their major processes (Fig. 11D-F). The presence of these two receptors *in vitro* was also confirmed with immunobloting: in both OPCs (d2) and OLs (d10) there was clear expression of TrkA (approximately 140 kDa) and p75^{NTR} (75 kDa) (Fig. 11M). Subsequently, we explored their expression *in vivo* by performing immunohistochemistry on CC cryosections for CC-1 (a specific marker for mature OLs) and for both receptors. CC-1^{+} OLs (Fig. 11G, J and inserts) express both receptors (Fig, 11H, I, K, L and inserts), however not all cells were positive (Fig. 11N). Altogether, these results indicate that OLs both *in vitro* and *in vivo* express the NGF receptors, TrkA and p75^{NTR}.

Figure 11 (next page). OLs express TrkA and p75NTR receptors in vitro and in vivo. TrkA and p75NTR expression in OL primary cultures and in CC cryosections. (A-F) Double immunocytochemistry of differentiated OLs, with stage-specific (MBP) and specific antibodies for TrkA (see also inserts in A-C for details) or p75NTR receptors. (G-L and inserts) Double immunostaining of coronal CC cryosections for CC-1 (OLs) and TrkA or p75NTR. (M) TrkA (~140 kDa) and p75NTR (75 kDa) protein levels in primary cultures of OPCs and OLs. (N) Quantification of the OLs (CC-1+ cells) positive for one of the two receptors, in the CC of control mice. Scale bar in A-F: 45 μm, in G-L: 35 μm.

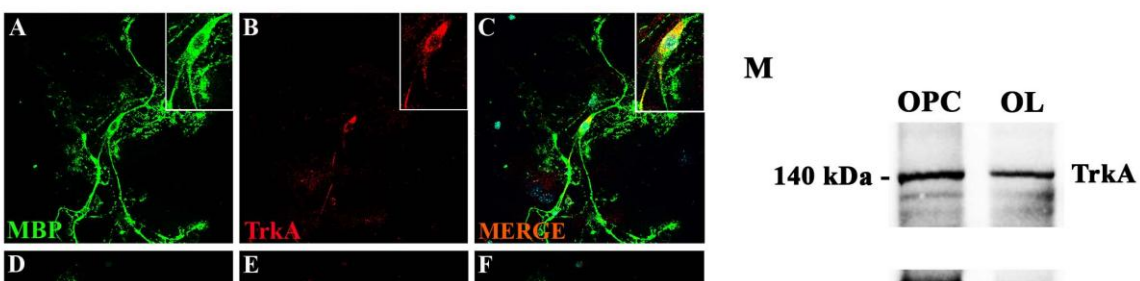

F.3. NGF and BNN27 rescue mature oligodendrocytes from cuprizone-induced apoptosis, increasing cell viability and myelin-like sheet formation *in vitro*

In the present study we sought to investigate the putative trophic action of a novel synthetic analog of NGF, the C17-spiroepoxy steroid BNN27, on OLs, after the addition of cuprizone *in vitro*. The copper chelator cuprizone (bis-cyclohexanone oxaldihydrazone) is able to induce the death of OLs in specific white matter tracts of the CNS, as well as the activation of microglia and the stimulation of the astrocytes (Matsushima and Morell 2001, Gudi, Gingele et al. 2014). To examine the putative protective role of NGF and BNN27 directly on OLs, we explored their ability to control the damaging effect of cuprizone toxin on primary OL cultures (Benardais, Kotsiari et al. 2013).

The apoptotic process in cultured cells was studied by evaluating two parameters of this phenomenon: the activated/cleaved Caspase-3 (aCaspase-3) and the number of apoptotic bodies (by DAPI nuclear staining), both being non-reversible stages of apoptotic cell death. aCaspase-3 staining was quantified by counting the ratio of MBP^+-aCaspase-3^+ OLs over the total number of MBP^+ OLs. For the DAPI analysis, apoptotic cells were recognized based on their characteristic morphology, mainly the presence of condensed, fragmented or degraded nuclei

(Collins, Schandi et al. 1997). Cuprizone (100 µM, for 48 h) induced the death of OLs *in vitro*, visualized by the aCaspase-3 staining (Fig. 12A and Fig. 13D-F), and the disrupted morphology of the nucleus (Fig. 12B and insert in Fig. 13E), compared to the control (Fig. 12A, B, Fig. 13A-C and insert in Fig. 13B). Addition of NGF (10 ng/ml) or BNN27 (100 nM) significantly reduced the toxic effect of cuprizone: in fact, the levels of aCaspase-3 and the morphology of the nuclei were comparable to the control group in NGF and BNN27-treated cells (Fig. 12A, B, Fig. 13G-L and inserts in Fig. 13H and K). To establish if NGF and BNN27 increased cell viability after cuprizone administration, we performed the MTT assay. As shown in figure 12C, cuprizone reduced cell viability compared to the control, while both NGF and BNN27 treatments were able to counteract this action.

To investigate the role of NGF and BNN27 in the later stages of oligodendrocyte development and maturation, we classified MBP^+ OLs in one of the three categories that reflected increasing branching complexity and myelin membrane sheet formation (Fig. 12D): type A included cells with low ramification branching, type B were recognized as cells with an increased branching level but lack of visible myelin membrane, whereas type C (fully myelinated) cells displayed myelin membrane in addition to an increased level of complexity. No differences were seen between the control and the cuprizone group, while both NGF and BNN27 increased the percentage of type C cells compared to the cuprizone group, with the BNN27 being also able to reduce the number of type A OLs compared both to the control and the cuprizone groups (Fig. 12F). Moreover, we analyzed the capacity of OLs to elaborate myelin-like membrane sheets *in vitro*, quantified by tracing the MBP^+ membrane sheets and measuring the occupied area (Fig. 12E). OLs grown in the presence of NGF or BNN27 exhibited a significant increase in the area of MBP^+ sheets compared to the cells in the cuprizone group (Fig. 12G). It is of note that NGF and BNN27 induced an incremented percentage of type C OLs, as well as an increased myelin-like membrane sheet area, when applied in the absence of the cuprizone toxin in control cultures (Fig. 17A and B), indicating that their effect is partially independent from cuprizone administration.

In short, NGF and BNN27 decreased the apoptotic effect of the cuprizone toxin on OLs, increasing their viability as well as their maturation.

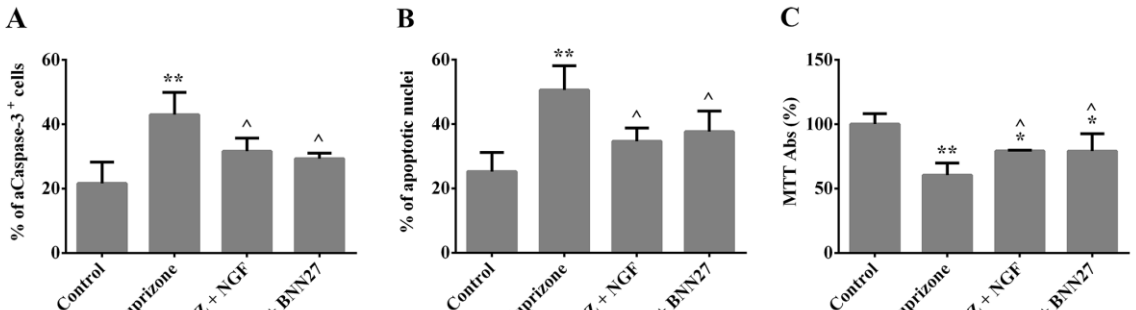

Figure 12. NGF and BNN27 induce in vitro OL survival, maturation and myelin-like membrane extension after cuprizone treatment. (A) Quantification of cleaved Caspase-3 (aCaspase-3). The histogram represents percentage of MBP+ OLs that are also aCaspase3+, over the total number of MBP+ cells, in control cultures and cultures exposed to cuprizone (100 μM), in the presence or absence of NGF (10 ng/ml) or BNN27 (100 nM). (B) Quantification of the apoptotic nuclei. The histogram represents percentage of MBP+ cells showing chromatin condensation over the total number of MBP+ cells, in control cultures and cultures exposed to cuprizone (100 μM), in the presence or absence of NGF (10 ng/ml) or BNN27 (100 nM). (C) Quantification of cell viability using the MTT assay. Data are expressed as an absorbance ratio to the control (untreated) OL cultures. (D) Representative examples of MBP-expressing OLs: type A shows low ramification branching, type B displays increasing levels of process outgrowth and branching without myelin membranes, whereas type C exhibits incremented levels of complexity and myelin membranes. (E) A type C MBP+ OL extending myelin-like membrane sheets. The area was quantified by tracing the MBP+ myelin-like membrane sheets (red outlines). (F) Quantification of OL complexity: the percentage of cells within each category is shown for control OLs, OLs in the presence of cuprizone (100 μM) and with or without NGF (10 ng/ml) or BNN27 (100 nM). (G) Quantification of MBP+-area calculated in type C OLs. For the statistics: One-way ANOVA with post-hoc Tukey test. Comparison with CONTROL

group: * p < 0,05; ** p < 0,01. Comparison with CUPRIZONE group: ^ p < 0,05; ^^ p < 0,01. For the quantification of OLs complexity, the Two-way ANOVA with post-hoc Tukey test was used. Comparison with CONTROL group: * p < 0,05. Comparison with CUPRIZONE group: ^ p < 0,05. Scale bar in D: 45 µm.

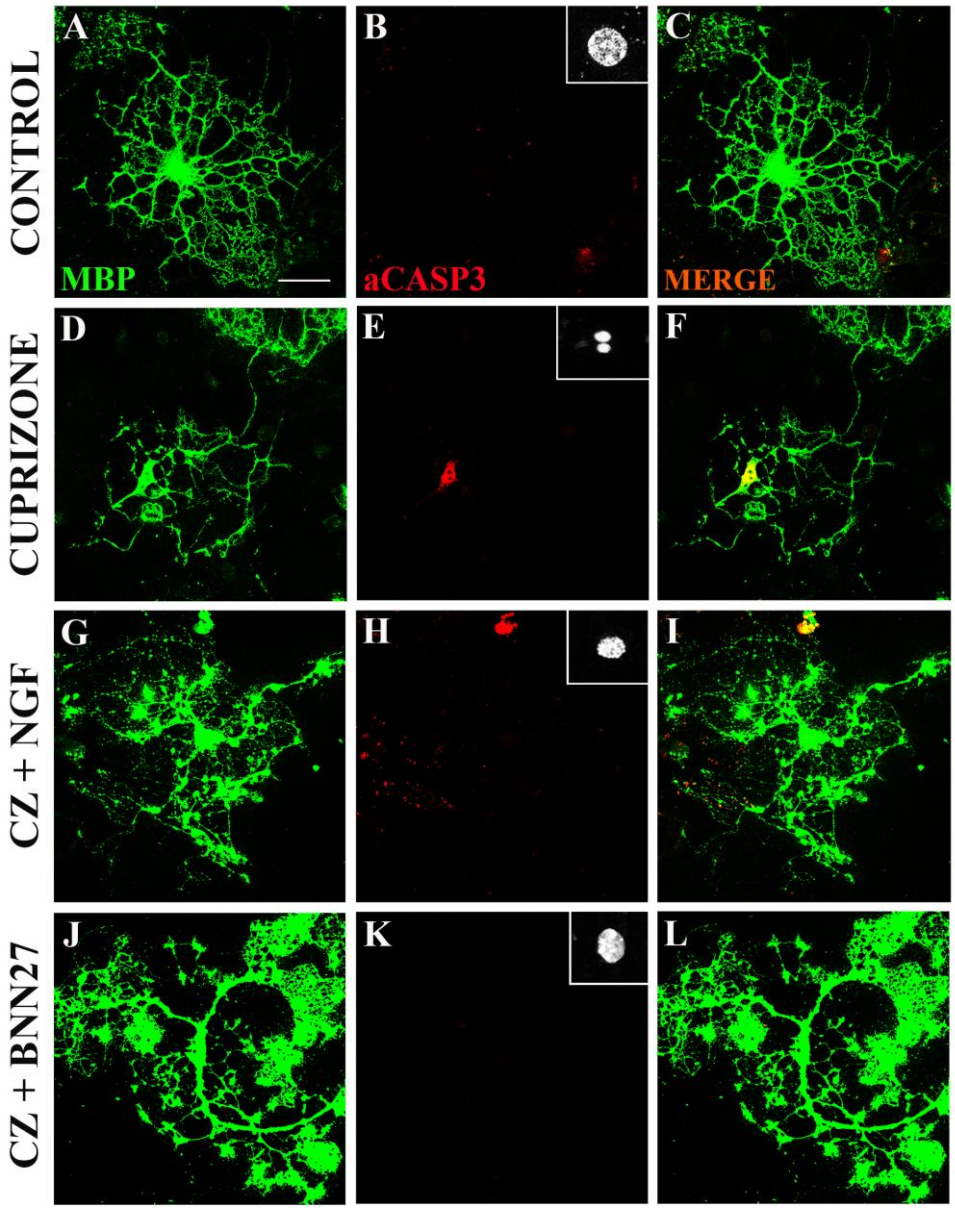

Figure 13. aCaspase-3 staining and nuclei morphology in OL primary cultures treated with cuprizone, NGF and BNN27. (A-L) To evaluate the trophic effect of NGF or BNN27 on OLs, apoptosis was measured after the administration of cuprizone (100 µM), with or withouth NGF (10 ng/ml) or BNN27 (100 nM) for 48 hours, using aCaspase-3 expression (B, E, H and K) and determining apoptotic bodies by DAPI nuclear staining (inserts in B, E, H and K). Scale bar in A-L: 60 µm.

F.4. The beneficial effect of NGF and BNN27 on mature oligodendrocytes is TrkA-dependent

To uncover the molecular mechanism through which NGF and BNN27 exert their protective role on OLs *in vitro*, we adopted two different approaches. In the first one, we added a specific TrkA inhibitor (10 nM) in cultures differentiated for 10 days, in the absence or the presence of cuprizone (100 μM), NGF (10 ng/ml) or BNN27 (100 nM). The percentage of aCaspase-3-positive cells, the apoptotic bodies as well as the cell viability were subsequently evaluated. No significant differences were seen after the addition of the sole inhibitor on control cells (Fig. 14A and B, 'Control' vs 'Control + TrkA Inh' bars), while cuprizone effectively induced the death of OLs even after the inclusion of the inhibitor (Fig. 14A and B), reducing cell viability (Fig. 14C). On the contrary, the trophic effect of NGF and BNN27 was abolished in the presence of the inhibitor (Fig. 14A, B and C).

To get additional insights on the role of TrkA in the activity of NGF and BNN27 on OLs, we investigated the OL complexity and the membrane-like sheet formation in the absence of the receptor's activity. NGF and BNN27 did not boost the OLs towards the fully myelinated (type C) class (Fig. 14D), nor increased the area of the myelin sheets (Fig. 14E), as they did in the presence of the TrkA receptor. The relevance of TrkA in NGF and BNN27 action was further confirmed by the addition of these two molecules on control cultures (i.e. without cuprizone), where they did not show any beneficial effect (Suppl. Fig. 17C and D).

Overall, these results indicate that the trophic effect of NGF and BNN27 on OLs, as well as the ability to enhance the maturation level on this cellular population, is dependent upon TrkA activation.

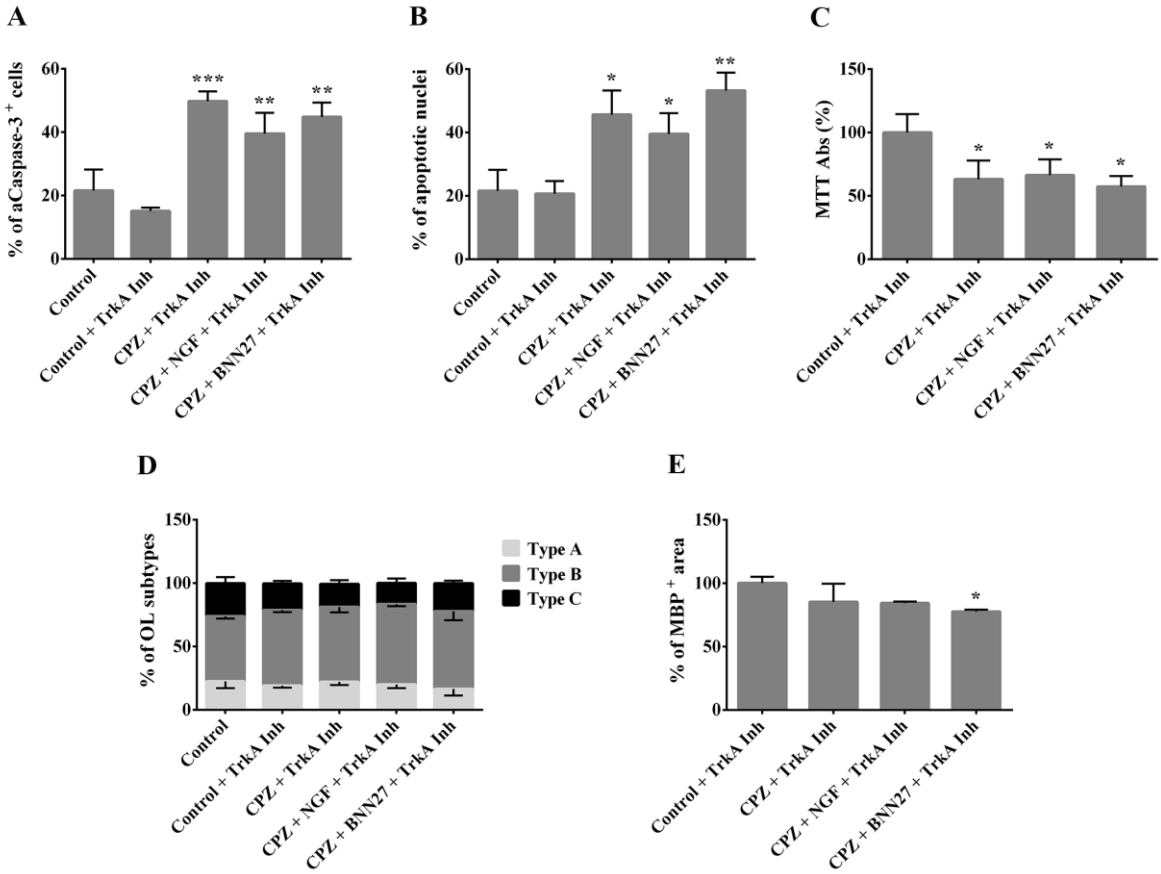

Figure 14. Inhibition of the TrkA receptor abolishes the trophic effect of NGF and BNN27. (A) Quantification of cleaved Caspase-3 (aCaspase-3). The histogram represents percentage of MBP^+ cells showing Caspase-3 cleavage over the total number of MBP^+ cells, in control cultures and cultures exposed to cuprizone (100 μM), in the presence or absence of NGF (10 ng/ml) or BNN27 (100 nM), after the addition of a specific TrkA inhibitor (10 nM). Values of the control cultures without the presence of the inhibitor are also shown. (B) Quantification of the apoptotic nuclei. The histogram represents percentage of MBP^+ cells showing chromatin condensation over the total number of MBP^+ cells, in control cultures and cultures exposed to cuprizone (100 μM), in the presence or absence of NGF (10 ng/ml) or BNN27 (100 nM), after the addition of the TrkA inhibitor (10 nM). Values of the control cultures without the presence of the inhibitor are also shown. (C) Quantification of cell viability using the MTT assay. Data are expressed as an absorbance ratio to the control cultures after the addition of the TrkA inhibitor (10 nM). (D) Quantification of OL complexity: the percentage of cells within each category is shown for control OLs and OLs in the presence of cuprizone (100 μM), with or without NGF (10 ng/ml) or BNN27 (100 nM), after the addition of the TrkA inhibitor (10 nM). Values of the control cultures without the presence of the inhibitor are also shown. (E) Quantification of MBP^+-area calculated in type C OLs, after the addition of the TrkA inhibitor (10 nM). For the statistics: One-way ANOVA with post-hoc Tukey test. Comparison with CONTROL group: * $p < 0,05$; ** $p < 0,01$; *** $p < 0,001$. For the quantification of OLs complexity, the Two-way ANOVA with post-hoc Tukey test was used, but no statistical significances were found.

F.5. Deletion of $p75^{NTR}$ receptor does not affect the protective activity of NGF or BNN27

The second approach used to investigate the mechanism of action of NGF and BNN27 was to take advantage of a murine line where this receptor is not expressed. We cultured OLs isolated from $p75^{NTR}$-null mice (Lee, Li et al. 1992), which carry a mutant allele that does not produce the functional protein. As expected, OLs from $p75^{NTR-/-}$ mice did not express the receptor (Suppl. Fig. 15D-F), while in OLs isolated from wild type mice the presence of the protein was clearly visible (Suppl. Fig. 15A-C). No major differences were evident, in terms of apoptotic levels, between wild type and null cells, in the untreated condition (Fig. 16A and B, 'Control' vs '$Control^{-/-}$' bars). The cuprizone toxin (100 μM) was able to induce cell death, as well as to reduce cell viability, in OLs devoid of the receptor, suggesting that its mechanism of action is not dependent on $p75^{NTR}$ (Fig. 16A, B and C). aCaspase3 levels were decreased after the addition of NGF (10 ng/ml) or BNN27 (100 nM) (Fig. 16A), and reduced apoptotis was evident when the analysis of the nuclei morphology was performed (Fig. 16B). Moreover, both NGF and BNN27 increased cell viability compared to the OLs treated only with cuprizone (Fig. 16C). To analyze the role of the $p75^{NTR}$ receptor in the maturation process, we studied the cell complexity and the formation of myelin-like membrane sheets in OLs derived from $p75^{NTR}$-null mice. As already seen for the apoptotic and the viability process, the absence of $p75^{NTR}$ did

not influence the capacity of NGF and BNN27 to improve maturation. In fact, both agents increased the number of type C cells compared to the cuprizone group, with BNN27 reducing type A cells as well (Fig. 16D). No main differences were present between OLs derived from wild type and knock-out mice. (Fig. 16D, 'Control' vs 'Control$^{-/-}$' bars). The addition of NGF and BNN27 enhanced the percentage of myelin-like membrane sheets compared to the cuprizone treatment and, for BNN27, also compared to the control group (Fig. 16E). The same outcome was visible when NGF and BNN27 were added to control cultures in the absence of the cuprizone toxin (Suppl. Fig. 17E and F).
Altogether, our data suggests that the absence of p75^{NTR} does not influence the capacity of NGF or BNN27 to induce OL survival or maturation.

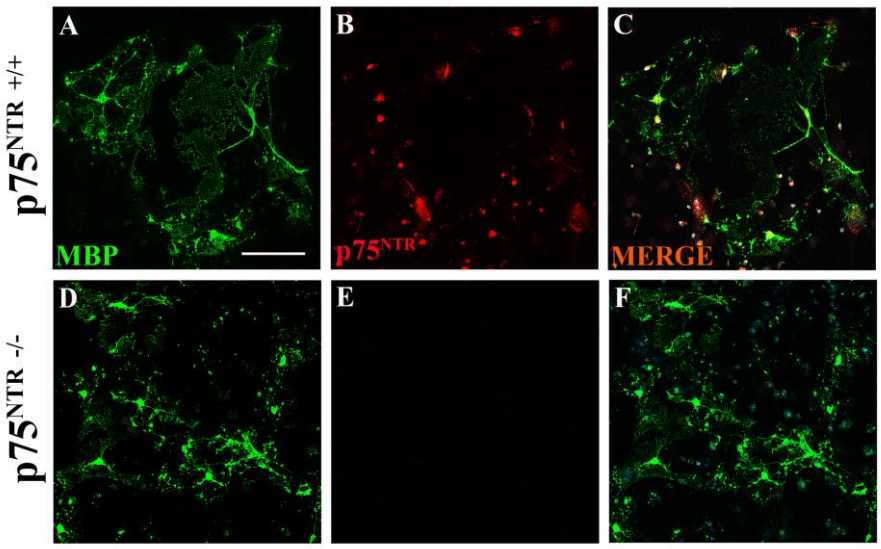

Figure 15. Expression of the p75^{NTR} receptor in cultures of p75$^{NTR\ +/+}$ and p75$^{NTR\ -/-}$ OLs. (A-F) Double immunostaining of mature oligodendrocytes, with the stage-specific marker MBP and p75^{NTR} antibody. No visible trace of the receptor is present in the KO culture (D-F), while a clear expression is visible in the wild type (A-C).

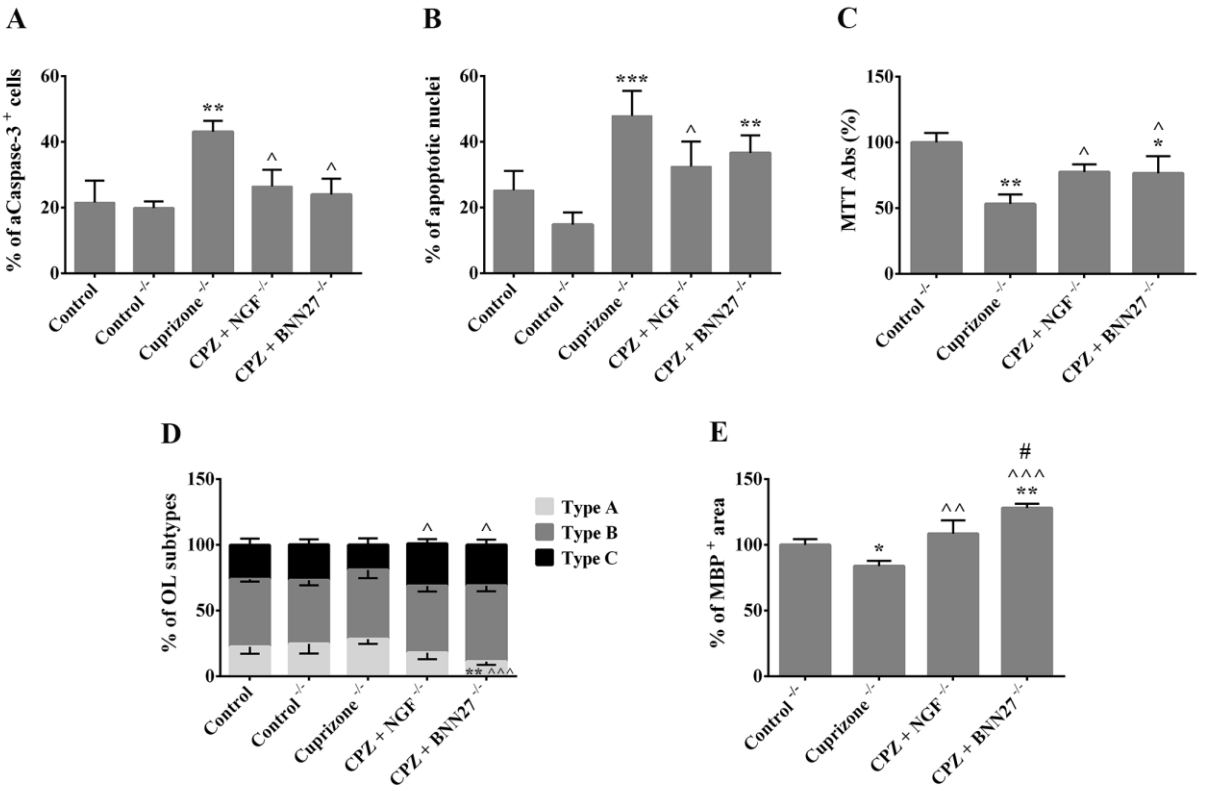

Figure 16. The absence of the p75^{NTR} receptor does not alter the trophic action of NGF or BNN27. (A) Quantification of the Caspase-3 cleavage (aCaspase-3) in cultures of p75$^{NTR-/-}$ OLs. The histogram represents percentage of MBP^{+} OLs showing Caspase-3 cleavage over the total number of MBP^{+} cells, in control cultures and cultures exposed to cuprizone (100 μM), in the presence or absence of NGF (10 ng/ml) or BNN27 (100 nM). Values referring to the wild type control cultures are also shown. (B) Quantification of the apoptotic nuclei in cultures of p75$^{NTR\ -/-}$ OLs. The histogram represents percentage of MBP^{+} OLs showing chromatin condensation over the total number of MBP^{+} cells, in control cultures and cultures exposed to cuprizone (100 μM), in the presence or absence of NGF (10 ng/ml) or BNN27 (100 nM). Values referring to the wild type control cultures are also included. (C) Quantification of cell viability in cultures of p75$^{NTR\ -/-}$ OLs using the MTT assay. Data are expressed as an absorbance ratio to control cultures of p75$^{NTR\ -/-}$ OLs. (D) Quantification of OLs complexity in p75$^{NTR\ -/-}$ cultures: the percentage of cells within each category is shown for control OLs and OLs in the presence of cuprizone (100 μM) and with or without NGF (10 ng/ml) or BNN27 (100 nM). Values referring to the wild type control cultures are also shown. (E) Quantification of MBP^{+}-area calculated in type C OLs from p75$^{NTR\ -/-}$ cultures. For the statistics: One-way ANOVA with post-hoc Tukey test. Comparison with CONTROL group: * $p < 0,05$; ** $p < 0,01$; *** $p < 0,001$. Comparison with CUPRIZONE group: ^ $p < 0,05$; ^^ $p < 0,01$; ^^^ $p < 0,001$. Comparison between NGF and BNN27 groups: # $p < 0,05$. For the quantification of OLs complexity, the Two-way ANOVA with post-hoc Tukey test was used. Comparison with CONTROL group: ** $p < 0,01$. Comparison with CUPRIZONE group: ^ $p < 0,05$; ^^^ $p < 0,001$.

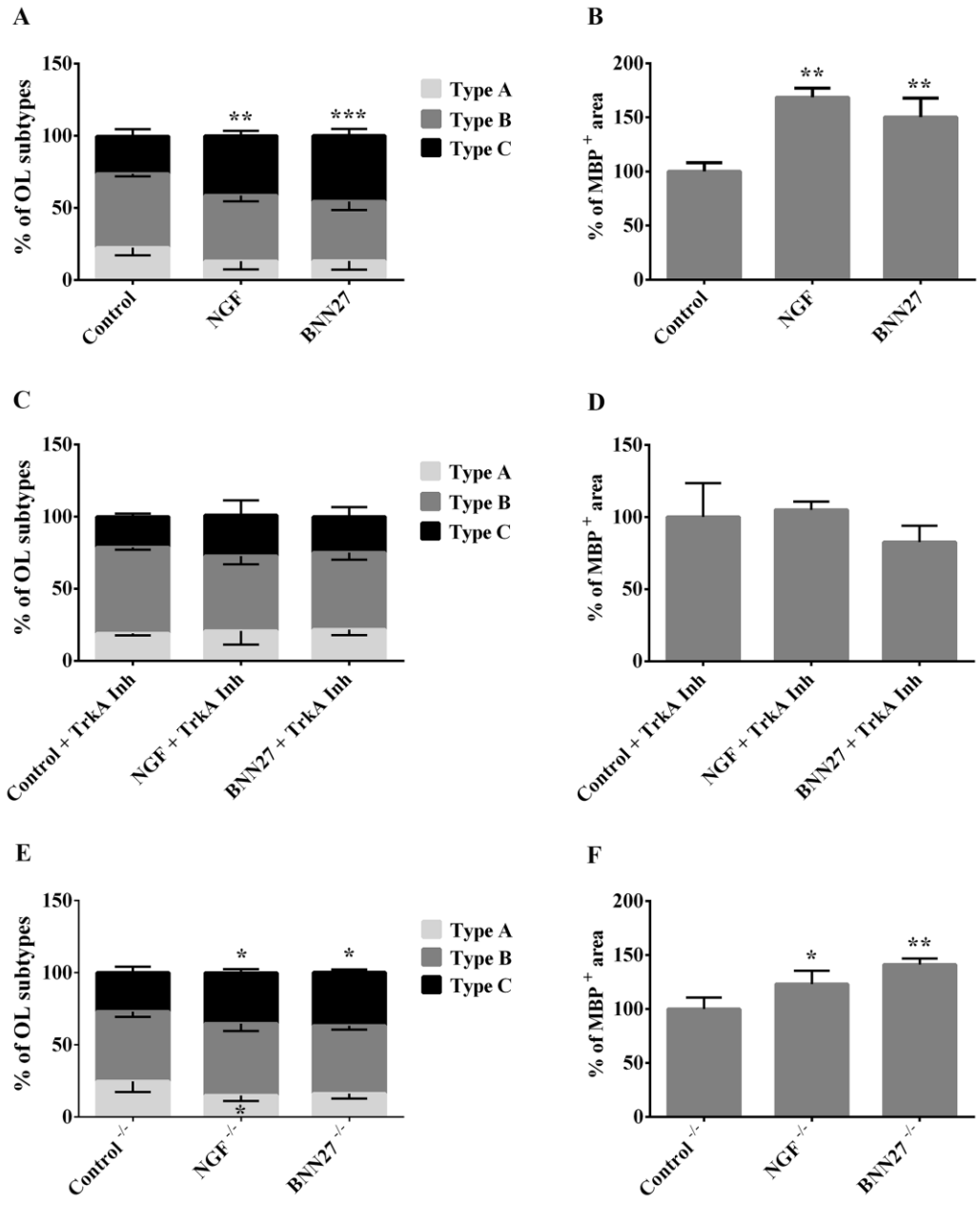

Figure 17. Effect of NGF and BNN27 on OL primary cultures, without cuprizone treatment. (A, C and E) Quantification of OL complexity in wild type cultures (A), after the addition of a specific TrkA inhibitor (10 nM) (C) and in OL cultures devoid of the $p75^{NTR}$ receptor (E): the percentage of cells within each category is shown for control OLs and for OLs with NGF (10 ng/ml) or BNN27 (100 nM). (B, D and F) Quantification of MBP^+-area calculated in type C OLs, in wild type cultures (B), after the addition of a specific TrkA inhibitor (10 nM) (D) and in OL cultures devoid of the $p75^{NTR}$ receptor (F). For the statistics: One-way ANOVA with post-hoc Tukey test. Comparison with CONTROL group: * $p < 0,05$; ** $p < 0,01$. For the quantification of OLs complexity, the Two-way ANOVA with post-hoc Tukey test was used. Comparison with CONTROL group: * $p < 0,05$; ** $p < 0,01$; *** $p < 0,001$.

F.6. BNN27 restores the myelin loss in cuprizone-induced demyelination *in vivo*

Our next goal was to analyze the action of BNN27 *in vivo*, using the cuprizone demyelinating model. 8-week-old animals were fed with 0.2% (w/w) of cuprizone for 6 weeks. At day 8 and 29 patches either containing BNN27 (BNN27 group) or devoid of it (CUPRIZONE group) were implanted subcutaneously (Fig. 18A). Untreated (CONTROL group) mice were used as controls. Two major areas of interest were selected to best represent the variations in demyelination, namely the central and the lateral part of the CC (Fig. 18B), since cuprizone is able to induce a reproducible demyelination pattern in these regions (Matsushima and Morell, 2001; Gudi et al, 2014). No statistically significant differences were observed in the weight of mice upon different treatments (Fig. 18C). To test if BNN27 influences the myelination levels, we analyzed the myelin protein composition, through immunoblotting and immunostaining for MBP, and the myelin lipid content, with the Luxol Fast Blue (LFB) histological staining. As depicted in fig. 18D and E, following cuprizone administration there was a significant decrease of MBP protein levels, which was partially recovered after BNN27 administration. In the LFB staining, the myelin in the CC of untreated mice is seen in blue while in the CUPRIZONE group only few blue stained myelin structures can be seen (Fig. 18F, G and O). BNN27 significantly diminished the myelin loss (Fig. 18H and O). Evaluation of the demyelinated areas by densitometric analysis for MBP immunohistochemistry revealed significant demyelination in the CUPRIZONE group compared to the CONTROL (Fig. 18I, J, L, M and P), while administration of BNN27 reduced the phenomenon (Fig. 18K, N and P).
Overall, our results indicate a protective role of BNN27 on the myelin compartment in the demyelination phase.

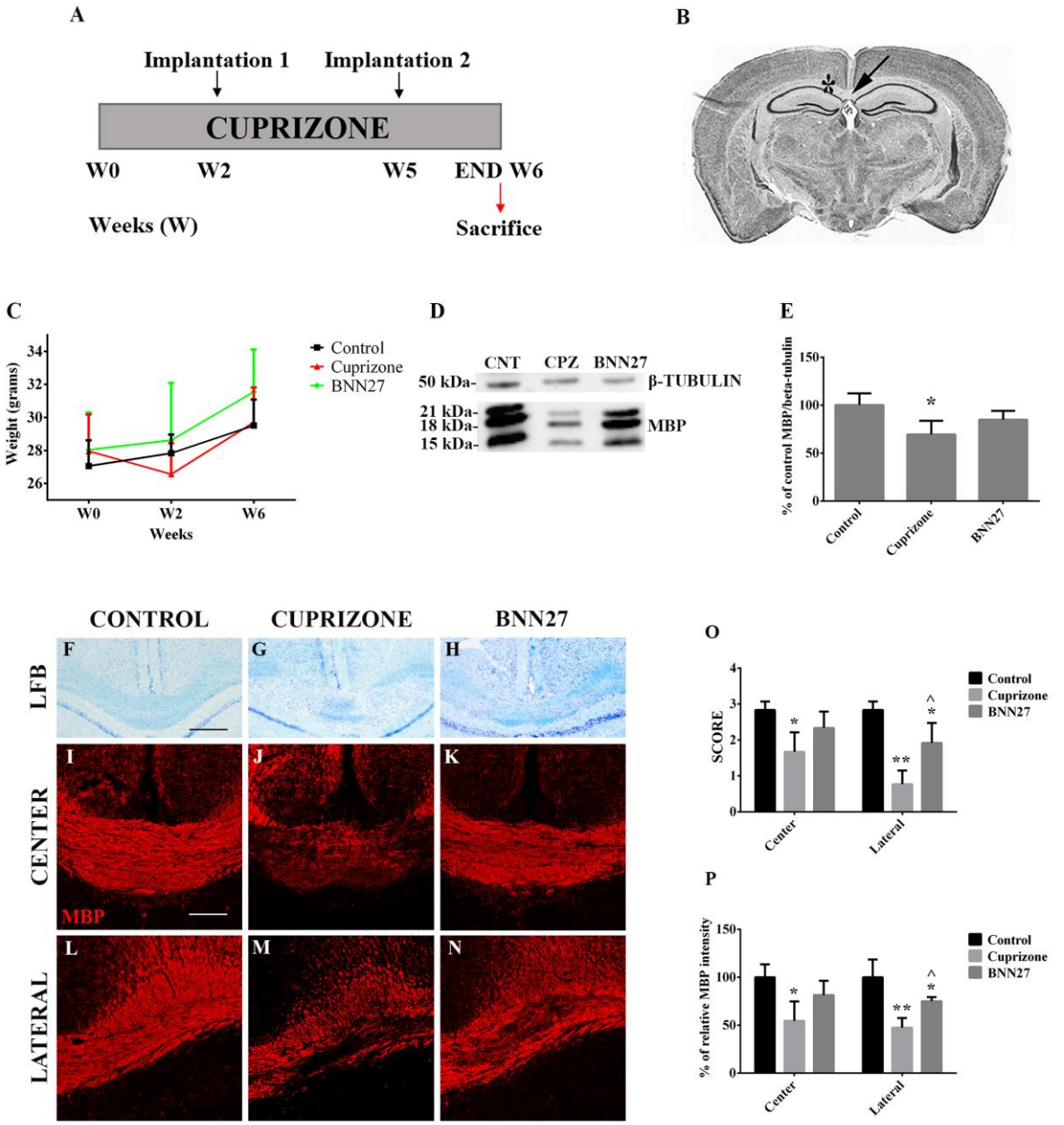

Figure 18. Experimental design and course of demyelination in the CC of 6 weeks cuprizone-treated mice. (A) Animals were fed with 0.2% w/w of cuprizone for 6 weeks. At day 8 (W2) and 29 (W5) patches either containing (BNN27 group) or not (CUPRIZONE group) BNN27 were implanted subcutaneously. Untreated (CONTROL group) mice were used as control. (B) The caudal area of CC was analyzed (Bregma -0,9 to -1,70): the central (arrow) and the lateral part (asterisk). (C) Body weights of the mice over the course of the experiment. (D-E) MBP protein levels in CC lysates of control, cuprizone-treated and BNN27-treated mice. (F-H) Representative Luxol Fast Blue (LFB) myelin stainings on coronal CC cryosections. (I-N) Representative MBP immunostainings on coronal CC cryosections. (O) Quantification of the LFB scoring. (P) Quantification of the MBP densitometric analysis. For the quantification of the protein levels and the densitometric analysis of MBP, the One-way ANOVA with post-hoc Tukey test was performed. Comparison with CONTROL group: * $p < 0,05$; ** $p < 0,01$.

Comparison with CUPRIZONE group: ^ $p < 0,05$. For the LFB scoring evaluation, the Friedman ANOVA on ranks as a non-parametric test, followed by the Tukey post-hoc test for pairwise multiple comparison procedures, was performed. Comparison with CONTROL group: * $p < 0,05$; ** $p < 0,01$. Comparison with CUPRIZONE group: ^ $p < 0,05$. Scale bar in F-H: 150 μm, in I-N: 75 μm.

F.7. BNN27 regulates mature oligodendrocyte and oligodendrocyte precursor numbers *in vivo*

To detect whether there was a variation in the number of OLs or OPCs upon BNN27 treatment *in vivo*, we analyzed the CC-1- (OLs) and PDGFRα- (OPCs) positive cells in the central and lateral part of the CC. As expected, the number of CC-1^+ cells was reduced in both areas of the CC after 6 weeks of cuprizone administration compared to the control mice (Fig. 19A, B, D, E, M and N). BNN27 partially but significantly counteracted the depletion of mature OLs (Fig. 19C, F, M and N). Furthermore, an increased number of OPCs (PDGFRα^+ cells) was visible in the CC of cuprizone-treated mice compared to the control (Fig. 19G, H, J, K, inserts, O and P), while mice treated with BNN27 showed a milder OPC recruitment (Fig. 19I, L, inserts, O and P). In summary, BNN27 exerts a positive *in vivo* effect on OLs, as seen in the *in vitro* experiments, while regulating the number of OPCs.

Figure 19 (next page). In vivo effect of BNN27 on mature oligodendrocytes and on oligodendrocyte precursors. (A-F) Representative immunohistochemistry of the central and lateral part of the CC for CC-1 (red) and TO-PRO3 (blue). (G-L and inserts) Representative immunohistochemistry of the central and the lateral part of the CC for PDGFRα (green) and TO-PRO3 (blue). (M-P) Quantification of the percentage of OLs stained with CC-1 (M and N), and of the percentage of OPCs stained with PDGFRα (O and P). For the statistics, One-way ANOVA with post-hoc Tukey test. Comparison with CONTROL group: * $p < 0,05$; ** $p < 0,01$; *** $p < 0,001$. Comparison with CUPRIZONE group: ^ $p < 0,05$; ^^ $p < 0,01$. Scale bar in A-L: 75 μm.

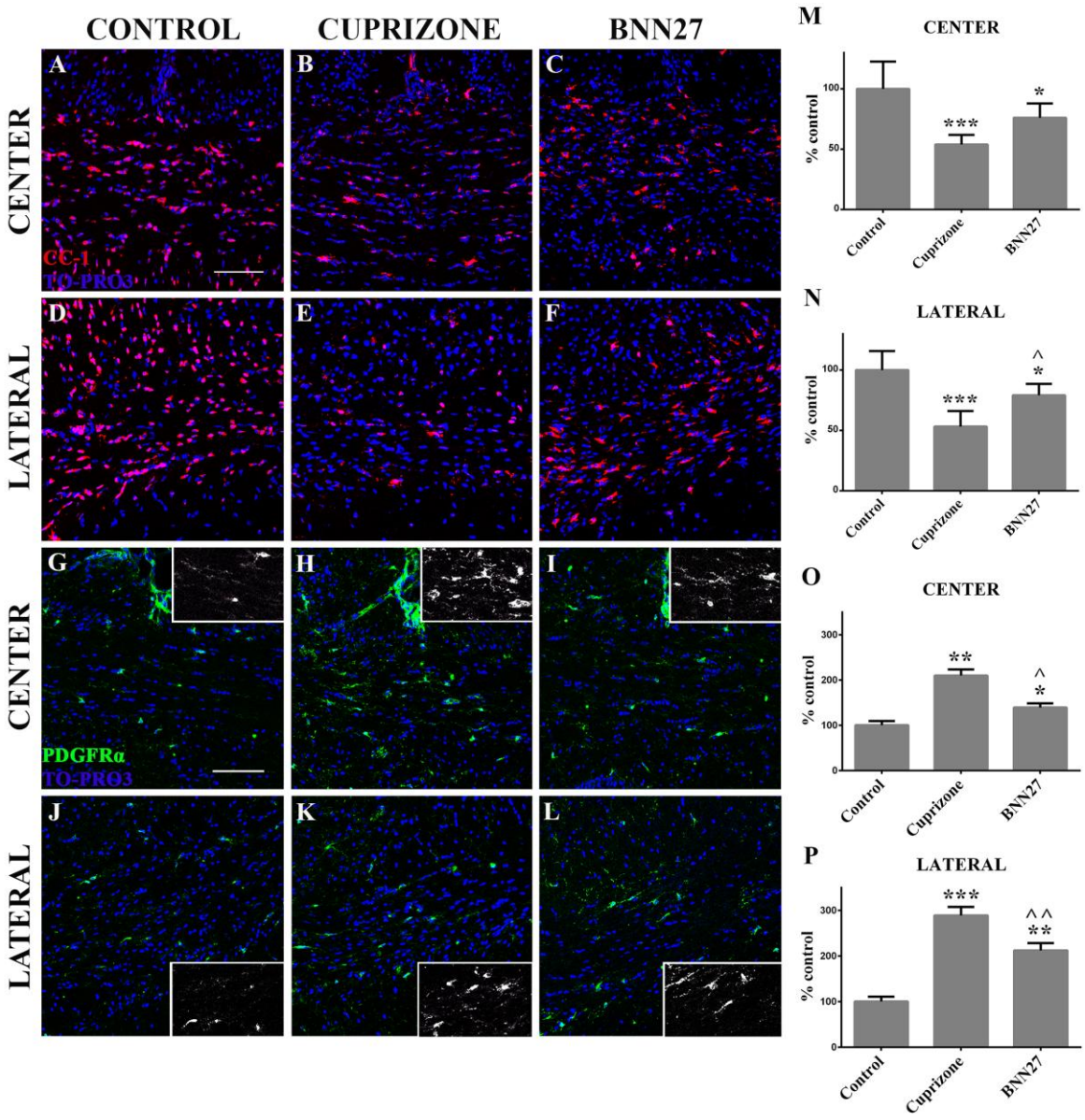

F.8. BNN27 treatment reduces microgliosis and astrogliosis During the cuprizone challenge

As aforementioned, cuprizone causes microglial activation without the breakdown of the BBB and without a marked lymphocytic response (Gudi, Gingele et al. 2014). After 6 weeks of cuprizone feeding, a significant accumulation of microglia (identified by IBA-1 staining) was visible in the two analyzed areas of the CC (Fig. 20A, B, D, E, M and N), followed by a statistically significant decrease in their number after BNN27 treatment (Fig. 20C, F, M and N). In the cuprizone model, the microglial activation initiates a cascade of signals that stimulate astrocytic activation and the expression of signaling molecules, which contribute to demyelination (Kang et al. 2012). In the CC of control mice, the GFAP marker was present in fine processes of astrocytes (Fig. 20G and J). After 6 weeks of cuprizone administration, astrocytes peaked in number and their reactivity was increased, as evident from the augmented

hypertrophy and disorganized process distribution (Fig. 20H, K, O and P). The treatment with BNN27 significantly reversed this increase (Fig. 20I, L, O and P). Overall, BNN27 has been shown to hold a diminishing effect on microglia and astrocyte proliferation.

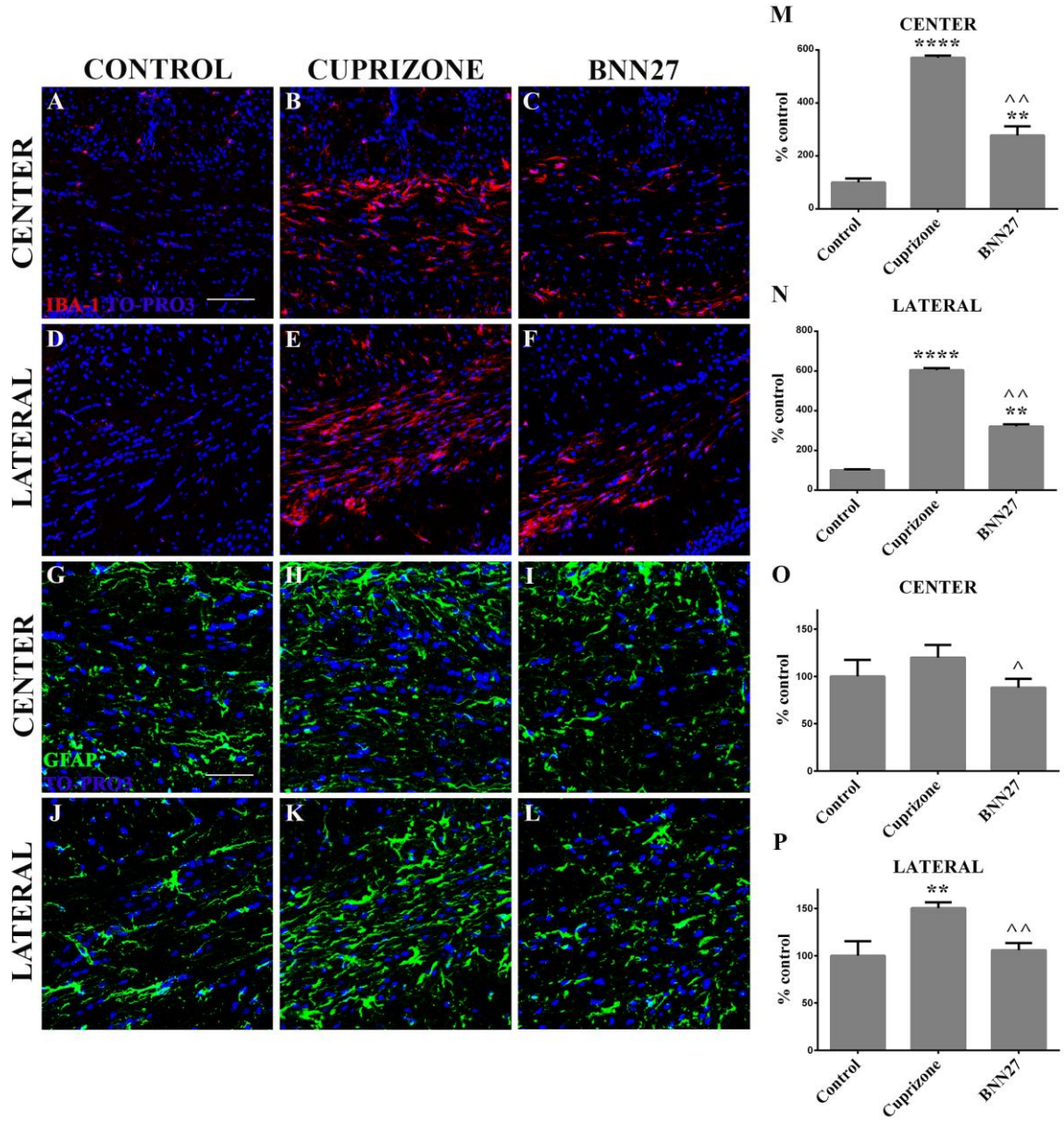

Figure 20. *In vivo* effect of BNN27 on microgliosis and astrogliosis. (A-F) Representative immunohistochemistry of the central and the lateral part of the CC for IBA-1 (red) and TO-PRO3 (blue). (G-L) Representative immunohistochemistry of the central and the lateral part of the CC for GFAP (green) and TO-PRO3 (blue). (M-P) Quantification of the percentage of microglial cells stained with IBA-1 (M and N) and of the percentage of astroglial cells stained with GFAP (O and P). For the statistics, One-way ANOVA with post-hoc Tukey test. Comparison with CONTROL group: ** $p < 0,01$; **** $p < 0,0001$. Comparison with CUPRIZONE group: ^ $p < 0,05$; ^^ $p < 0,01$. Scale bar in A-F: 75 µm. Scale bar in G-L: 37,5 µm.

F.9. BNN27 does not affect the remyelination process *in vivo*

The cuprizone model is a useful experimental approach because its termination leads to spontaneous remyelination; furthermore, a partial remyelinating event occurs simultaneously with ongoing demyelination (Matsushima and Morell 2001, Lindner, Heine et al. 2008, Kipp, Clarner et al. 2009). We investigated the remyelinating potential of BNN27 by two different means: in a first set of experiments, we analyzed shorter-term cuprizone feedings (3 and 5 weeks, Fig. 21A). The intrinsic remyelinating process (i.e. ongoing during cuprizone feeding) is evident from the increased level of OPCs at 3 and 5 weeks of cuprizone administration in the CUPRIZONE group, in an attempt of remyelinating the lesions. On the contrary, BNN27 treatment reduced the death of the OLs (Fig. 21B and D), while decreasing the OPC number (Suppl. Fig. 21C and E). In addition, BNN27 decreased the activation of the microglia and astrocytic compartments (data not shown).

We then evaluated the later aspect of the remyelinating event. Demyelination was induced by treating the mice with cuprizone for 6 weeks, after which the toxin was removed to allow remyelination to occur for 3 additional weeks. Patches containing BNN27 were implanted at the end of the demyelinating period (END W6) (Fig. 22A). The remyelination process in the CUPRIZONE group was confirmed as previously described (Matsushima and Morell, 2001), with reduced lesion extension and increased intensity in the MBP staining compared to 6 weeks of cuprizone treatment. However, no evident differences were present between the CUPRIZONE and the BNN27 groups in the MBP densitometric analysis (data not shown), or OL number (Fig. 22B). In BNN27-treated mice, the OPC number was reduced compared to the CUPRIZONE group (Fig. 22C). Furthermore, BNN27 decreased the activation of microglia (Fig. 22D), as well as astrogliosis (Fig. 22E).

These data led us to speculate that BNN27 does not exert a remyelinating effect *per se*, since it does not increase the number of OPC cells in the CC (both during cuprizone feeding and remyelinating period), which is a critical step in the remyelination process.

Figure 21 (next page). BNN27 does not influence in vivo remyelination during the cuprizone challenge. (A) Animals were fed with 0.2% w/w of cuprizone for 3 or 5 weeks. At day 8 (W2) and 29 (W5) patches either containing (BNN27 group) or not (CUPRIZONE group) BNN27 were implanted subcutaneously. Untreated (CONTROL group) mice were used as control. (B-E) Quantification of the percentage of OLs stained for CC-1 (B and D) and OPCs stained for PDGFRα (C and E), after 3 and 5 weeks of cuprizone administration. For the statistics: One-way ANOVA with post-hoc Tukey test. Comparison with CONTROL group: * $p < 0,05$; ** $p < 0,01$; *** $p < 0,001$. Comparison with CUPRIZONE group: ^ $p < 0,05$; ^^^ $p < 0,001$.

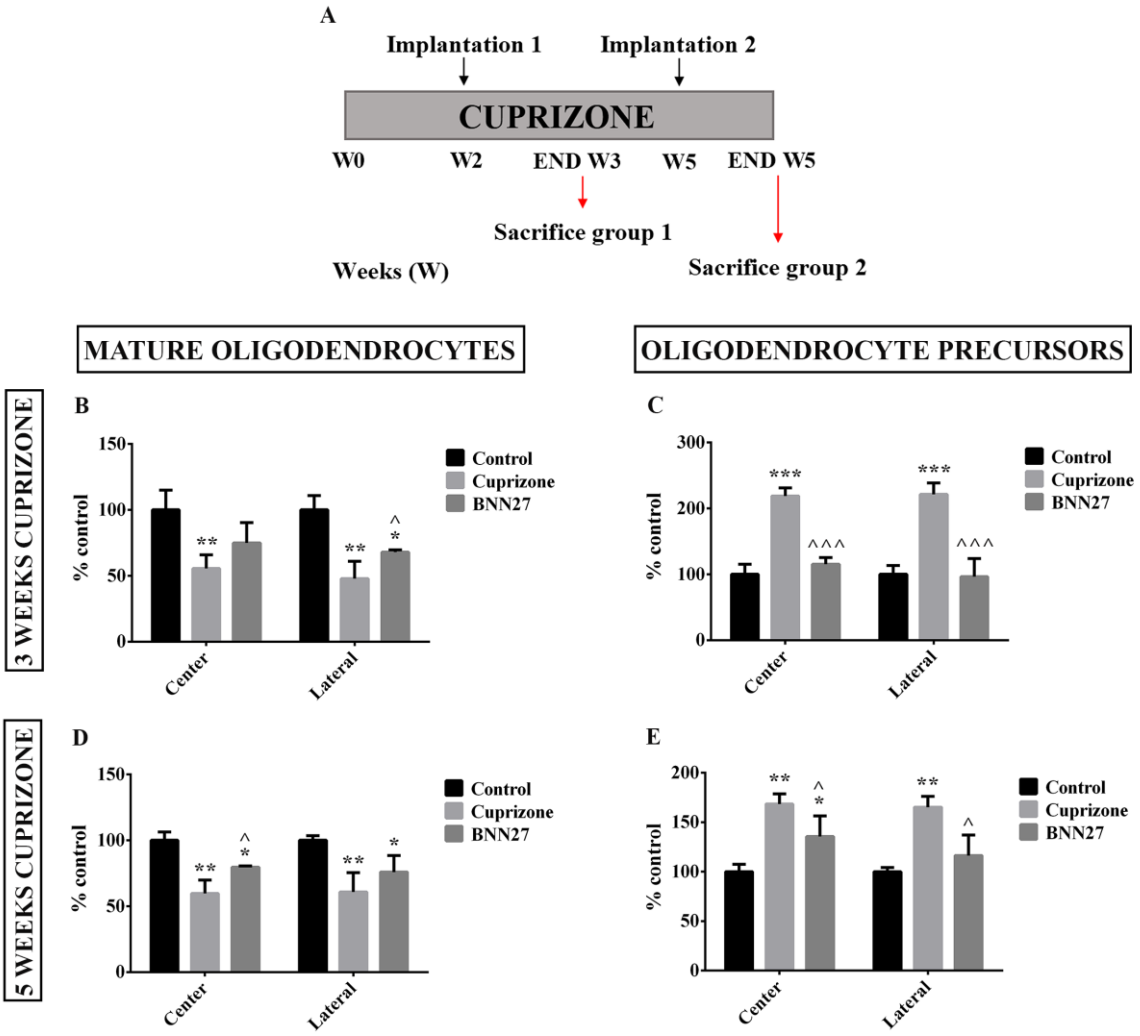

Figure 22 (next page). BNN27 does not have an evident effect after 3 weeks of remyelination, in vivo. (A) Animals were fed with 0.2% w/w of cuprizone for 6 weeks and then returned to normal chow while being implanted (END W6) with patches either containing (BNN27 group) or not (CUPRIZONE group). Untreated (CONTROL group) mice were used as control. Remyelination was allowed to occur for 3 weeks, after which animals were sacrificed (END W9). (B-E) Quantification of the percentage of cells stained with CC-1 (OLs), PDGFRα (OPCs), IBA-1 (microglia) and GFAP (astrocytes). For the statistics: One-way ANOVA with post-hoc Tukey test. Comparison with CONTROL group: * $p < 0,05$; ** $p < 0,01$; *** $p < 0,001$. Comparison with CUPRIZONE group: ^ $p < 0,05$; ^^ $p < 0,01$; ^^^ $p < 0,001$.

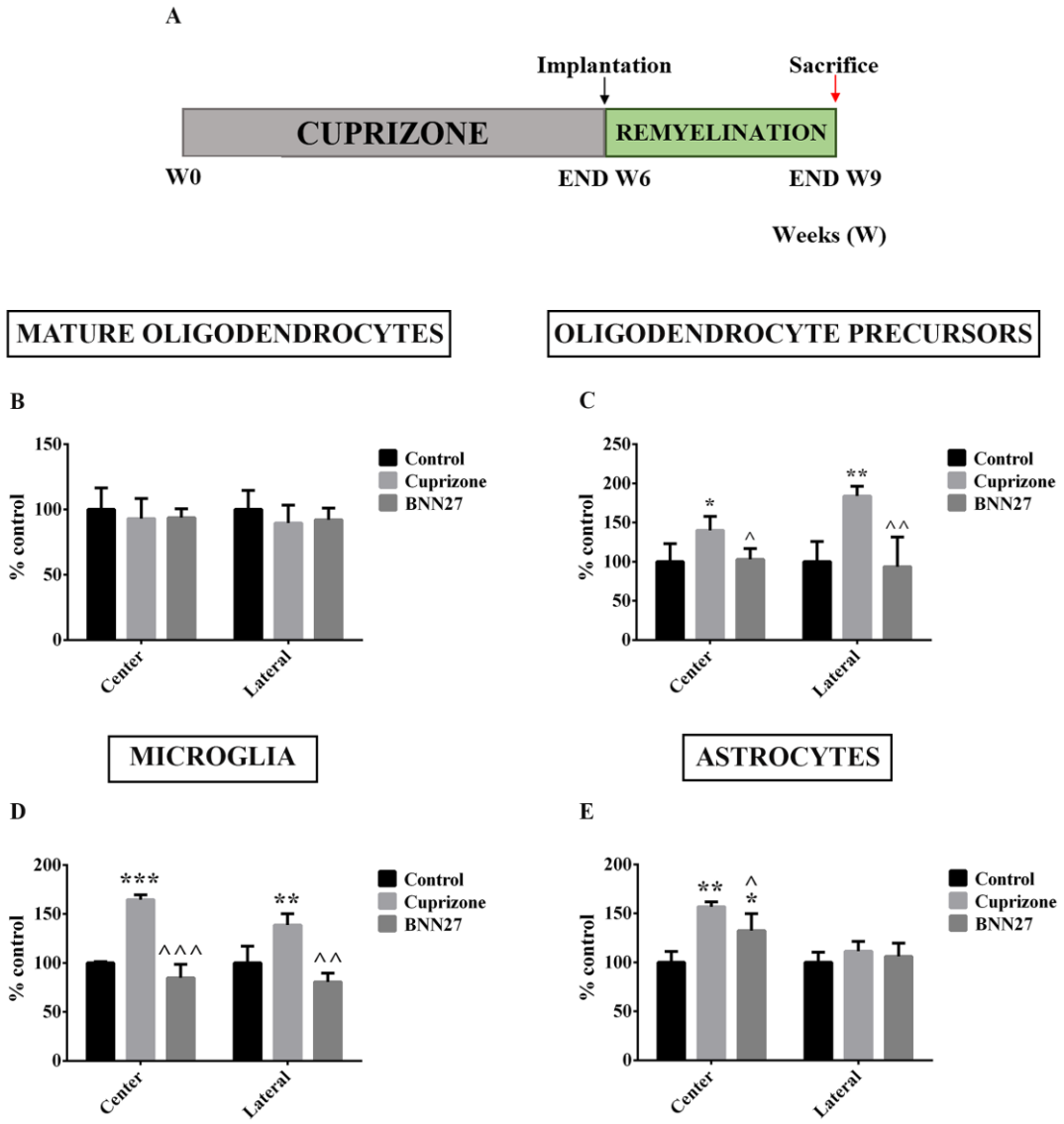

F.10. BNN27 reduces microglia activation and proliferation *in vitro*

To investigate if BNN27 acts exclusively on OLs *in vivo*, or if other cell types can be affected by its action, we decided to analyze its effect on microglia primary cultures (Fig. 8), since this cell type also expresses the NGF receptors, TrkA and $p75^{NTR}$ (Heese, Fiebich et al. 1998, Nordell, Lewis et al. 2005). To activate microglia, the cultures were exposed for 24 or 48 hours to LPS (100 µg/ml), which induced cell proliferation, as visible by the increased level of Ki67 nuclear staining, compared to the control (NO SERUM group) situation (Fig. 23A, B, F, G and K). Addition of BNN27 (100 nM) reduced the proliferation, with a significant effect at 48 hours (Fig. 23D, I and K). As further control, microglia cells were treated only with BNN27 or cuprizone (100 µM), which did not affect the number of $Ki67^{+}$-cells (Fig. 23C, E, H, J and K).

Addition of LPS (i.e. activation of the microglia) is able to induce a shift in the cell morphology, from a non-active (ramified morphology) to an active (amoeboid morphology) state (see IBA-1^+ cells in fig. 23L). Indeed, in the LPS GROUP a decreased number of ramified microglia and an increased level of amoeboid cells was evident, compared to the control (NO SERUM group), with significant differences observed at 48 hours (Fig. 23M and N). BNN27 reduced this modification after 48 hours of administration (Fig. 23M and N). Inclusion of BNN27 or cuprizone alone decreased the number of IBA-1^+ amoeboid cells compared to the LPS GROUP (at 24 and 48 hours), increasing the amount of ramified microglia (only at 48 hours, fig. 23M and N). Overall, these results indicate that BNN27 holds a direct effect on microglia activation, *in vitro*.

Figure 23 (next page). In vitro effect of BNN27 on microglia proliferation and morphology. (A-J) Representative immunocytochemistry of microglia primary cultures showing proliferating microglia (nuclear staining of Ki67+ cells, in red), in control cultures (NO SERUM group) and in cultures after LPS addition (100 μg/ml), in the absence or presence of BNN27 (100 nM), or with the sole inclusion of BNN27 or cuprizone (100 μM). (K) Quantification of the number of cells found positive for Ki67. (L) Representative images of IBA-1-expressing microglia, classified on their morphology: ramified (inactive) and amoeboid (reactive). (M, N) Quantification of the percentage of IBA-1+ microglia showing a specific morphology at 24 (M) and 48 (N) hours after LPS addition (100 μg/ml). For the statistics: One-way ANOVA with post-hoc Tukey test. Comparison with NO SERUM (control) group: * $p < 0,05$; ** $p < 0,01$; *** $p < 0,001$. Comparison with LPS GROUP: ^^ $p < 0,01$; ^^^ $p < 0,001$. Comparison with LPS + BNN27 GROUP: ## $p < 0,01$. For the evaluation of the microglia morphology, the Two-way ANOVA with post-hoc Tukey test was performed. Comparison with NO SERUM (control) group: * $p < 0,05$; *** $p < 0,001$. Comparison with LPS group: ^^ $p < 0,01$; ^^^ $p < 0,001$. Scale bar in A-J: 60 μm. Scale bar in L: 35 μm.

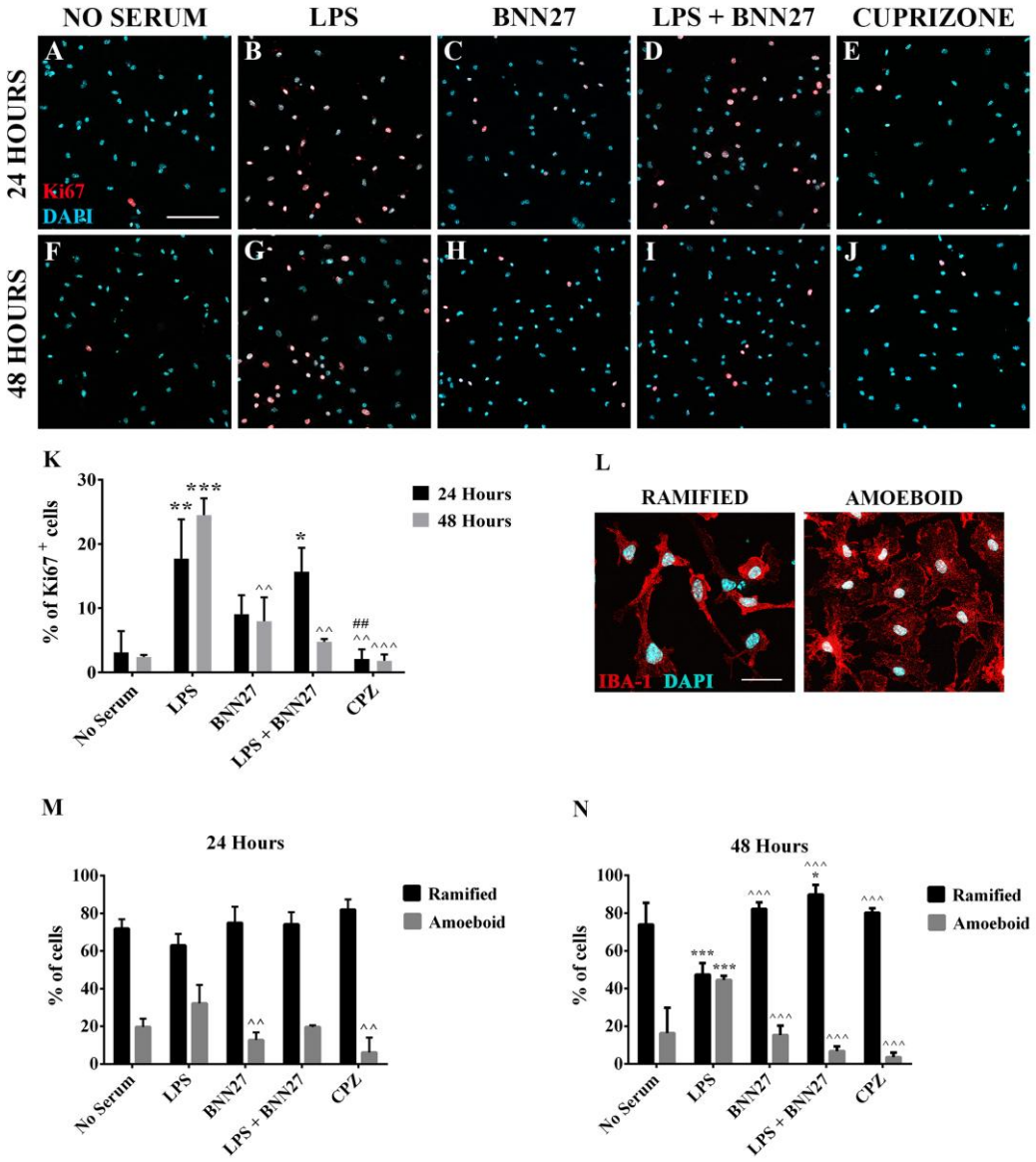
NO SERUM
LPS
BNN27
LPS + BNN27
CUPRIZONE
24 HOURS
48 HOURS
A
B
C
D
E
F
G
H
I
J
Ki67
DAPI
K
% of Ki67+ cells
24 Hours
48 Hours
No Serum
LPS
BNN27
LPS + BNN27
CPZ
L
RAMIFIED
AMOEBOID
IBA-1 DAPI
M
24 Hours
% of cells
Ramified
Amoeboid
N
48 Hours

G. RESULTS II

G.1. Broadening the TAG-1/Contactin-2 interaction network

The second aim of the present doctoral research concerned the identification of novel partners of TAG-1/Contactin-2 (CNTN-2) protein. To do that, we took advantage of a new computational tool, called UniReD, developed by our collaborator Dr Ioannis Iliopoulos and his team: this software not only identifies known protein-protein interactions (PPIs) described in biomedical literature, but also predicts new interactions not yet documented. The method revealed a number of known protein interactors for the target molecule TAG-1, including itself (CNTN2 Q61330, cluster score: 0.431685497809, Tsiotra et al., 1996), L1CAM (P11627, cluster score: 0.351247667577, Kuhn et al., 1991), NRCAM (Q810U4, cluster score: 0.384952668058, Pavlou et al, MCN, 2002), CNTNAP2/CASPR2 (Q9CPW0, cluster score: 0.384952668058, Traka et al., 2003), potassium voltage-gated channel subfamily A member 1 (KCNA1 P16388, cluster score: 0.384952668058, Poliak et al., 2003) and protein CD24 (P24807, cluster score: 0.434840323837, Lieberoth et al., 2009).
Apart from the known molecules that interact with TAG-1, several other putative interactors were identified. Five of them were validated with co-immunoprecipitation studies. TAG-1 was found to interact with MAP1B (P14873, cluster score: 0.421539019305) both in embryonic (Fig. 24A and B) and adult mouse brain tissue (Fig. 24C and D), while a second interaction between TAG-1 and Reelin was also verified (RELN Q60841, cluster score: 0.341662298037) (Fig. 24E and F). On the contrary, no interaction was found between TAG-1 and Tenascin-R, as well as between TAG-1 and MAP2 (Fig. 25).

Figure 24 (next page). Co-immunoprecipitation analysis of mouse embryonic and adult brain tissue. (A-F) Interaction of TAG-1 with MAP1B in mouse adult (A, B) and embryonic tissue (C, D), and Reelin (E, F) in embryonic tissue. Immunoprecipitation was performed with the rabbit polyclonal antibody against TAG-1 TG2. Western blot analysis of the lysates (Lys), G-beads used for the preclearance step (G) and immunoprecipitates (IPTG2) revealed the interaction of TAG-1 with MAP1B (B, D) and Reelin (F).

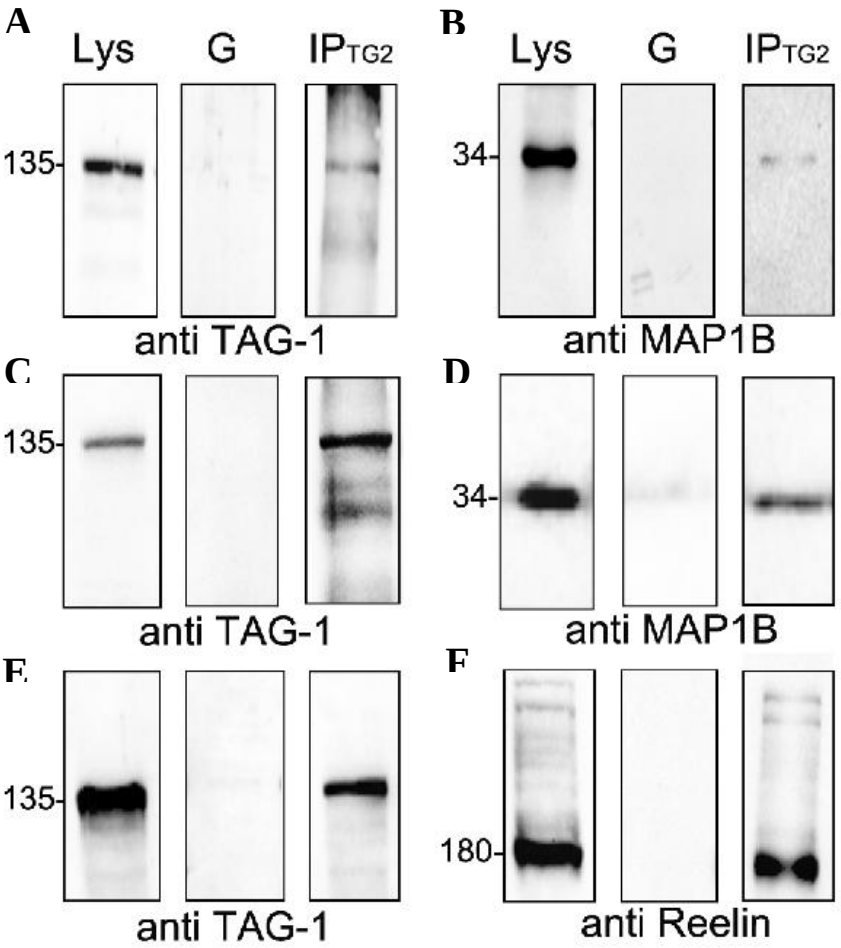

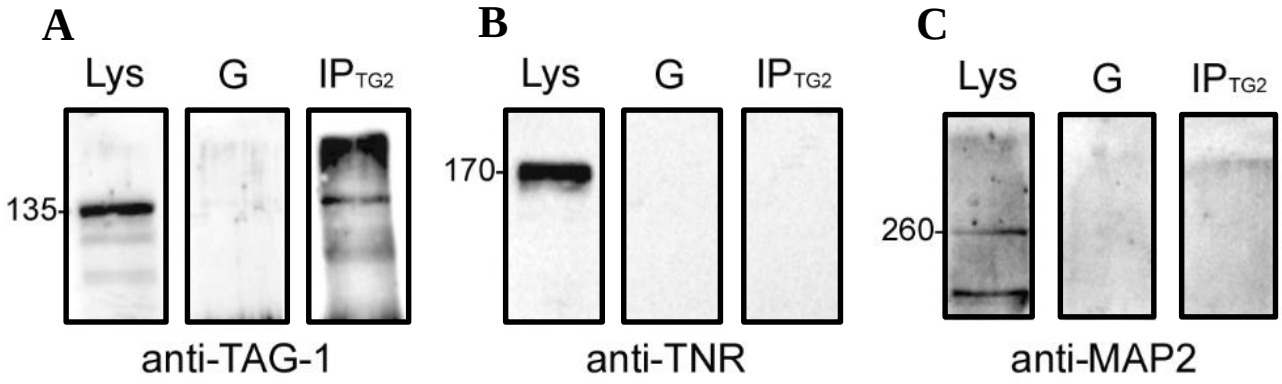

Figure 25. Co-immunoprecipitation analysis of mouse adult brain tissue. (A-C) Immunoprecipitation was performed with the rabbit polyclonal antibody against TAG-1 TG2. Western blot analysis of the lysates (Lys), G-beads used for the preclearance step (G) and immunoprecipitates (IP_{TG2}) revealed no interaction of TAG-1 (A) with Tenascin-R (B) and MAP2 (C).

G.2. Production of recombinant Reelin

Having found the interaction between TAG-1 and Reelin using a biochemical approach (Co-IP), hence not being sure that this is a direct interaction, we decided to utilize immunocytochemical methods. The first step was the preparation of a concentrated source of Reelin that could be used in neuronal cultures to verify the direct interaction with TAG-1. We took advantage of a stable cell line secreting high levels of full-length Reelin (1–2 mg/ml). Briefly, these HEK 293-cells were maintained DMEM in the presence of the selection antibiotic G418. Approximately 24 h after seeding cells into fresh medium, the DMEM was removed and the subconfluent cell monolayer was washed three times with 10 ml DMEM per 15 cm dish. Following washing, cultures were incubated in 30 ml of serum-free DMEM. After incubation for 48 h Reelin-containing medium was harvested. Supernatants were clarified by centrifugation, decanted and stored at 4 °C. Control media was harvested from 293T cells transfected with the empty CEP4 vector. All further purification procedures were performed identically on the Reelin-containing supernatants and the control supernatants. After purification, Reelin migrated at 300 kDa on SDS-Page, with minor position product present at 180 kDa (Fig. 26).

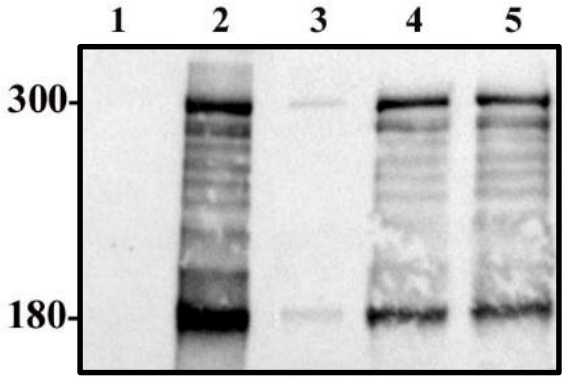

1: Serum free GFP-transfected supernatant (50 µg of protein)
2: Serum free Reelin-conditioned supernatant (50 µg of protein)
3: Reelin-conditioned supernatant (10 µl)
4: Reelin-conditioned supernatant (50 µl)
5: Reelin-conditioned supernatant (100 µl)

Figure 26. Western blots for Reelin under the different experimental conditions. Supernatants from stably transfected HEK 293-cells expressing either full-length Reelin or from control cells transfected with a control vector (MOCK) were collected and the proteins were separated through SDS-Page. Two different isoforms of Reelin are represented (180 kDa and 300 kDa). No visible proteins were detected in the supernatant of control 293 cells (lane 1), differently from the freshly prepared conditioned supernatant from Reelin-transfected 293 cells (lanes 2-5).

H. DISCUSSION I

The aim of the first part of my thesis was to investigate the role of the novel C17-spiroepoxy analog of DHEA, BNN27, in demyelination and remyelination. Specifically, we decided to take advantage of the experimentally-induced demyelination model called cuprizone and to focus on the population which is under attack in this paradigm, i.e. the OLs.

We described the beneficial effect of BNN27 on the rescue of OL death and in demyelination processes. BNN27 effectively protected OLs from cuprizone-induced apoptosis in a TrkA-dependent manner. Additionally, it enhanced OL maturation *in vitro*, through its interaction with the TrkA receptor. *In vivo* experiments indicated that BNN27 preserved OLs from cuprizone-induced cell death by regulating OL survival, and it reduced microgliosis and astrogliosis. These data point to a significant protective effect of the synthetic molecule BNN27, a BBB-permeable analog of DHEA devoid of interactions with steroid receptors but acting through the NGF receptors, on the oligodendrocyte population and myelin.

The nervous system is not only a target for endocrine effects exerted by hormonal steroids released by peripheral steroidogenic tissues, but is also controlled in a paracrine or autocrine manner by neurosteroids, which are synthesized within the brain and peripheral nerves by glial cells and neurons (Baulieu 1999). In addition to endogenous steroids (hormonal steroids and neurosteroids) naturally produced in the body, several exogenous or synthetic steroids also have the ability to regulate the activity of the nervous system. It appears that a wide variety of steroids, acting through different mechanisms, exert a large array of biological effects on the nervous system.

Over the three past decades, neurosteroids have received a great amount of attention because of their capacity to control both homeostatic parameters and crucial pathophysiological mechanisms such as neurodegenerative processes and signaling pathways involved in neuronal cell death (Charalampopoulos, Alexaki et al. 2006, Melcangi and Garcia-Segura 2006, Melcangi and Panzica 2006). Particularly, the production of specific neurosteroids has been shown to play an important role in the myelinating process (Baulieu 1991, Robel and Baulieu 1994). For instance, progesterone increases the formation of new myelin sheaths after lesion of the rodent sciatic nerve as well as in explant cultures of DRGs (Koenig, Schumacher et al. 1995). It is also able to trigger central myelination, stimulating MBP expression in organotypic cerebellar slice cultures (Ghoumari, Ibanez et al. 2003). Allopregnanolone and progesterone protect against the loss of membrane integrity and against motor neuron death in injured organotypic spinal cord cultures from young mice (Labombarda, Ghoumari et al. 2013). Moreover, progesterone treatment has been shown to reduce the severity of EAE clinical symptoms, maintaining myelin protein expression and modulating inflammatory responses (Garay, Gonzalez Deniselle et al. 2007, Yates, Li et al. 2010, Giatti, Caruso et al. 2012). Finally, progesterone triggers myelin regeneration after chronic demyelination induced by the cuprizone toxin (El-Etr, Rame et al. 2015).

Interestingly, OPCs synthesize progesterone and produce its reduced metabolite allopregnanolone, a potent positive allosteric modulator of $GABA_A$ receptors. Progesterone indirectly stimulates the proliferation of OPCs through its metabolite allopregnanolone, via a bicuculline-sensitive mechanism involving $GABA_A$ receptors (Gago, El-Etr et al. 2004). Importantly, OPCs express $GABA_A$ receptors and also synthesize GABA (Gago, El-Etr et al. 2004). These results reveal complex autocrine/paracrine loops in the control of OPCs proliferation, involving interactive neurosteroid and GABA signaling.

Several studies have described the role of another neurosteroid, DHEA, in the treatment of neuroinflammatory or demyelinating pathologies. DHEA is protective after rat sciatic nerve transection, reducing the extent of denervation atrophy and inducing an earlier onset of axonal regeneration (Ayhan, Markal et al. 2003). After crush injury of rat sciatic nerve, it induces a faster return to normal values of sciatic function index and increases the number of myelinated fibers and fiber diameters (Gudemez, Ozer et al. 2002). It preserves rat chromaffin cells and the rat pheochromocytoma PC12 cell line against serum deprivation-induced apoptosis (Charalampopoulos, Tsatsanis et al. 2004). Moreover, an effect of DHEA in preventing vascular and neuronal dysfunction in the sciatic nerve of streptozotocin-rats (an experimental model of diabetic neuropathy) has also been observed (Yorek, Coppey et al. 2002). In EAE, *in vivo* administration of DHEA inhibits Th1-mediated inflammatory responses in the CNS and ameliorates the development of the disease (Du, Khalil et al. 2001). In accordance to these results, DHEA appears to inhibit Th17 cells by inducing IL-10-producing regulatory T cells in EAE in an estrogen receptor β-dependent fashion (Aggelakopoulou, Kourepini et al. 2016).

DHEA is a multifaceted agent, interacting with steroid and neurotransmitter receptors, and acting as an endogenous precursor for the biosynthesis of androgens, estrogens and their metabolites (Charalampopoulos, Margioris et al. 2008). It has been recently reported that DHEA exerts part of its aforementioned properties via binding at nanomolar concentrations to and activation of both NGF receptors, TrkA and $p75^{NTR}$ (Lazaridis, Charalampopoulos et al. 2011). Binding of DHEA to TrkA results in the receptor tyrosine phosphorylation, activation of the transcription factors CREB and NFkB and the transcriptional control of the production of anti-apoptotic protein Bcl-2 (Charalampopoulos, Tsatsanis et al. 2004, Lazaridis, Charalampopoulos et al. 2011). It is worth noticing that DHEA binds to all mammalian and invertebrate Trk receptors, although with affinity lower by two orders of magnitude compared to that of the polypeptidic neurotrophins (Pediaditakis, Iliopoulos et al. 2015).

Several synthetic C17-spiro derivatives of DHEA with neurotrophic properties have been synthesized (Calogeropoulou, Avlonitis et al. 2009), named microneurotrophins (MNT), devoid of any estrogenic or androgenic activities and unable to bind to and activate steroid hormone receptors (Calogeropoulou, Avlonitis et al. 2009). The MNTs act as agonists of Trks and $p75^{NTR}$ membrane receptors and efficiently activate their downstream pathways (Pediaditakis, Efstathopoulos et al. 2016, Pediaditakis, Kourgiantaki et al. 2016). BNN27 is the most studied member of this group: it attenuates the loss of motor neurons co-cultured with astrocytes derived from Amyotrophic Lateral Sclerosis (ALS) patients with SOD1 mutations, via the

reduction of oxidative stress (Glajch, Ferraiuolo et al. 2016). It also inhibits apoptosis of NGF-deprived sympathetic neurons and reverses apoptosis of $TrkA^+$ sensory neurons in E13.5 NGF-deficient mouse embryos (Pediaditakis, Efstathopoulos et al. 2016). Additionally, it promotes the internalization and fast turnover of TrkA into neuronal membranes in a different manner than NGF, securing higher levels of surface TrkA and potentiating the efficacy of low levels of NGF (Pediaditakis, Efstathopoulos et al. 2016) (see Fig. 28). Finally, it facilitates the interaction of $p75^{NTR}$ with its effector proteins, RhoGDI, RIP2 and TRAF6, in neuronal cells (Pediaditakis, Kourgiantaki et al. 2016).

In the present study, we tested the action of BNN27 on OLs. Although NGF plays an important role in the regulation of OL development (Cohen, Marmur et al. 1996), the expression of its receptors (TrkA and $p75^{NTR}$) and the stages at which it exerts its trophic action have not been fully defined. Therefore, we first confirmed that OLs in *vitro*, as well as in the CC of mice, express both TrkA and $p75^{NTR}$ receptors, in agreement with previous reports (Cohen, Marmur et al. 1996, Takano, Hisahara et al. 2000). Cohen and colleagues showed that developing rat brain OLs express full-length transcripts for TrkA and its protein products. By contrast, $p75^{NTR}$ was expressed at low levels in OPCs ($O\text{-}2A^+$-cells), but was upregulated in OLs (Cohen, Marmur et al. 1996). We could not detect this upregulation in our hands, and we have seen a stable expression of the $p75^{NTR}$ receptor both in primary cultures of OPCs and OLs.

To determine whether NGF and BNN27 support OL survival, we assessed cellular viability using two related methods: the MTT cell survival assay and quantitation of apoptotic OLs. Both NGF and BNN27 exhibited a protective, trophic effect in primary mouse OLs in culture when the cells were challenged with the cuprizone, decreasing the expression of the apoptotic executor aCaspase3 in cells exposed only to the toxin.

In addition to the above, we also showed that both NGF and BNN27 increased the formation of myelin-like membrane sheets. In *in vivo* conditions, OPCs differentiate, becoming increasingly branched and finally convert into post-mitotic OLs, which extend their processes to search for unmyelinated axons. Upon contact with axons, OLs produce compact myelin (Lee and Zheng 2012, Simons, Misgeld et al. 2014). Although the role of NGF on CNS myelination is still controversial (Cohen, Marmur et al. 1996, Chan, Cosgaya et al. 2001), it is of note that it effectively enhances the extent of fiber elongation and branching in pig OLs (Althaus, Kloppner et al. 1992). We hypothesize that the increased percentage of fully mature OLs (type C), as well as the augmented formation of myelin-like membrane sheets detected in the presence of NGF and BNN27 *in vitro*, may be attributed to an increased myelinating potential *in vivo*. Further studies, including neuron-OL co-cultures, will conclusively address this hypothesis.

Interestingly, the trophic action of NGF and BNN27 is lost in OLs cultured in the presence of a specific TrkA inhibitor, indicating the primary role of this receptor in the rescue of OLs undergoing apoptosis. The inhibition of TrkA also decreased the beneficial effect of NGF and BNN27 on OL maturation. It is of note that NGF and BNN27 exert their primary trophic action mainly through the TrkA receptor: in fact, when they were tested on OLs from $p75^{NTR\text{-}/\text{-}}$ mice, no evident differences were seen compared to those isolated from wild type animals. These

results are in agreement with a previous study, where it has been shown that TNF-α-induced OL death can be efficiently prevented by NGF, through the activation of the Akt-mediated signal transduction pathway (Takano, Hisahara et al. 2000).

Neuronal cell survival by neurotrophins requires the activation of Trk tyrosine kinase, which transduces signals via a Ras-dependent pathway and leads to the activation of the MAP kinases (Greene and Kaplan 1995) and PI3K (Speight, Yao et al. 1993). The $p75^{NTR}$ receptor forms high-affinity binding sites with TrkA, and this complex can lower the concentration of NGF required for signal transduction (Yao and Cooper 1995). Without TrkA expression, $p75^{NTR}$ can act as an inducer of apoptosis in mature rodent OLs (Casaccia-Bonnefil, Carter et al. 1996), but not in mature human OLs (Ladiwala, Lachance et al. 1998). Activation of TrkA in OLs negates the cell death mediated by $p75^{NTR}$ (Yoon, Casaccia-Bonnefil et al. 1998), suggesting that the expression levels of TrkA and $p75^{NTR}$ determine the rodent OL response to NGF. Overall, our data support increased formation of myelin-like membrane sheets, as well as pro-survival effect on OLs, due to NGF and BNN27 action via TrkA.

We also investigated the effect of BNN27 on OLs *in vivo*, taking advantage of the cuprizone model of demyelination. BNN27 has shown effective BBB penetrance (differently from NGF) and is not a major substrate for ABC drug transporters (Bennett, O'Brien et al. 2016). Administration of cuprizone induces the formation of lesions in specific areas within the CNS, most notably the CC, inducing death of OLs (Matsushima and Morell 2001). Moreover, this rodent model affords a unique opportunity to examine the role of microglia and astrocytes in de- and remyelination processes. The treatment with BNN27 significantly rescued the demyelinating effect of cuprizone (as shown by myelin lipids and protein levels), likely by reducing OL cell death and microglia activation, as supported by the *in vitro* data (i.e. OL and microglia primary cultures). Upon BNN27 treatment, we observed a significant reduction in the activation of microglial cells and astrocytes. One possible explanation is that BNN27, by diminishing OL death, reduces the activation of the microglial and/or the astrocyte population, in agreement with a previous report (Kang, Liu et al. 2012). This study described the so-called 'two-hit' model (see Fig. 27): upon cuprizone treatment, OLs undergo apoptosis, leading to the release of molecules such as reactive oxygen species (ROS) and heat shock proteins (HSPs), which up-regulate the expression and release of the inflammatory cytokines, targeting astrocytes to produce TNF-α and ROS, which can promote cell death and enhance cuprizone-induced demyelination. Hence, the direct effect of BNN27 on OLs would decrease the activation of the microglia and the astrocytes, reducing also an additional demyelinating event.

Microglia constitutes the resident macrophage population of the CNS and, together with astrocytes, express TrkA and $p75^{NTR}$ receptors (Rudge, Li et al. 1994, Heese, Fiebich et al. 1998, Wang, Hagel et al. 1998, Nordell, Lewis et al. 2005). Once stimulated they undergo a process called 'activation' (Rock, Gekker et al. 2004), which includes proliferation, changes in cell shape (from a ramified to an amoeboid morphology) and secretion of a variety of cytokines and free radicals (Streit 2002) that are believed to contribute to neurodegeneration (Rock, Gekker et al. 2004). To clarify the role of BNN27 specifically on microglia, we performed

primary cultures, using LPS to activate the cells. BNN27 reduced cell proliferation, leading to an increased percentage of ramified (i.e. inactive) cells. In agreement with these results, we have recently shown that BNN27 effectively induces TrkA phosphorylation in BV2 mouse glial cells (used as primary microglia substitute) (Blasi, Barluzzi et al. 1990, Henn, Lund et al. 2009) *in vitro*, decreasing the mRNA levels of IL6 (Pediaditakis, Efstathopoulos et al. 2016). It is interesting to note that serum levels of IL6 are elevated in MS patients (Maimone, Guazzi et al. 1997, Malmestrom, Andersson et al. 2006), while in EAE, IL6 seems to play a detrimental role, promoting the diversion of T helper (Th) cell population toward pathogenic Th17 and Th1 cells, thus aggravating the disease (Serada, Fujimoto et al. 2008). A deleterious role of the microglial compartment in the cuprizone-induced demyelination has also been observed (Millet, Moiola et al. 2009, Yoshikawa, Palumbo et al. 2011). However, there is also evidence suggesting beneficial effects of microglia in clearing myelin debris (Jurevics, Largent et al. 2002, Olah, Amor et al. 2012), promoting the recruitment of the OPCs to the lesion area (Arnett, Mason et al. 2001, Arnett, Wang et al. 2003) and releasing cytokines beneficial to the remyelinating process (Skripuletz, Hackstette et al. 2013). The results from our study indicate a direct action of BNN27 on microglia *in vitro*, which is to maintain this population in the resting state. Experiments directly addressing the role of BNN27 on microglia *in vivo* should contribute to the understanding of the role of this glial population in the demyelination process.

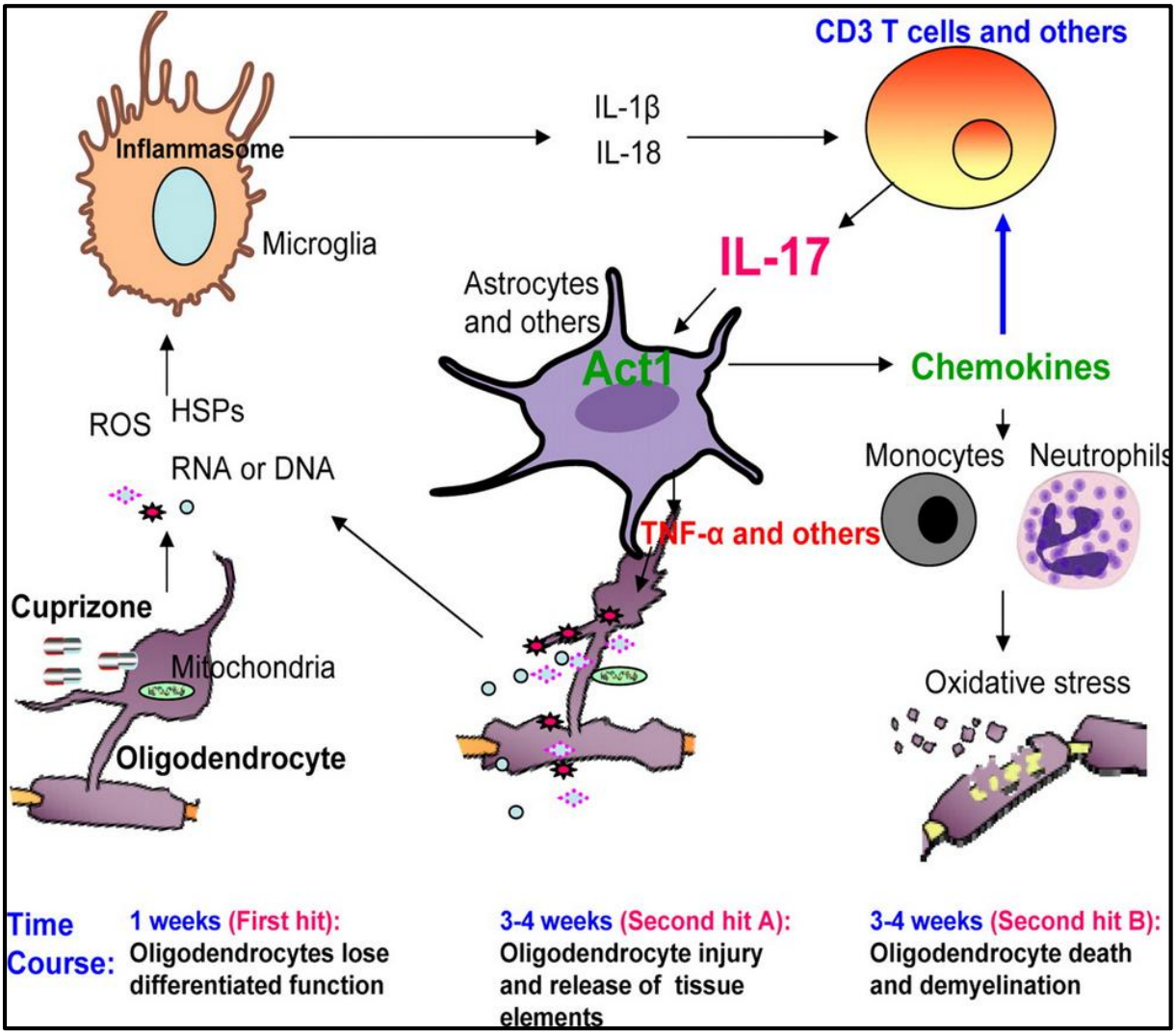

Figure 27. 'Two-hit' model in the cuprizone paradigm. First hit: Upon cuprizone treatment, most of the oligodendrocytes lose differentiated function and partially undergo apoptosis, leading to the release of intracellular substances such as HSPs, ATP, ROS and nucleic acids. While HSPs and nucleic acids activate TLR signaling in microglia to upregulate the expression of pro-IL-1β and pro-IL-18, ATP and ROS activate inflammasomes in microglia to promote the release of IL-18 and IL-1β, which then in turn act on T cells to polarize them to IL-17-producing cells. Second hits: IL-17 targets CNS resident cells such as astrocytes to produce chemokines, TNF-α, and ROS. While chemokines lead to the recruitment of neutrophils and monocytes, TNF and ROS can promote cell death in the CNS and enhance cuprizone-induced demyelination. Adapted from Kang et al. (Kang, Liu et al. 2012).

In the *in vivo* remyelinating protocol (3 weeks remyelination after 6 weeks of cuprizone), BNN27 neither improved myelin recovery, nor affected the number of OLs. The *in vitro* data showing that BNN27 has a positive effect on OL maturation led us to speculate that the same would occur *in vivo* as increased remyelination. However, the experiments so far do not support this hypothesis. We want to highlight that in this experimental design BNN27 was administered after the cuprizone treatment, therefore in a period when the number of OLs is expected to be decreased due to the toxin action. Hence, the results are in agreement with the hypothesis that BNN27 exerts a direct trophic action on OLs *in vivo*, as confirmed by the *in vitro* experiments. BNN27 reduced the number of microglia and astrocytes, confirming the effect observed both in the *in vivo* demyelinating protocol (i.e. 6 weeks of cuprizone treatment) and on microglia primary cultures, while it did not affect the OPC compartment. We completed the analysis by studying the intrinsic remyelinating potential that BNN27 could hold during cuprizone administration. In fact, it has been previously described that a considerable extent of remyelination is ongoing within acutely demyelinated lesions during cuprizone treatment (Matsushima and Morell 2001, Lindner, Heine et al. 2008, Kipp, Clarner et al. 2009). Analyzing shorter-term cuprizone feedings (3 and 5 weeks), we observed that BNN27 reduced OL death, decreasing microglia and astrocytes activation, without affecting OPCs. Our data are compatible with two interpretations related to the lack of a BNN27 effect on remyelination: either BNN27 does not have a direct effect on OPC proliferation or the reduced activation of the microglia and/or astrocytic compartments results in a reduced recruitment of OPCs. May be for the purpose of discussion you should add here what type if different protocol (ie time of BNN administration etc) you could use to test remyelination more directly
BNN27 enters the mouse brain within 30 min after peripheral (i.p. or patch pellet) administration. Additionally, the mono-oxidation metabolites of the compound were also detected in the mouse brain. Indeed, BNN27 is rapidly metabolized in the mouse liver by the cytochrome P450 system, producing ring-single hydroxylation metabolites (Bennett, O'Brien et al. 2016). In contrast, experiments with human liver preparations *ex vivo* suggest a much

slower metabolism of BNN27 in humans (Bennett, O'Brien et al. 2016). Thus, our study cannot exclude the possibility that some of the *in vivo* effects of BNN27 on OL survival and proliferation may be mediated by its BBB-permeable metabolites. Studies are now underway to fully characterize the exact chemical identity as well as the pharmacological properties of BNN27 metabolites, produced by mouse and human liver preparations *ex vivo*.
In summary, our results point towards a beneficial effect of BNN27 in OLs, when they are subjected to stress induced by the cuprizone toxin. Our *in vitro* studies support the hypothesis that this effect is mediated mainly by the TrkA receptor expressed in the OLs. Our *in vitro* findings also suggest that BNN27 keeps microglia at a resting state. Taken together, BNN27 might serve as a lead molecule to develop BBB-permeable synthetic agonists of neurotrophin receptors with strong neurotrophic and neuroprotective effects. Such molecules, with beneficial actions on oligodendrocytes (and possibly other glial populations) as well as neurons, may prove more effective in diseases with demyelinating as well as neurodegenerative components, such as MS.

Outlook and future directions

We aimed to investigate the role of the 17-spiro analog of DHEA, BNN27, in experimentally-induced demyelination of the CNS, taking advantage of the cuprizone neurotoxicity model.

The main findings of the first part of the study are (see also the graphical summary below):

- ✓ OLs and OPCs express TrkA and $p75^{NTR}$ receptors, both *in vitro* and *in vivo*;
- ✓ NGF and BNN27 reduce the toxic effect of cuprizone on OL *in vitro*, increasing their cellular viability;
- ✓ NGF and BNN27 enhance OL maturation *in vitro*;
- ✓ Inhibition of TrkA receptor impairs the effect of NGF and BNN27;
- ✓ $p75^{NTR}$ does not seem to hold a role in the OL survival and maturation process;
- ✓ NGF and BNN27 diminish the LPS-induced microglial activation, leading to an increased percentage of ramified (i.e. inactive) cells;
- ✓ BNN27 ameliorates the myelin status in the cuprizone-treated mice;
- ✓ BNN27 decreases the death of OLs in the *in vivo* cuprizone demyelinating model;

- ✓ BNN27 treatment reduces astrocytic reaction and macrophages accumulation during the cuprizone challenge;

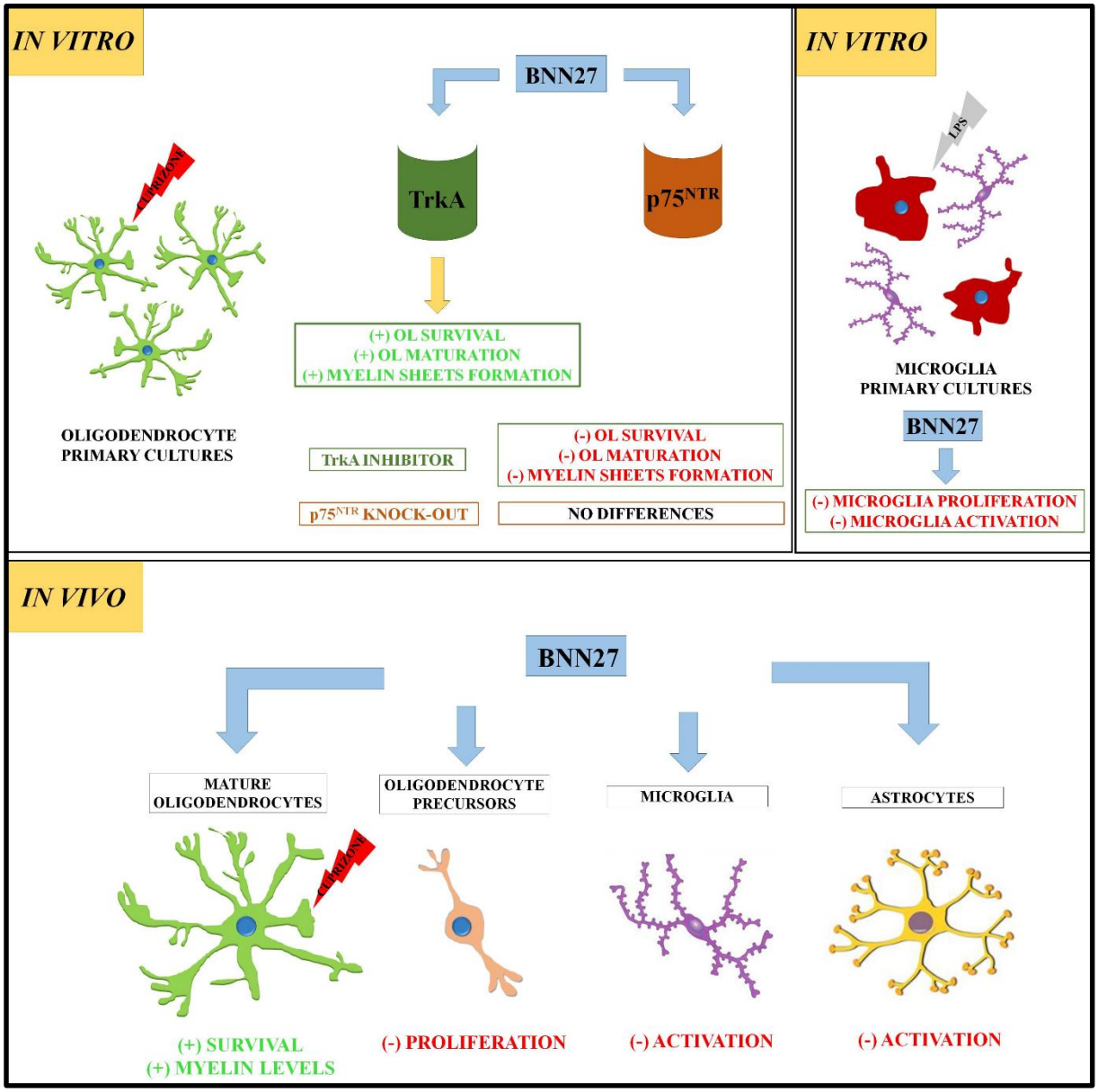

Future plans of the project include the study of the molecular mechanisms underlying the *in vitro* and *in vivo* effect of BNN27 in the cuprizone-induced demyelination. It is known that the binding of NGF to TrkA on the cell surface causes receptor dimerization and leads to the activation of the intrinsic tyrosine kinase activity of TrkA (Jing, Tapley et al. 1992). Consequently, NGF promotes cell survival by activating the PI3K/Akt and Ras/MAP kinase signaling pathways (Burgering and Coffer 1995).

We would like to decipher the intracellular pathway(s) activated by BNN27 on OLs. BNN27 induces a different pattern of TrkA turnover compared to that of NGF (Pediaditakis,

Efstathopoulos et al. 2016) (see Fig. 28). Specifically, BNN27 facilitates an internalization and fast translocation of the receptor back to cell surface through the persistent association of Rab5 with TrkA, docking of the receptor in the recycling endosomes (Rab11) and blocking the interaction of TrkA with the late endosomes (Rab7) and thus the maintenance of their signaling capacity. BNN27 secures higher levels of surface TrkA, inducing its faster recycling into the membranes, and potentiating the effects of low concentrations of NGF in axonal growth sprouting. BNN27 was also shown to be ineffective in inducing differentiation and neurite outgrowth of mouse sensory neurons in culture. However, when it was combined with low concentrations of NGF it significantly increased the efficacy of the latter in inducing the percentage of enhanced axonal length in both cell systems. These data suggest that the combination of BNN27 and NGF will act in parallel by the BNN27-driven fast returning of the internalized TrkA receptor in the membrane through early endosomes, increasing thus the levels of functional TrkA receptors occupied by NGF which afterwards induce full late endocytosis signaling of the NGF-TrkA complex, enhancing neurite outgrowth.

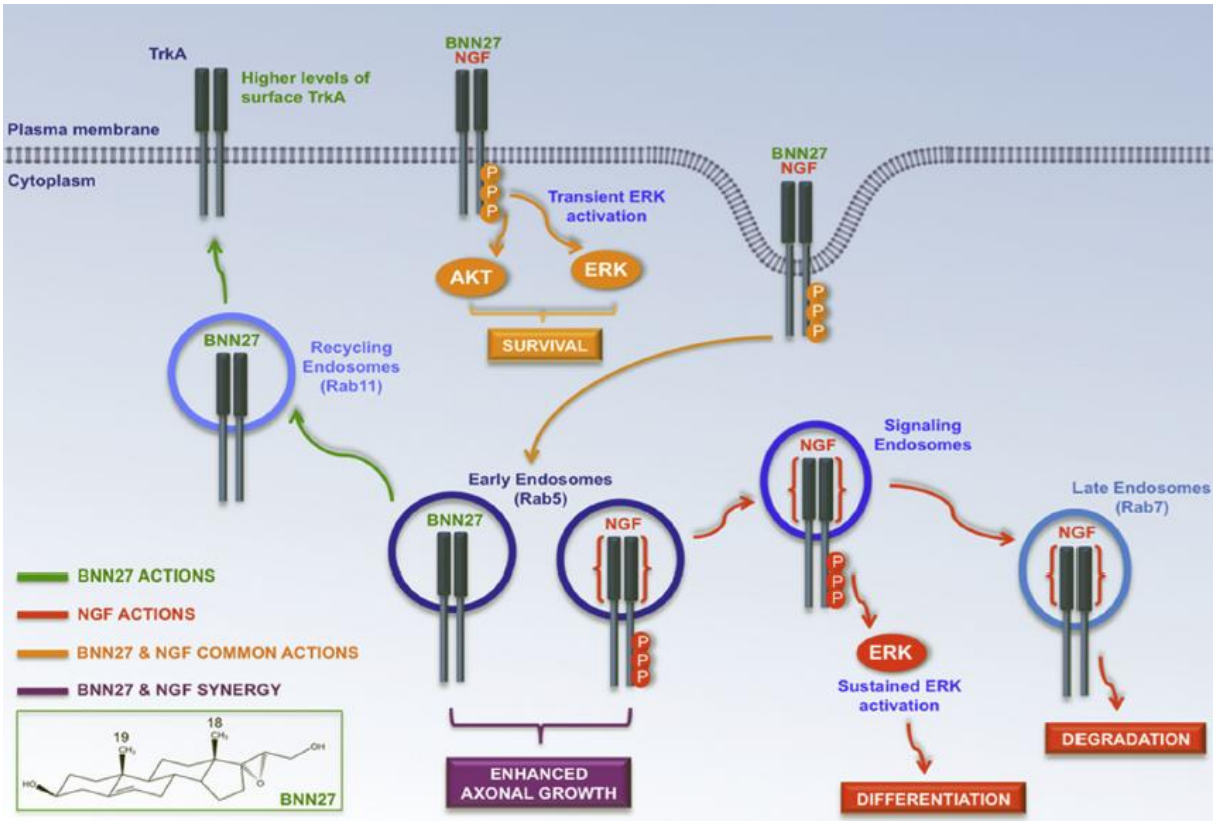

Figure 28. Schematic representation of the actions of BNN27 on TrkA receptor signaling and turnover. BNN27 specifically interacts with TrkA receptor at nanomolar concentrations and induces TrkA tyrosine phosphorylation, affecting downstream signaling of ERK and AKT in a different time pattern than that of NGF. BNN27 induces internalization and fast return of the receptor into the membrane through activation of Rab5 protein, docking the receptor in early/recycling endosomes. In contrast, NGF-activated TrkA receptors maintained their

signaling capacity and trafficking from early into late endosomes, ending in lysosomal degradation. BNN27 exerts strong anti-apoptotic, neuroprotective actions via NGF receptors and potentiates the effects of NGF in the induction of neurite elongation. Adapted from Pediaditakis et al. (Pediaditakis, Efstathopoulos et al. 2016).

A second open question is if BNN27 is able to induce OPC proliferation. It is known that NGF alone does not induce the proliferation of brain-derived OPCs (O-2A+ cells), but co-application of NGF and FGF-2 enhances FGF-2-mediated proliferation of O-2A progenitors (Cohen, Marmur et al. 1996). By contrast, solitary application of NGF supports the survival of differentiated cells and causes a robust and prolonged increase in the amount of phosphorylated MAPK (Cohen, Marmur et al. 1996). Because both OPCs and OLs express TrkA, the reasons for these differences are yet to be determined.

K. DISCUSSION II

The organization and maintenance of the domains that are encountered along mammalian myelinated fibers (i.e. nodes of Ranvier, paranodes and juxtaparanodes), depends on several molecular complexes that are restricted at these sites, found either on the axonal or glial membrane (Susuki and Rasband 2008, Zoupi, Savvaki et al. 2011). Although some of the cellular/molecular mechanisms underlying axoglial interactions in the node and paranode have been revealed in the last few years, the interactions and the molecular composition of juxtaparanodes have only started being deciphered.

TAG-1 is a GPI-anchored protein interacting with the transmembrane protein Caspr2 and the VGKCs expressed on the axon, forming a cluster in the juxtaparanodal area. Caspr2 has been identified as the transmembrane partner of axonal TAG-1 that links the complex to the axonal cytoskeleton (Poliak, Salomon et al. 2003, Traka, Goutebroze et al. 2003). The loss of either Caspr2 or TAG-1 causes juxtaparanodal disruption, while TAG-1 is considered to interact also homophilically with its counterpart found on the glial membrane (Poliak, Salomon et al. 2003, Traka, Goutebroze et al. 2003, Savvaki, Panagiotaropoulos et al. 2008). It has been shown that the exclusive expression of glial TAG-1 is sufficient to rescue the hypomyelination defect present in homozygous mutants (Savvaki, Theodorakis et al. 2010), suggesting that the glial TAG-1 plays an important role in myelination.

In this part of the study, we set out to identify novel partners of the TAG-1 protein. Taking advantage of a new computational tool, called UniReD, we not only identified known proteins interacting with TAG-1 (described in the biomedical literature), but also predicted new interactions not yet documented. Four putative TAG-1 interactors (MAP1B, MAP2, Reelin and TenascinR) were identified and we sought to use co-immunoprecipitation (co-IP) experiments to validate these presumptive interactions.

We want to emphasize that whereas direct protein/protein interactions are typically determined by techniques such as fluorescence resonance energy transfer (FRET), surface plasmon resonance, or pulldown assays with purified proteins, co-IP assay cannot discriminate between the direct and indirect interaction, therefore we cannot confirm that the interactions validated in our experiment are direct.

TAG-1 was found to interact with MAP1B, both in embryonic and adult mouse brain tissue. MAP1B is a protein that can induce cytoskeletal rearrangements by regulating actin and microtubule dynamics, and promote axonal growth, development, branching and regeneration (Kuo, Hong et al. 2009). Moreover, it plays an important role in axon guidance and neuronal migration (Meixner, Haverkamp et al. 2000). A variety of signaling molecules associated with axonal development and guidance, such as netrins (Del Rio, Gonzalez-Billault et al. 2004), Wnt (Ciani, Krylova et al. 2004), and signaling molecules associated with neuronal migration, such as Reelin (Gonzalez-Billault, Del Rio et al. 2005), modulate MAP1B function. Intriguingly, Reelin may promote CNS development through phosphorylation of MAP1B (Jimenez-Mateos, Paglini et al. 2005). Reelin induces disabled 1 phosphorylation through very low density

lipoprotein receptor and apolipoprotein receptor 2. Activated disabled 1 activates GSK3 and Cdk5, which synergistically increase levels of P1-MAP1B. The PI3K pathway regulates P1-MAP1B levels by inhibiting GSK3 activity to maintain microtubular instability and promote neuronal migration (Gonzalez-Billault, Del Rio et al. 2005).

MAP1B contains microtubule and actin binding domains: thus, it can regulate microtubule and actin stability (Cueille, Blanc et al. 2007). Neuronal cultures from MAP1B knockout mice exhibit delayed neuronal migration and suppressed neurite elongation, but microtubule extension into growth cones is increased (Jimenez-Mateos, Paglini et al. 2005). Inhibition of MAP1B phosphorylation increases the size of growth cones and leads to shortened and thickened axons (Goold, Owen et al. 1999). Overall, these results indicate that MAP1B can stabilize microtubules and induce the formation of microfilaments.

Kv1 channels, Caspr2 and Adam22 (another protein found at the juxtaparanodal region), have a PDZ domain binding motifs in their citoplasmatic domains that can interact with Psd93 and Psd95 (see Fig. 29). Hence, Caspr2/TAG-1, Kv1 channels, Adam 22, Psd93 and Psd95 may form a macromolecular protein complex (Rasband, Park et al. 2002, Ogawa, Oses-Prieto et al. 2010). The proteins 4.1B, αII spectrin and βII spectrin are also present in the juxtaparanodal domain in the axon (Ogawa, Schafer et al. 2006). Caspr2 has a 4.1B-binding site and may link the whole complex to the actin cytoskeleton through 4.1B and αII/ βII spectrin (Chang and Rasband 2013). Therefore, we hypothesize a possible indirect interaction between TAG-1, found in the aforementioned protein complex, and MAP1B, which direct interacts with the actin net found underneath the juxtaparanodal domain.

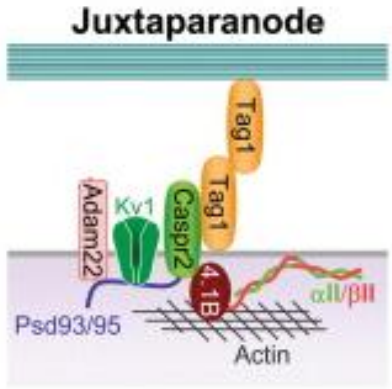

Figure 29. Molecular composition of the juxtaparanodal domain. This domain includes a cis complex of TAG-1 and Caspr2, which binds to TAG-1 on the glial membrane and interacts with 4.1B in the cytoplasm via a multidomain PDZ protein in the juxtaparanodes, which in turn is linked to Kv1.1 and 1.2 on the axon membrane. Juxtaparanodes are also enriched in Psd93, Psd95 and Adam22. Adapted from Chang & Rasband (Chang and Rasband 2013).

Our co-IP experiments also showed an interaction between TAG-1 and Reelin, a large secreted ECM that helps regulate processes of neuronal migration and positioning in the developing brain by controlling cell-cell interactions (Weeber, Beffert et al. 2002).

Two germinative zones of the telencephalon, the dorsal (pallial) and the ventral (subpallial) ventricular zones (VZ), provide new neurons to the cerebral cortex. Postmitotic cells from the dorsal VZ differentiate into excitatory projection neurons after a radial migration whereas the ventral part of the VZ generates neurons of the basal ganglia and cortical interneurons (Nery, Fishell et al. 2002). The cortical neurons, born early to form the preplate, are thought to function as a scaffold for the assembly of the cortical architecture (Landry, Pribyl et al. 1998). Other cortical neurons, born later, migrate radially and insert themselves into the preplate to generate the cortical plate (CP), which splits the preplate into the MZ and the subplate (SP) (Landry, Pribyl et al. 1998). Cajal–Retzius cells, which reside in the preplate and thereafter in the MZ, are considered to be the earliest neurons to differentiate in the developing neocortex (Landry, Pribyl et al. 1998). These cells secrete Reelin (Hevner, Neogi et al. 2003), which is crucial for cortical lamination (Rice and Curran 2001). Pioneer neurons are also preplate derived; they guide thalamocortical afferent axons into the cortex, and cortical efferent axons to their subcortical targets (Allendoerfer and Shatz 1994). It has been described a population of pioneer neurons in the MZ, that migrate tangentially to the MZ from subpallial sources in a Reelin-dependent way (Fairen, Morante-Oria et al. 2002). TAG-1, as well as the adhesion molecule L1, are reliable markers of such neurons. This pioneer neurons in the MZ are the cellular substrate of TAG-1 functions in regulating migrations. TAG-1 is present in cell body and processes of MZ cells before it is detected in descending axonal projections from that layer (Morante-Oria, Carleton et al. 2003) (see Fig. 30). In this context, it is interesting to notice an interaction between Reelin and TAG-1. This putative interaction may have nothing to do with the juxtaparanodal partners of TAG-1 but it may be important for its developmental function.

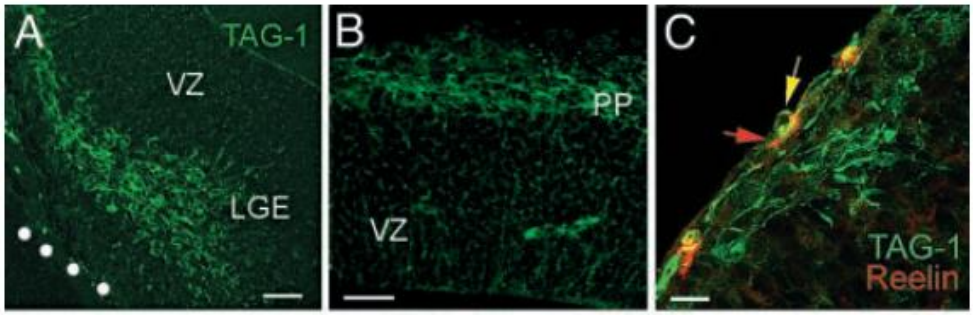

Figure 30. Immunohistochemical experiments supporting the subcortical origin of MZ pioneer neurons. (A) Cell bodies immunoreactive for TAG-1 populate the mantle of the LGE and form a continuum toward a putative pioneer migratory stream to the neocortex. (B) TAG-1-immunoreactive cell bodies in the neocortical PP. (C) TAG-1-immunoreactive cell bodies and dendrites (green) lie deep in the preplate, deeper than Reelin^{+} neurons (red). A red arrow points to a Reelin-immunoreactive cell in the MZ; in rare instances, Reelin and TAG-1 colocalize (yellow arrow). Adapted from Morante-Oria et al. (Morante-Oria, Carleton et al. 2003).

REFERENCES

Ackerman, S. D., C. Garcia, X. Piao, D. H. Gutmann and K. R. Monk (2015). "The adhesion GPCR Gpr56 regulates oligodendrocyte development via interactions with Galpha12/13 and RhoA." Nat Commun **6**: 6122.

Aggelakopoulou, M., E. Kourepini, N. Paschalidis, D. C. Simoes, D. Kalavrizioti, N. Dimisianos, P. Papathanasopoulos, A. Mouzaki and V. Panoutsakopoulou (2016). "ERbeta-Dependent Direct Suppression of Human and Murine Th17 Cells and Treatment of Established Central Nervous System Autoimmunity by a Neurosteroid." J Immunol **197**(7): 2598-2609.

Allendoerfer, K. L. and C. J. Shatz (1994). "The subplate, a transient neocortical structure: its role in the development of connections between thalamus and cortex." Annu Rev Neurosci **17**: 185-218.

Althaus, H. H., S. Kloppner, T. Schmidt-Schultz and P. Schwartz (1992). "Nerve growth factor induces proliferation and enhances fiber regeneration in oligodendrocytes isolated from adult pig brain." Neurosci Lett **135**(2): 219-223.

Amor, S., P. A. Smith, B. Hart and D. Baker (2005). "Biozzi mice: of mice and human neurological diseases." J Neuroimmunol **165**(1-2): 1-10.

Anastasia, A., P. A. Barker, M. V. Chao and B. L. Hempstead (2015). "Detection of p75NTR Trimers: Implications for Receptor Stoichiometry and Activation." J Neurosci **35**(34): 11911-11920.

Antony, J. M., G. van Marle, W. Opii, D. A. Butterfield, F. Mallet, V. W. Yong, J. L. Wallace, R. M. Deacon, K. Warren and C. Power (2004). "Human endogenous retrovirus glycoprotein-mediated induction of redox reactants causes oligodendrocyte death and demyelination." Nat Neurosci **7**(10): 1088-1095.

Arnett, H. A., J. Mason, M. Marino, K. Suzuki, G. K. Matsushima and J. P. Ting (2001). "TNF alpha promotes proliferation of oligodendrocyte progenitors and remyelination." Nat Neurosci **4**(11): 1116-1122.

Arnett, H. A., Y. Wang, G. K. Matsushima, K. Suzuki and J. P. Ting (2003). "Functional genomic analysis of remyelination reveals importance of inflammation in oligodendrocyte regeneration." J Neurosci **23**(30): 9824-9832.

Ayhan, S., N. Markal, K. Siemionow, B. Araneo and M. Siemionow (2003). "Effect of subepineurial dehydroepiandrosterone treatment on healing of transected nerves repaired with the epineurial sleeve technique." Microsurgery **23**(1): 49-55.

Bansal, R., M. Kumar, K. Murray, R. S. Morrison and S. E. Pfeiffer (1996). "Regulation of FGF receptors in the oligodendrocyte lineage." Mol Cell Neurosci **7**(4): 263-275.

Barateiro, A. and A. Fernandes (2014). "Temporal oligodendrocyte lineage progression: in vitro models of proliferation, differentiation and myelination." Biochim Biophys Acta **1843**(9): 1917-1929.

Barde, Y. A., D. Edgar and H. Thoenen (1982). "Purification of a new neurotrophic factor from mammalian brain." EMBO J **1**(5): 549-553.

Barnett, M. H. and J. W. Prineas (2004). "Relapsing and remitting multiple sclerosis: pathology of the newly forming lesion." Ann Neurol **55**(4): 458-468.

Barres, B. A. (2008). "The mystery and magic of glia: a perspective on their roles in health and disease." Neuron **60**(3): 430-440.

Bartsch, U., A. Faissner, J. Trotter, U. Dorries, S. Bartsch, H. Mohajeri and M. Schachner (1994). "Tenascin demarcates the boundary between the myelinated and nonmyelinated part of retinal ganglion cell axons in the developing and adult mouse." J Neurosci **14**(8): 4756-4768.

Baulieu, E. E. (1991). "Neurosteroids: a new function in the brain." Biol Cell **71**(1-2): 3-10.

Baulieu, E. E. (1999). "Neuroactive neurosteroids: dehydroepiandrosterone (DHEA) and DHEA sulphate." Acta Paediatr Suppl **88**(433): 78-80.

Baulieu, E. E. and P. Robel (1990). "Neurosteroids: a new brain function?" J Steroid Biochem Mol Biol **37**(3): 395-403.

Baulieu, E. E. and P. Robel (1998). "Dehydroepiandrosterone (DHEA) and dehydroepiandrosterone sulfate (DHEAS) as neuroactive neurosteroids." Proc Natl Acad Sci U S A **95**(8): 4089-4091.

Becker, C. G., J. Schweitzer, J. Feldner, M. Schachner and T. Becker (2004). "Tenascin-R as a repellent guidance molecule for newly growing and regenerating optic axons in adult zebrafish." Mol Cell Neurosci **26**(3): 376-389.

Becker, T., B. Anliker, C. G. Becker, J. Taylor, M. Schachner, R. L. Meyer and U. Bartsch (2000). "Tenascin-R inhibits regrowth of optic fibers in vitro and persists in the optic nerve of mice after injury." Glia **29**(4): 330-346.

Belelli, D., N. L. Harrison, J. Maguire, R. L. Macdonald, M. C. Walker and D. W. Cope (2009). "Extrasynaptic GABAA receptors: form, pharmacology, and function." J Neurosci **29**(41): 12757-12763.

Belelli, D. and J. J. Lambert (2005). "Neurosteroids: endogenous regulators of the GABA(A) receptor." Nat Rev Neurosci **6**(7): 565-575.

Benardais, K., A. Kotsiari, J. Skuljec, P. N. Koutsoudaki, V. Gudi, V. Singh, F. Vulinovic, T. Skripuletz and M. Stangel (2013). "Cuprizone [bis(cyclohexylidenehydrazide)] is selectively toxic for mature oligodendrocytes." Neurotox Res **24**(2): 244-250.

Bennett, J. P., Jr., L. C. O'Brien and D. G. Brohawn (2016). "Pharmacological properties of microneurotrophin drugs developed for treatment of amyotrophic lateral sclerosis." Biochem Pharmacol **117**: 68-77.

Berezin, V., P. S. Walmod, M. Filippov and A. Dityatev (2014). "Targeting of ECM molecules and their metabolizing enzymes and receptors for the treatment of CNS diseases." Prog Brain Res **214**: 353-388.

Blakemore, W. F. and R. J. Franklin (2008). "Remyelination in experimental models of toxin-induced demyelination." Curr Top Microbiol Immunol **318**: 193-212.

Blasi, E., R. Barluzzi, V. Bocchini, R. Mazzolla and F. Bistoni (1990). "Immortalization of murine microglial cells by a v-raf/v-myc carrying retrovirus." J Neuroimmunol **27**(2-3): 229-237.

Block, M. L., L. Zecca and J. S. Hong (2007). "Microglia-mediated neurotoxicity: uncovering the molecular mechanisms." Nat Rev Neurosci **8**(1): 57-69.

Bogler, O., D. Wren, S. C. Barnett, H. Land and M. Noble (1990). "Cooperation between two growth factors promotes extended self-renewal and inhibits differentiation of oligodendrocyte-type-2 astrocyte (O-2A) progenitor cells." Proc Natl Acad Sci U S A **87**(16): 6368-6372.

Brenneke, F., O. Bukalo, A. Dityatev and A. A. Lie (2004). "Mice deficient for the extracellular matrix glycoprotein tenascin-r show physiological and structural hallmarks of increased hippocampal excitability, but no increased susceptibility to seizures in the pilocarpine model of epilepsy." Neuroscience **124**(4): 841-855.

Brinkmann, B. G., A. Agarwal, M. W. Sereda, A. N. Garratt, T. Muller, H. Wende, R. M. Stassart, S. Nawaz, C. Humml, V. Velanac, K. Radyushkin, S. Goebbels, T. M. Fischer, R. J. Franklin, C. Lai, H. Ehrenreich, C. Birchmeier, M. H. Schwab and K. A. Nave (2008). "Neuregulin-1/ErbB signaling serves distinct functions in myelination of the peripheral and central nervous system." Neuron **59**(4): 581-595.

Bruck, W., R. Pfortner, T. Pham, J. Zhang, L. Hayardeny, V. Piryatinsky, U. K. Hanisch, T. Regen, D. van Rossum, L. Brakelmann, K. Hagemeier, T. Kuhlmann, C. Stadelmann, G. R. John, N. Kramann and C. Wegner (2012). "Reduced astrocytic NF-kappaB activation by laquinimod protects from cuprizone-induced demyelination." Acta Neuropathol **124**(3): 411-424.

Burgering, B. M. and P. J. Coffer (1995). "Protein kinase B (c-Akt) in phosphatidylinositol-3-OH kinase signal transduction." Nature **376**(6541): 599-602.

Cai, J., Y. Qi, X. Hu, M. Tan, Z. Liu, J. Zhang, Q. Li, M. Sander and M. Qiu (2005). "Generation of oligodendrocyte precursor cells from mouse dorsal spinal cord independent of Nkx6 regulation and Shh signaling." Neuron **45**(1): 41-53.

Calogeropoulou, T., N. Avlonitis, V. Minas, X. Alexi, A. Pantzou, I. Charalampopoulos, M. Zervou, V. Vergou, E. S. Katsanou, I. Lazaridis, M. N. Alexis and A. Gravanis (2009). "Novel dehydroepiandrosterone derivatives with antiapoptotic, neuroprotective activity." J Med Chem **52**(21): 6569-6587.

Carlton, W. W. (1967). "Studies on the induction of hydrocephalus and spongy degeneration by cuprizone feeding and attempts to antidote the toxicity." Life Sci **6**(1): 11-19.

Casaccia-Bonnefil, P., B. D. Carter, R. T. Dobrowsky and M. V. Chao (1996). "Death of oligodendrocytes mediated by the interaction of nerve growth factor with its receptor p75." Nature **383**(6602): 716-719.

Chan, J. R., J. M. Cosgaya, Y. J. Wu and E. M. Shooter (2001). "Neurotrophins are key mediators of the myelination program in the peripheral nervous system." Proc Natl Acad Sci U S A **98**(25): 14661-14668.

Chang, K. J. and M. N. Rasband (2013). "Excitable domains of myelinated nerves: axon initial segments and nodes of Ranvier." Curr Top Membr **72**: 159-192.

Chao, M. V. (2003). "Neurotrophins and their receptors: a convergence point for many signalling pathways." Nat Rev Neurosci **4**(4): 299-309.

Chao, M. V., R. Rajagopal and F. S. Lee (2006). "Neurotrophin signalling in health and disease." Clin Sci (Lond) **110**(2): 167-173.

Charalampopoulos, I., V. I. Alexaki, C. Tsatsanis, V. Minas, E. Dermitzaki, I. Lasaridis, L. Vardouli, C. Stournaras, A. N. Margioris, E. Castanas and A. Gravanis (2006). "Neurosteroids as endogenous inhibitors of neuronal cell apoptosis in aging." Ann N Y Acad Sci **1088**: 139-152.

Charalampopoulos, I., A. N. Margioris and A. Gravanis (2008). "Neurosteroid dehydroepiandrosterone exerts anti-apoptotic effects by membrane-mediated, integrated genomic and non-genomic pro-survival signaling pathways." J Neurochem **107**(5): 1457-1469.

Charalampopoulos, I., C. Tsatsanis, E. Dermitzaki, V. I. Alexaki, E. Castanas, A. N. Margioris and A. Gravanis (2004). "Dehydroepiandrosterone and allopregnanolone protect sympathoadrenal medulla cells against apoptosis via antiapoptotic Bcl-2 proteins." Proc Natl Acad Sci U S A **101**(21): 8209-8214.

Chen, J. Y., J. R. Lin, K. A. Cimprich and T. Meyer (2012). "A two-dimensional ERK-AKT signaling code for an NGF-triggered cell-fate decision." Mol Cell **45**(2): 196-209.

Chiquet-Ehrismann, R. and R. P. Tucker (2011). "Tenascins and the importance of adhesion modulation." Cold Spring Harb Perspect Biol **3**(5).

Ciani, L., O. Krylova, M. J. Smalley, T. C. Dale and P. C. Salinas (2004). "A divergent canonical WNT-signaling pathway regulates microtubule dynamics: dishevelled signals locally to stabilize microtubules." J Cell Biol **164**(2): 243-253.

Ciccarelli, O., F. Barkhof, B. Bodini, N. De Stefano, X. Golay, K. Nicolay, D. Pelletier, P. J. Pouwels, S. A. Smith, C. A. Wheeler-Kingshott, B. Stankoff, T. Yousry and D. H. Miller (2014). "Pathogenesis of multiple sclerosis: insights from molecular and metabolic imaging." Lancet Neurol **13**(8): 807-822.

Clarke, L. E., K. M. Young, N. B. Hamilton, H. Li, W. D. Richardson and D. Attwell (2012). "Properties and fate of oligodendrocyte progenitor cells in the corpus callosum, motor cortex, and piriform cortex of the mouse." J Neurosci **32**(24): 8173-8185.

Clary, D. O. and L. F. Reichardt (1994). "An alternatively spliced form of the nerve growth factor receptor TrkA confers an enhanced response to neurotrophin 3." Proc Natl Acad Sci U S A **91**(23): 11133-11137.

Coggan, J. S., S. Bittner, K. M. Stiefel, S. G. Meuth and S. A. Prescott (2015). "Physiological Dynamics in Demyelinating Diseases: Unraveling Complex Relationships through Computer Modeling." Int J Mol Sci **16**(9): 21215-21236.

Cohen, J. A. (2009). "Emerging therapies for relapsing multiple sclerosis." Arch Neurol **66**(7): 821-828.

Cohen, R. I., R. Marmur, W. T. Norton, M. F. Mehler and J. A. Kessler (1996). "Nerve growth factor and neurotrophin-3 differentially regulate the proliferation and survival of developing rat brain oligodendrocytes." J Neurosci **16**(20): 6433-6442.

Collins, J. A., C. A. Schandi, K. K. Young, J. Vesely and M. C. Willingham (1997). "Major DNA fragmentation is a late event in apoptosis." J Histochem Cytochem **45**(7): 923-934.

Colombo, F., G. Racchetti and J. Meldolesi (2014). "Neurite outgrowth induced by NGF or L1CAM via activation of the TrkA receptor is sustained also by the exocytosis of enlargeosomes." Proc Natl Acad Sci U S A **111**(47): 16943-16948.

Compagnone, N. A. and S. H. Mellon (2000). "Neurosteroids: biosynthesis and function of these novel neuromodulators." Front Neuroendocrinol **21**(1): 1-56.

Corley, S. M., U. Ladiwala, A. Besson and V. W. Yong (2001). "Astrocytes attenuate oligodendrocyte death in vitro through an alpha(6) integrin-laminin-dependent mechanism." Glia **36**(3): 281-294.

Corpechot, C., P. Robel, M. Axelson, J. Sjovall and E. E. Baulieu (1981). "Characterization and measurement of dehydroepiandrosterone sulfate in rat brain." Proc Natl Acad Sci U S A **78**(8): 4704-4707.

Crang, A. J., R. J. Franklin, W. F. Blakemore, J. Trotter, M. Schachner, S. C. Barnett and M. Noble (1991). "Transplantation of normal and genetically engineered glia into areas of demyelination." Ann N Y Acad Sci **633**: 563-565.

Cueille, N., C. T. Blanc, S. Popa-Nita, S. Kasas, S. Catsicas, G. Dietler and B. M. Riederer (2007). "Characterization of MAP1B heavy chain interaction with actin." Brain Res Bull **71**(6): 610-618.

D'Amico, E., F. Patti, A. Zanghi and M. Zappia (2016). "A Personalized Approach in Progressive Multiple Sclerosis: The Current Status of Disease Modifying Therapies (DMTs) and Future Perspectives." Int J Mol Sci **17**(10).

de Bergeyck, V., B. Naerhuyzen, A. M. Goffinet and C. Lambert de Rouvroit (1998). "A panel of monoclonal antibodies against reelin, the extracellular matrix protein defective in reeler mutant mice." J Neurosci Methods **82**(1): 17-24.

Del Rio, J. A., C. Gonzalez-Billault, J. M. Urena, E. M. Jimenez, M. J. Barallobre, M. Pascual, L. Pujadas, S. Simo, A. La Torre, F. Wandosell, J. Avila and E. Soriano (2004). "MAP1B is required for Netrin 1 signaling in neuronal migration and axonal guidance." Curr Biol **14**(10): 840-850.

Derfuss, T., K. Parikh, S. Velhin, M. Braun, E. Mathey, M. Krumbholz, T. Kumpfel, A. Moldenhauer, C. Rader, P. Sonderegger, W. Pollmann, C. Tiefenthaller, J. Bauer, H. Lassmann, H. Wekerle, D. Karagogeos, R. Hohlfeld, C. Linington and E. Meinl (2009). "Contactin-2/TAG-1-directed autoimmunity is identified in multiple sclerosis patients and mediates gray matter pathology in animals." Proc Natl Acad Sci U S A **106**(20): 8302-8307.

DeSilva, U., G. D'Arcangelo, V. V. Braden, J. Chen, G. G. Miao, T. Curran and E. D. Green (1997). "The human reelin gene: isolation, sequencing, and mapping on chromosome 7." Genome Res **7**(2): 157-164.

Dityatev, A. and M. Schachner (2003). "Extracellular matrix molecules and synaptic plasticity." Nat Rev Neurosci **4**(6): 456-468.

Du, C., M. W. Khalil and S. Sriram (2001). "Administration of dehydroepiandrosterone suppresses experimental allergic encephalomyelitis in SJL/J mice." J Immunol **167**(12): 7094-7101.

Du, J., L. Feng, F. Yang and B. Lu (2000). "Activity- and Ca(2+)-dependent modulation of surface expression of brain-derived neurotrophic factor receptors in hippocampal neurons." J Cell Biol **150**(6): 1423-1434.

Du, J., L. Feng, E. Zaitsev, H. S. Je, X. W. Liu and B. Lu (2003). "Regulation of TrkB receptor tyrosine kinase and its internalization by neuronal activity and Ca2+ influx." J Cell Biol **163**(2): 385-395.

Edgar, J. M., M. McLaughlin, D. Yool, S. C. Zhang, J. H. Fowler, P. Montague, J. A. Barrie, M. C. McCulloch, I. D. Duncan, J. Garbern, K. A. Nave and I. R. Griffiths (2004). "Oligodendroglial modulation of fast axonal transport in a mouse model of hereditary spastic paraplegia." J Cell Biol **166**(1): 121-131.

Ehrhard, P. B., P. Erb, U. Graumann and U. Otten (1993). "Expression of nerve growth factor and nerve growth factor receptor tyrosine kinase Trk in activated CD4-positive T-cell clones." Proc Natl Acad Sci U S A **90**(23): 10984-10988.

Eide, F. F., E. R. Vining, B. L. Eide, K. Zang, X. Y. Wang and L. F. Reichardt (1996). "Naturally occurring truncated trkB receptors have dominant inhibitory effects on brain-derived neurotrophic factor signaling." J Neurosci **16**(10): 3123-3129.

Einheber, S., G. Zanazzi, W. Ching, S. Scherer, T. A. Milner, E. Peles and J. L. Salzer (1997). "The axonal membrane protein Caspr, a homologue of neurexin IV, is a component of the septate-like paranodal junctions that assemble during myelination." J Cell Biol **139**(6): 1495-1506.

El-Etr, M., M. Rame, C. Boucher, A. M. Ghoumari, N. Kumar, P. Liere, A. Pianos, M. Schumacher and R. Sitruk-Ware (2015). "Progesterone and nestorone promote myelin regeneration in chronic demyelinating lesions of corpus callosum and cerebral cortex." Glia **63**(1): 104-117.

Fairen, A., J. Morante-Oria and C. Frassoni (2002). "The surface of the developing cerebral cortex: still special cells one century later." Prog Brain Res **136**: 281-291.

Faivre-Sarrailh, C. and J. J. Devaux (2013). "Neuro-glial interactions at the nodes of Ranvier: implication in health and diseases." Front Cell Neurosci **7**: 196.

Farrer, R. G. and R. H. Quarles (1999). "GT3 and its O-acetylated derivative are the principal A2B5-reactive gangliosides in cultured O2A lineage cells and are down-regulated along with O-acetyl GD3 during differentiation to oligodendrocytes." J Neurosci Res **57**(3): 371-380.

Forster, E., H. H. Bock, J. Herz, X. Chai, M. Frotscher and S. Zhao (2010). "Emerging topics in Reelin function." Eur J Neurosci **31**(9): 1511-1518.

Frade, J. M. and Y. A. Barde (1998). "Microglia-derived nerve growth factor causes cell death in the developing retina." Neuron **20**(1): 35-41.

Frade, J. M. and Y. A. Barde (1999). "Genetic evidence for cell death mediated by nerve growth factor and the neurotrophin receptor p75 in the developing mouse retina and spinal cord." Development **126**(4): 683-690.

Franklin, R. J., A. J. Crang and W. F. Blakemore (1991). "Transplanted type-1 astrocytes facilitate repair of demyelinating lesions by host oligodendrocytes in adult rat spinal cord." J Neurocytol **20**(5): 420-430.

Franklin, R. J. and V. Gallo (2014). "The translational biology of remyelination: past, present, and future." Glia **62**(11): 1905-1915.

Franklin, R. J. and S. A. Goldman (2015). "Glia Disease and Repair-Remyelination." Cold Spring Harb Perspect Biol **7**(7): a020594.

Gago, N., M. El-Etr, N. Sananes, F. Cadepond, D. Samuel, V. Avellana-Adalid, A. Baron-Van Evercooren and M. Schumacher (2004). "3alpha,5alpha-Tetrahydroprogesterone (allopregnanolone) and gamma-aminobutyric acid: autocrine/paracrine interactions in the control of neonatal PSA-NCAM+ progenitor proliferation." J Neurosci Res **78**(6): 770-783.

Garay, L., M. C. Gonzalez Deniselle, A. Lima, P. Roig and A. F. De Nicola (2007). "Effects of progesterone in the spinal cord of a mouse model of multiple sclerosis." J Steroid Biochem Mol Biol **107**(3-5): 228-237.

Gard, A. L., M. R. Burrell, S. E. Pfeiffer, J. S. Rudge and W. C. Williams, 2nd (1995). "Astroglial control of oligodendrocyte survival mediated by PDGF and leukemia inhibitory factor-like protein." Development **121**(7): 2187-2197.

Ghoumari, A. M., C. Ibanez, M. El-Etr, P. Leclerc, B. Eychenne, B. W. O'Malley, E. E. Baulieu and M. Schumacher (2003). "Progesterone and its metabolites increase myelin basic protein expression in organotypic slice cultures of rat cerebellum." J Neurochem **86**(4): 848-859.

Giatti, S., D. Caruso, M. Boraso, F. Abbiati, E. Ballarini, D. Calabrese, M. Pesaresi, R. Rigolio, M. Santos-Galindo, B. Viviani, G. Cavaletti, L. M. Garcia-Segura and R. C. Melcangi (2012). "Neuroprotective effects of progesterone in chronic experimental autoimmune encephalomyelitis." J Neuroendocrinol **24**(6): 851-861.

Gibon, J., S. M. Buckley, N. Unsain, V. Kaartinen, P. Seguela and P. A. Barker (2015). "proBDNF and p75NTR Control Excitability and Persistent Firing of Cortical Pyramidal Neurons." J Neurosci **35**(26): 9741-9753.

Glajch, K. E., L. Ferraiuolo, K. A. Mueller, M. J. Stopford, V. Prabhkar, A. Gravanis, P. J. Shaw and G. Sadri-Vakili (2016). "MicroNeurotrophins Improve Survival in Motor Neuron-Astrocyte Co-Cultures but Do Not Improve Disease Phenotypes in a Mutant SOD1 Mouse Model of Amyotrophic Lateral Sclerosis." PLoS One **11**(10): e0164103.

Gonzalez-Billault, C., J. A. Del Rio, J. M. Urena, E. M. Jimenez-Mateos, M. J. Barallobre, M. Pascual, L. Pujadas, S. Simo, A. L. Torre, R. Gavin, F. Wandosell, E. Soriano and J. Avila (2005). "A role of MAP1B in Reelin-dependent neuronal migration." Cereb Cortex **15**(8): 1134-1145.

Goold, R. G., R. Owen and P. R. Gordon-Weeks (1999). "Glycogen synthase kinase 3beta phosphorylation of microtubule-associated protein 1B regulates the stability of microtubules in growth cones." J Cell Sci **112 (Pt 19)**: 3373-3384.

Greene, L. A. and D. R. Kaplan (1995). "Early events in neurotrophin signalling via Trk and p75 receptors." Curr Opin Neurobiol **5**(5): 579-587.

Gudemez, E., K. Ozer, B. Cunningham, K. Siemionow, E. Browne and M. Siemionow (2002). "Dehydroepiandrosterone as an enhancer of functional recovery following crush injury to rat sciatic nerve." Microsurgery **22**(6): 234-241.

Gudi, V., S. Gingele, T. Skripuletz and M. Stangel (2014). "Glial response during cuprizone-induced de- and remyelination in the CNS: lessons learned." Front Cell Neurosci **8**: 73.

Guo, W., Y. Ji, S. Wang, Y. Sun and B. Lu (2014). "Neuronal activity alters BDNF-TrkB signaling kinetics and downstream functions." J Cell Sci **127**(Pt 10): 2249-2260.

Hall, S. M. (1972). "The effect of injections of lysophosphatidyl choline into white matter of the adult mouse spinal cord." J Cell Sci **10**(2): 535-546.

Hallbook, F. (1999). "Evolution of the vertebrate neurotrophin and Trk receptor gene families." Curr Opin Neurobiol **9**(5): 616-621.

Hamilton, S. P. and L. H. Rome (1994). "Stimulation of in vitro myelin synthesis by microglia." Glia **11**(4): 326-335.

Hanisch, U. K. and H. Kettenmann (2007). "Microglia: active sensor and versatile effector cells in the normal and pathologic brain." Nat Neurosci **10**(11): 1387-1394.

Hartline, D. K. and D. R. Colman (2007). "Rapid conduction and the evolution of giant axons and myelinated fibers." Curr Biol **17**(1): R29-35.

Havelock, J. C., R. J. Auchus and W. E. Rainey (2004). "The rise in adrenal androgen biosynthesis: adrenarche." Semin Reprod Med **22**(4): 337-347.

He, X. L. and K. C. Garcia (2004). "Structure of nerve growth factor complexed with the shared neurotrophin receptor p75." Science **304**(5672): 870-875.

Heese, K., B. L. Fiebich, J. Bauer and U. Otten (1998). "NF-kappaB modulates lipopolysaccharide-induced microglial nerve growth factor expression." Glia **22**(4): 401-407.

Henderson, A. P., M. H. Barnett, J. D. Parratt and J. W. Prineas (2009). "Multiple sclerosis: distribution of inflammatory cells in newly forming lesions." Ann Neurol **66**(6): 739-753.

Henn, A., S. Lund, M. Hedtjarn, A. Schrattenholz, P. Porzgen and M. Leist (2009). "The suitability of BV2 cells as alternative model system for primary microglia cultures or for animal experiments examining brain inflammation." ALTEX **26**(2): 83-94.

Herculano-Houzel, S. (2014). "The glia/neuron ratio: how it varies uniformly across brain structures and species and what that means for brain physiology and evolution." Glia **62**(9): 1377-1391.

Hernandez, M. and P. Casaccia (2015). "Interplay between transcriptional control and chromatin regulation in the oligodendrocyte lineage." Glia **63**(8): 1357-1375.

Hesp, Z. C., E. Z. Goldstein, C. J. Miranda, B. K. Kaspar and D. M. McTigue (2015). "Chronic oligodendrogenesis and remyelination after spinal cord injury in mice and rats." J Neurosci **35**(3): 1274-1290.

Hevner, R. F., T. Neogi, C. Englund, R. A. Daza and A. Fink (2003). "Cajal-Retzius cells in the mouse: transcription factors, neurotransmitters, and birthdays suggest a pallial origin." Brain Res Dev Brain Res **141**(1-2): 39-53.

Hiremath, M. M., Y. Saito, G. W. Knapp, J. P. Ting, K. Suzuki and G. K. Matsushima (1998). "Microglial/macrophage accumulation during cuprizone-induced demyelination in C57BL/6 mice." J Neuroimmunol **92**(1-2): 38-49.

Huang, E. J. and L. F. Reichardt (2003). "Trk receptors: roles in neuronal signal transduction." Annu Rev Biochem **72**: 609-642.

Hughes, E. G., S. H. Kang, M. Fukaya and D. E. Bergles (2013). "Oligodendrocyte progenitors balance growth with self-repulsion to achieve homeostasis in the adult brain." Nat Neurosci **16**(6): 668-676.

Jessen, K. R. and R. Mirsky (2005). "The origin and development of glial cells in peripheral nerves." Nat Rev Neurosci **6**(9): 671-682.

Jimenez-Mateos, E. M., G. Paglini, C. Gonzalez-Billault, A. Caceres and J. Avila (2005). "End binding protein-1 (EB1) complements microtubule-associated protein-1B during axonogenesis." J Neurosci Res **80**(3): 350-359.

Jing, S., P. Tapley and M. Barbacid (1992). "Nerve growth factor mediates signal transduction through trk homodimer receptors." Neuron **9**(6): 1067-1079.

Joo, W., S. Hippenmeyer and L. Luo (2014). "Neurodevelopment. Dendrite morphogenesis depends on relative levels of NT-3/TrkC signaling." Science **346**(6209): 626-629.

Jossin, Y., N. Ignatova, T. Hiesberger, J. Herz, C. Lambert de Rouvroit and A. M. Goffinet (2004). "The central fragment of Reelin, generated by proteolytic processing in vivo, is critical to its function during cortical plate development." J Neurosci **24**(2): 514-521.

Jossin, Y., M. Ogawa, C. Metin, F. Tissir and A. M. Goffinet (2003). "Inhibition of SRC family kinases and non-classical protein kinases C induce a reeler-like malformation of cortical plate development." J Neurosci **23**(30): 9953-9959.

Jurevics, H., C. Largent, J. Hostettler, D. W. Sammond, G. K. Matsushima, A. Kleindienst, A. D. Toews and P. Morell (2002). "Alterations in metabolism and gene expression in brain regions during cuprizone-induced demyelination and remyelination." J Neurochem **82**(1): 126-136.

Kalman, B., K. Laitinen and S. Komoly (2007). "The involvement of mitochondria in the pathogenesis of multiple sclerosis." J Neuroimmunol **188**(1-2): 1-12.

Kang, Z., L. Liu, R. Spangler, C. Spear, C. Wang, M. F. Gulen, M. Veenstra, W. Ouyang, R. M. Ransohoff and X. Li (2012). "IL-17-induced Act1-mediated signaling is critical for cuprizone-induced demyelination." J Neurosci **32**(24): 8284-8292.

Kawakami, N., S. Lassmann, Z. Li, F. Odoardi, T. Ritter, T. Ziemssen, W. E. Klinkert, J. W. Ellwart, M. Bradl, K. Krivacic, H. Lassmann, R. M. Ransohoff, H. D. Volk, H. Wekerle, C. Linington and A. Flugel (2004). "The activation status of neuroantigen-specific T cells in the target organ determines the clinical outcome of autoimmune encephalomyelitis." J Exp Med **199**(2): 185-197.

Kessaris, N., M. Fogarty, P. Iannarelli, M. Grist, M. Wegner and W. D. Richardson (2006). "Competing waves of oligodendrocytes in the forebrain and postnatal elimination of an embryonic lineage." Nat Neurosci **9**(2): 173-179.

Kessaris, N., N. Pringle and W. D. Richardson (2008). "Specification of CNS glia from neural stem cells in the embryonic neuroepithelium." Philos Trans R Soc Lond B Biol Sci **363**(1489): 71-85.

Kipp, M., T. Clarner, J. Dang, S. Copray and C. Beyer (2009). "The cuprizone animal model: new insights into an old story." Acta Neuropathol **118**(6): 723-736.

Knapp, P. E., W. P. Bartlett and R. P. Skoff (1987). "Cultured oligodendrocytes mimic in vivo phenotypic characteristics: cell shape, expression of myelin-specific antigens, and membrane production." Dev Biol **120**(2): 356-365.

Koenig, H. L., M. Schumacher, B. Ferzaz, A. N. Thi, A. Ressouches, R. Guennoun, I. Jung-Testas, P. Robel, Y. Akwa and E. E. Baulieu (1995). "Progesterone synthesis and myelin formation by Schwann cells." Science **268**(5216): 1500-1503.

Kohno, T., Y. Nakano, N. Kitoh, H. Yagi, K. Kato, A. Baba and M. Hattori (2009). "C-terminal region-dependent change of antibody-binding to the Eighth Reelin repeat reflects the signaling activity of Reelin." J Neurosci Res **87**(14): 3043-3053.

Komoly, S. (2005). "Experimental demyelination caused by primary oligodendrocyte dystrophy. Regional distribution of the lesions in the nervous system of mice [corrected]." Ideggyogy Sz **58**(1-2): 40-43.

Kotter, M. R., W. W. Li, C. Zhao and R. J. Franklin (2006). "Myelin impairs CNS remyelination by inhibiting oligodendrocyte precursor cell differentiation." J Neurosci **26**(1): 328-332.

Kumar, S., J. C. Biancotti, M. Yamaguchi and J. de Vellis (2007). "Combination of growth factors enhances remyelination in a cuprizone-induced demyelination mouse model." Neurochem Res **32**(4-5): 783-797.

Kuno, R., Y. Yoshida, A. Nitta, T. Nabeshima, J. Wang, Y. Sonobe, J. Kawanokuchi, H. Takeuchi, T. Mizuno and A. Suzumura (2006). "The role of TNF-alpha and its receptors in the production of NGF and GDNF by astrocytes." Brain Res **1116**(1): 12-18.

Kuo, T. Y., C. J. Hong and Y. P. Hsueh (2009). "Bcl11A/CTIP1 regulates expression of DCC and MAP1b in control of axon branching and dendrite outgrowth." Mol Cell Neurosci **42**(3): 195-207.

Labombarda, F., A. M. Ghoumari, P. Liere, A. F. De Nicola, M. Schumacher and R. Guennoun (2013). "Neuroprotection by steroids after neurotrauma in organotypic spinal cord cultures: a key role for progesterone receptors and steroidal modulators of GABA(A) receptors." Neuropharmacology **71**: 46-55.

Ladiwala, U., C. Lachance, S. J. Simoneau, A. Bhakar, P. A. Barker and J. P. Antel (1998). "p75 neurotrophin receptor expression on adult human oligodendrocytes: signaling without cell death in response to NGF." J Neurosci **18**(4): 1297-1304.

Landry, C. F., T. M. Pribyl, J. A. Ellison, M. I. Givogri, K. Kampf, C. W. Campagnoni and A. T. Campagnoni (1998). "Embryonic expression of the myelin basic protein gene: identification of a promoter region that targets transgene expression to pioneer neurons." J Neurosci **18**(18): 7315-7327.

Lappe-Siefke, C., S. Goebbels, M. Gravel, E. Nicksch, J. Lee, P. E. Braun, I. R. Griffiths and K. A. Nave (2003). "Disruption of Cnp1 uncouples oligodendroglial functions in axonal support and myelination." Nat Genet **33**(3): 366-374.

Lassmann, H. (1998). "Neuropathology in multiple sclerosis: new concepts." Mult Scler **4**(3): 93-98.

Laudiero, L. B., L. Aloe, R. Levi-Montalcini, C. Buttinelli, D. Schilter, S. Gillessen and U. Otten (1992). "Multiple sclerosis patients express increased levels of beta-nerve growth factor in cerebrospinal fluid." Neurosci Lett **147**(1): 9-12.

Lazaridis, I., I. Charalampopoulos, V. I. Alexaki, N. Avlonitis, I. Pediaditakis, P. Efstathopoulos, T. Calogeropoulou, E. Castanas and A. Gravanis (2011). "Neurosteroid dehydroepiandrosterone interacts with nerve growth factor (NGF) receptors, preventing neuronal apoptosis." PLoS Biol **9**(4): e1001051.

Le Moan, N., D. M. Houslay, F. Christian, M. D. Houslay and K. Akassoglou (2011). "Oxygen-dependent cleavage of the p75 neurotrophin receptor triggers stabilization of HIF-1alpha." Mol Cell **44**(3): 476-490.

Lee, G. H. and G. D'Arcangelo (2016). "New Insights into Reelin-Mediated Signaling Pathways." Front Cell Neurosci **10**: 122.

Lee, J. K. and B. Zheng (2012). "Role of myelin-associated inhibitors in axonal repair after spinal cord injury." Exp Neurol **235**(1): 33-42.

Lee, K. F., E. Li, L. J. Huber, S. C. Landis, A. H. Sharpe, M. V. Chao and R. Jaenisch (1992). "Targeted mutation of the gene encoding the low affinity NGF receptor p75 leads to deficits in the peripheral sensory nervous system." Cell **69**(5): 737-749.

Lee, R., P. Kermani, K. K. Teng and B. L. Hempstead (2001). "Regulation of cell survival by secreted proneurotrophins." Science **294**(5548): 1945-1948.

Lee, S., M. K. Leach, S. A. Redmond, S. Y. Chong, S. H. Mellon, S. J. Tuck, Z. Q. Feng, J. M. Corey and J. R. Chan (2012). "A culture system to study oligodendrocyte myelination processes using engineered nanofibers." Nat Methods **9**(9): 917-922.

Leon, A., A. Buriani, R. Dal Toso, M. Fabris, S. Romanello, L. Aloe and R. Levi-Montalcini (1994). "Mast cells synthesize, store, and release nerve growth factor." Proc Natl Acad Sci U S A **91**(9): 3739-3743.

Levi-Montalcini, R. (1987). "The nerve growth factor 35 years later." Science **237**(4819): 1154-1162.

Levine, J. M., R. Reynolds and J. W. Fawcett (2001). "The oligodendrocyte precursor cell in health and disease." Trends Neurosci **24**(1): 39-47.

Levine, J. M., F. Stincone and Y. S. Lee (1993). "Development and differentiation of glial precursor cells in the rat cerebellum." Glia **7**(4): 307-321.

Levison, S. W. and J. E. Goldman (1993). "Both oligodendrocytes and astrocytes develop from progenitors in the subventricular zone of postnatal rat forebrain." Neuron **10**(2): 201-212.

Li, J., E. R. Ramenaden, J. Peng, H. Koito, J. J. Volpe and P. A. Rosenberg (2008). "Tumor necrosis factor alpha mediates lipopolysaccharide-induced microglial toxicity to developing oligodendrocytes when astrocytes are present." J Neurosci **28**(20): 5321-5330.

Liao, H., W. Y. Bu, T. H. Wang, S. Ahmed and Z. C. Xiao (2005). "Tenascin-R plays a role in neuroprotection via its distinct domains that coordinate to modulate the microglia function." J Biol Chem **280**(9): 8316-8323.

Lieberman, S. (1995). "An abbreviated account of some aspects of the biochemistry of DHEA, 1934-1995." Ann N Y Acad Sci **774**: 1-15.

Lindner, M., J. Fokuhl, F. Linsmeier, C. Trebst and M. Stangel (2009). "Chronic toxic demyelination in the central nervous system leads to axonal damage despite remyelination." Neurosci Lett **453**(2): 120-125.

Lindner, M., S. Heine, K. Haastert, N. Garde, J. Fokuhl, F. Linsmeier, C. Grothe, W. Baumgartner and M. Stangel (2008). "Sequential myelin protein expression during remyelination reveals fast and efficient repair after central nervous system demyelination." Neuropathol Appl Neurobiol **34**(1): 105-114.

Longo, F. M. and S. M. Massa (2013). "Small-molecule modulation of neurotrophin receptors: a strategy for the treatment of neurological disease." Nat Rev Drug Discov **12**(7): 507-525.

Lubetzki, C. and B. Stankoff (2014). "Demyelination in multiple sclerosis." Handb Clin Neurol **122**: 89-99.

Lucchinetti, C., W. Bruck, J. Parisi, B. Scheithauer, M. Rodriguez and H. Lassmann (2000). "Heterogeneity of multiple sclerosis lesions: implications for the pathogenesis of demyelination." Ann Neurol **47**(6): 707-717.

Lucchinetti, C. F., W. Bruck, M. Rodriguez and H. Lassmann (1996). "Distinct patterns of multiple sclerosis pathology indicates heterogeneity on pathogenesis." Brain Pathol **6**(3): 259-274.

Lugaresi, A., M. di Ioia, D. Travaglini, E. Pietrolongo, E. Pucci and M. Onofrj (2013). "Risk-benefit considerations in the treatment of relapsing-remitting multiple sclerosis." Neuropsychiatr Dis Treat **9**: 893-914.

Maimone, D., G. C. Guazzi and P. Annunziata (1997). "IL-6 detection in multiple sclerosis brain." J Neurol Sci **146**(1): 59-65.

Malmestrom, C., B. A. Andersson, S. Haghighi and J. Lycke (2006). "IL-6 and CCL2 levels in CSF are associated with the clinical course of MS: implications for their possible immunopathogenic roles." J Neuroimmunol **175**(1-2): 176-182.

Maninger, N., O. M. Wolkowitz, V. I. Reus, E. S. Epel and S. H. Mellon (2009). "Neurobiological and neuropsychiatric effects of dehydroepiandrosterone (DHEA) and DHEA sulfate (DHEAS)." Front Neuroendocrinol **30**(1): 65-91.

Mao, J. R., G. Taylor, W. B. Dean, D. R. Wagner, V. Afzal, J. C. Lotz, E. M. Rubin and J. Bristow (2002). "Tenascin-X deficiency mimics Ehlers-Danlos syndrome in mice through alteration of collagen deposition." Nat Genet **30**(4): 421-425.

Martinez-Serrano, A. and A. Bjorklund (1996). "Protection of the neostriatum against excitotoxic damage by neurotrophin-producing, genetically modified neural stem cells." J Neurosci **16**(15): 4604-4616.

Matsushima, G. K. and P. Morell (2001). "The neurotoxicant, cuprizone, as a model to study demyelination and remyelination in the central nervous system." Brain Pathol **11**(1): 107-116.

McCarthy, K. D. and J. de Vellis (1980). "Preparation of separate astroglial and oligodendroglial cell cultures from rat cerebral tissue." J Cell Biol **85**(3): 890-902.

McTigue, D. M., P. Wei and B. T. Stokes (2001). "Proliferation of NG2-positive cells and altered oligodendrocyte numbers in the contused rat spinal cord." J Neurosci **21**(10): 3392-3400.

Mei, F., S. P. Fancy, Y. A. Shen, J. Niu, C. Zhao, B. Presley, E. Miao, S. Lee, S. R. Mayoral, S. A. Redmond, A. Etxeberria, L. Xiao, R. J. Franklin, A. Green, S. L. Hauser and J. R. Chan (2014). "Micropillar arrays as a high-throughput screening platform for therapeutics in multiple sclerosis." Nat Med **20**(8): 954-960.

Meixner, A., S. Haverkamp, H. Wassle, S. Fuhrer, J. Thalhammer, N. Kropf, R. E. Bittner, H. Lassmann, G. Wiche and F. Propst (2000). "MAP1B is required for axon guidance and Is involved in the development of the central and peripheral nervous system." J Cell Biol **151**(6): 1169-1178.

Melcangi, R. C. and L. M. Garcia-Segura (2006). "Therapeutic approaches to peripheral neuropathy based on neuroactive steroids." Expert Rev Neurother **6**(8): 1121-1125.

Melcangi, R. C. and G. C. Panzica (2006). "Neuroactive steroids: old players in a new game." Neuroscience **138**(3): 733-739.

Mesiano, S. and R. B. Jaffe (1997). "Developmental and functional biology of the primate fetal adrenal cortex." Endocr Rev **18**(3): 378-403.

Micera, A., R. De Simone and L. Aloe (1995). "Elevated levels of nerve growth factor in the thalamus and spinal cord of rats affected by experimental allergic encephalomyelitis." Arch Ital Biol **133**(2): 131-142.

Micera, A., F. Properzi, V. Triaca and L. Aloe (2000). "Nerve growth factor antibody exacerbates neuropathological signs of experimental allergic encephalomyelitis in adult lewis rats." J Neuroimmunol **104**(2): 116-123.

Miller, D. J., K. Asakura and M. Rodriguez (1996). "Central nervous system remyelination clinical application of basic neuroscience principles." Brain Pathol **6**(3): 331-344.

Millet, V., C. P. Moiola, J. M. Pasquini, E. F. Soto and L. A. Pasquini (2009). "Partial inhibition of proteasome activity enhances remyelination after cuprizone-induced demyelination." Exp Neurol **217**(2): 282-296.

Miron, V. E., A. Boyd, J. W. Zhao, T. J. Yuen, J. M. Ruckh, J. L. Shadrach, P. van Wijngaarden, A. J. Wagers, A. Williams, R. J. Franklin and C. ffrench-Constant (2013). "M2 microglia and macrophages drive oligodendrocyte differentiation during CNS remyelination." Nat Neurosci **16**(9): 1211-1218.

Mitew, S., C. M. Hay, H. Peckham, J. Xiao, M. Koenning and B. Emery (2014). "Mechanisms regulating the development of oligodendrocytes and central nervous system myelin." Neuroscience **276**: 29-47.

Monk, K. R., S. G. Naylor, T. D. Glenn, S. Mercurio, J. R. Perlin, C. Dominguez, C. B. Moens and W. S. Talbot (2009). "A G protein-coupled receptor is essential for Schwann cells to initiate myelination." Science **325**(5946): 1402-1405.

Morante-Oria, J., A. Carleton, B. Ortino, E. J. Kremer, A. Fairen and P. M. Lledo (2003). "Subpallial origin of a population of projecting pioneer neurons during corticogenesis." Proc Natl Acad Sci U S A **100**(21): 12468-12473.

Morell, P., C. V. Barrett, J. L. Mason, A. D. Toews, J. D. Hostettler, G. W. Knapp and G. K. Matsushima (1998). "Gene expression in brain during cuprizone-induced demyelination and remyelination." Mol Cell Neurosci **12**(4-5): 220-227.

Nash, B., K. Ioannidou and S. C. Barnett (2011). "Astrocyte phenotypes and their relationship to myelination." J Anat **219**(1): 44-52.

Nave, K. A. (2010). "Myelination and support of axonal integrity by glia." Nature **468**(7321): 244-252.

Nave, K. A. (2010). "Myelination and the trophic support of long axons." Nat Rev Neurosci **11**(4): 275-283.

Nery, S., G. Fishell and J. G. Corbin (2002). "The caudal ganglionic eminence is a source of distinct cortical and subcortical cell populations." Nat Neurosci **5**(12): 1279-1287.

Nicholas, R. S., M. G. Wing and A. Compston (2001). "Nonactivated microglia promote oligodendrocyte precursor survival and maturation through the transcription factor NF-kappa B." Eur J Neurosci **13**(5): 959-967.

Noble, M. and K. Murray (1984). "Purified astrocytes promote the in vitro division of a bipotential glial progenitor cell." EMBO J **3**(10): 2243-2247.

Noble, M., K. Murray, P. Stroobant, M. D. Waterfield and P. Riddle (1988). "Platelet-derived growth factor promotes division and motility and inhibits premature differentiation of the oligodendrocyte/type-2 astrocyte progenitor cell." Nature **333**(6173): 560-562.

Nordell, V. L., D. K. Lewis, S. Bake and F. Sohrabji (2005). "The neurotrophin receptor p75NTR mediates early anti-inflammatory effects of estrogen in the forebrain of young adult rats." BMC Neurosci **6**: 58.

Offner, H., A. Zamora, H. Drought, A. Matejuk, D. L. Auci, E. E. Morgan, A. A. Vandenbark and C. L. Reading (2002). "A synthetic androstene derivative and a natural androstene metabolite inhibit relapsing-remitting EAE." J Neuroimmunol **130**(1-2): 128-139.

Ogawa, Y., J. Oses-Prieto, M. Y. Kim, I. Horresh, E. Peles, A. L. Burlingame, J. S. Trimmer, D. Meijer and M. N. Rasband (2010). "ADAM22, a Kv1 channel-interacting protein, recruits membrane-associated guanylate kinases to juxtaparanodes of myelinated axons." J Neurosci **30**(3): 1038-1048.

Ogawa, Y., D. P. Schafer, I. Horresh, V. Bar, K. Hales, Y. Yang, K. Susuki, E. Peles, M. C. Stankewich and M. N. Rasband (2006). "Spectrins and ankyrinB constitute a specialized paranodal cytoskeleton." J Neurosci **26**(19): 5230-5239.

Oh, L. Y. and V. W. Yong (1996). "Astrocytes promote process outgrowth by adult human oligodendrocytes in vitro through interaction between bFGF and astrocyte extracellular matrix." Glia **17**(3): 237-253.

Olah, M., S. Amor, N. Brouwer, J. Vinet, B. Eggen, K. Biber and H. W. Boddeke (2012). "Identification of a microglia phenotype supportive of remyelination." Glia **60**(2): 306-321.

Oleszak, E. L., J. R. Chang, H. Friedman, C. D. Katsetos and C. D. Platsoucas (2004). "Theiler's virus infection: a model for multiple sclerosis." Clin Microbiol Rev **17**(1): 174-207.

Orentreich, N., J. L. Brind, J. H. Vogelman, R. Andres and H. Baldwin (1992). "Long-term longitudinal measurements of plasma dehydroepiandrosterone sulfate in normal men." J Clin Endocrinol Metab **75**(4): 1002-1004.

Oudega, M. and T. Hagg (1996). "Nerve growth factor promotes regeneration of sensory axons into adult rat spinal cord." Exp Neurol **140**(2): 218-229.

Pang, Y., Z. Cai and P. G. Rhodes (2000). "Effects of lipopolysaccharide on oligodendrocyte progenitor cells are mediated by astrocytes and microglia." J Neurosci Res **62**(4): 510-520.

Pang, Y., L. Campbell, B. Zheng, L. Fan, Z. Cai and P. Rhodes (2010). "Lipopolysaccharide-activated microglia induce death of oligodendrocyte progenitor cells and impede their development." Neuroscience **166**(2): 464-475.

Pang, Y., L. W. Fan, L. T. Tien, X. Dai, B. Zheng, Z. Cai, R. C. Lin and A. Bhatt (2013). "Differential roles of astrocyte and microglia in supporting oligodendrocyte development and myelination in vitro." Brain Behav **3**(5): 503-514.

Papadopoulos, D., D. Pham-Dinh and R. Reynolds (2006). "Axon loss is responsible for chronic neurological deficit following inflammatory demyelination in the rat." Exp Neurol **197**(2): 373-385.

Papadopoulos, V., M. Baraldi, T. R. Guilarte, T. B. Knudsen, J. J. Lacapere, P. Lindemann, M. D. Norenberg, D. Nutt, A. Weizman, M. R. Zhang and M. Gavish (2006). "Translocator protein (18kDa): new nomenclature for the peripheral-type benzodiazepine receptor based on its structure and molecular function." Trends Pharmacol Sci **27**(8): 402-409.

Pasquini, L. A., C. A. Calatayud, A. L. Bertone Una, V. Millet, J. M. Pasquini and E. F. Soto (2007). "The neurotoxic effect of cuprizone on oligodendrocytes depends on the presence of pro-inflammatory cytokines secreted by microglia." Neurochem Res **32**(2): 279-292.

Patel, J. R., J. L. Williams, M. M. Muccigrosso, L. Liu, T. Sun, J. B. Rubin and R. S. Klein (2012). "Astrocyte TNFR2 is required for CXCL12-mediated regulation of oligodendrocyte progenitor proliferation and differentiation within the adult CNS." Acta Neuropathol **124**(6): 847-860.

Pediaditakis, I., P. Efstathopoulos, K. C. Prousis, M. Zervou, J. C. Arevalo, V. I. Alexaki, V. Nikoletopoulou, E. Karagianni, C. Potamitis, N. Tavernarakis, T. Chavakis, A. N. Margioris, M. Venihaki, T. Calogeropoulou, I. Charalampopoulos and A. Gravanis (2016). "Selective and differential interactions of BNN27, a novel C17-spiroepoxy steroid derivative, with TrkA receptors, regulating neuronal survival and differentiation." Neuropharmacology **111**: 266-282.

Pediaditakis, I., I. Iliopoulos, I. Theologidis, N. Delivanoglou, A. N. Margioris, I. Charalampopoulos and A. Gravanis (2015). "Dehydroepiandrosterone: an ancestral ligand of neurotrophin receptors." Endocrinology **156**(1): 16-23.

Pediaditakis, I., A. Kourgiantaki, K. C. Prousis, C. Potamitis, K. P. Xanthopoulos, M. Zervou, T. Calogeropoulou, I. Charalampopoulos and A. Gravanis (2016). "BNN27, a 17-Spiroepoxy Steroid Derivative, Interacts With and Activates p75 Neurotrophin Receptor, Rescuing Cerebellar Granule Neurons from Apoptosis." Front Pharmacol **7**: 512.

Pfeiffer, S. E., A. E. Warrington and R. Bansal (1993). "The oligodendrocyte and its many cellular processes." Trends Cell Biol **3**(6): 191-197.

Philippidou, P., G. Valdez, W. Akmentin, W. J. Bowers, H. J. Federoff and S. Halegoua (2011). "Trk retrograde signaling requires persistent, Pincher-directed endosomes." Proc Natl Acad Sci U S A **108**(2): 852-857.

Pohlkamp, T., C. David, B. Cauli, T. Gallopin, E. Bouche, A. Karagiannis, P. May, J. Herz, M. Frotscher, J. F. Staiger and H. H. Bock (2014). "Characterization and distribution of Reelin-positive interneuron subtypes in the rat barrel cortex." Cereb Cortex **24**(11): 3046-3058.

Poliak, S. and E. Peles (2003). "The local differentiation of myelinated axons at nodes of Ranvier." Nat Rev Neurosci **4**(12): 968-980.

Poliak, S., D. Salomon, H. Elhanany, H. Sabanay, B. Kiernan, L. Pevny, C. L. Stewart, X. Xu, S. Y. Chiu, P. Shrager, A. J. Furley and E. Peles (2003). "Juxtaparanodal clustering of Shaker-like K+ channels in myelinated axons depends on Caspr2 and TAG-1." J Cell Biol **162**(6): 1149-1160.

Poliani, P. L., Y. Wang, E. Fontana, M. L. Robinette, Y. Yamanishi, S. Gilfillan and M. Colonna (2015). "TREM2 sustains microglial expansion during aging and response to demyelination." J Clin Invest **125**(5): 2161-2170.

Prineas, J. W., E. E. Kwon, P. Z. Goldenberg, A. A. Ilyas, R. H. Quarles, J. A. Benjamins and T. J. Sprinkle (1989). "Multiple sclerosis. Oligodendrocyte proliferation and differentiation in fresh lesions." Lab Invest **61**(5): 489-503.

Pringle, N. P., S. Guthrie, A. Lumsden and W. D. Richardson (1998). "Dorsal spinal cord neuroepithelium generates astrocytes but not oligodendrocytes." Neuron **20**(5): 883-893.

Prinz, M. and J. Priller (2014). "Microglia and brain macrophages in the molecular age: from origin to neuropsychiatric disease." Nat Rev Neurosci **15**(5): 300-312.

Psachoulia, K., F. Jamen, K. M. Young and W. D. Richardson (2009). "Cell cycle dynamics of NG2 cells in the postnatal and ageing brain." Neuron Glia Biol **5**(3-4): 57-67.

Rasband, M. N., E. W. Park, D. Zhen, M. I. Arbuckle, S. Poliak, E. Peles, S. G. Grant and J. S. Trimmer (2002). "Clustering of neuronal potassium channels is independent of their interaction with PSD-95." J Cell Biol **159**(4): 663-672.

Rathjen, F. G., J. M. Wolff and R. Chiquet-Ehrismann (1991). "Restrictin: a chick neural extracellular matrix protein involved in cell attachment co-purifies with the cell recognition molecule F11." Development **113**(1): 151-164.

Reddy, D. S. (2010). "Neurosteroids: endogenous role in the human brain and therapeutic potentials." Prog Brain Res **186**: 113-137.

Regelson, W. and M. Kalimi (1994). "Dehydroepiandrosterone (DHEA)--the multifunctional steroid. II. Effects on the CNS, cell proliferation, metabolic and vascular, clinical and other effects. Mechanism of action?" Ann N Y Acad Sci **719**: 564-575.

Remington, L. T., A. A. Babcock, S. P. Zehntner and T. Owens (2007). "Microglial recruitment, activation, and proliferation in response to primary demyelination." Am J Pathol **170**(5): 1713-1724.

Rice, D. S. and T. Curran (2001). "Role of the reelin signaling pathway in central nervous system development." Annu Rev Neurosci **24**: 1005-1039.

Robel, P. and E. E. Baulieu (1994). "Neurosteroids Biosynthesis and function." Trends Endocrinol Metab **5**(1): 1-8.

Robinson, A. P., C. T. Harp, A. Noronha and S. D. Miller (2014). "The experimental autoimmune encephalomyelitis (EAE) model of MS: utility for understanding disease pathophysiology and treatment." Handb Clin Neurol **122**: 173-189.

Rock, R. B., G. Gekker, S. Hu, W. S. Sheng, M. Cheeran, J. R. Lokensgard and P. K. Peterson (2004). "Role of microglia in central nervous system infections." Clin Microbiol Rev **17**(4): 942-964, table of contents.

Rodriguez-Tebar, A., G. Dechant and Y. A. Barde (1990). "Binding of brain-derived neurotrophic factor to the nerve growth factor receptor." Neuron **4**(4): 487-492.

Rose, C. R., R. Blum, B. Pichler, A. Lepier, K. W. Kafitz and A. Konnerth (2003). "Truncated TrkB-T1 mediates neurotrophin-evoked calcium signalling in glia cells." Nature **426**(6962): 74-78.

Rosen, C. L., R. P. Bunge, M. D. Ard and P. M. Wood (1989). "Type 1 astrocytes inhibit myelination by adult rat oligodendrocytes in vitro." J Neurosci **9**(10): 3371-3379.

Rosenberg, S. S., E. E. Kelland, E. Tokar, A. R. De la Torre and J. R. Chan (2008). "The geometric and spatial constraints of the microenvironment induce oligodendrocyte differentiation." Proc Natl Acad Sci U S A **105**(38): 14662-14667.

Rotola, A., I. Merlotti, L. Caniatti, E. Caselli, E. Granieri, M. R. Tola, D. Di Luca and E. Cassai (2004). "Human herpesvirus 6 infects the central nervous system of multiple sclerosis patients in the early stages of the disease." Mult Scler **10**(4): 348-354.

Rowitch, D. H. and A. R. Kriegstein (2010). "Developmental genetics of vertebrate glial-cell specification." Nature **468**(7321): 214-222.

Rudge, J. S., Y. Li, E. M. Pasnikowski, K. Mattsson, L. Pan, G. D. Yancopoulos, S. J. Wiegand, R. M. Lindsay and N. Y. Ip (1994). "Neurotrophic factor receptors and their signal transduction capabilities in rat astrocytes." Eur J Neurosci **6**(5): 693-705.

Rutishauser, U. and L. Landmesser (1996). "Polysialic acid in the vertebrate nervous system: a promoter of plasticity in cell-cell interactions." Trends Neurosci **19**(10): 422-427.

Saijo, K., J. G. Collier, A. C. Li, J. A. Katzenellenbogen and C. K. Glass (2011). "An ADIOL-ERbeta-CtBP transrepression pathway negatively regulates microglia-mediated inflammation." Cell **145**(4): 584-595.

Sakurai, Y., D. Nishimura, K. Yoshimura, Y. Tsuruo, C. Seiwa and H. Asou (1998). "Differentiation of oligodendrocyte occurs in contact with astrocyte." J Neurosci Res **52**(1): 17-26.

Santambrogio, L., M. Benedetti, M. V. Chao, R. Muzaffar, K. Kulig, N. Gabellini and G. Hochwald (1994). "Nerve growth factor production by lymphocytes." J Immunol **153**(10): 4488-4495.

Savvaki, M., T. Panagiotaropoulos, A. Stamatakis, I. Sargiannidou, P. Karatzioula, K. Watanabe, F. Stylianopoulou, D. Karagogeos and K. A. Kleopa (2008). "Impairment of learning and memory in TAG-1 deficient mice associated with shorter CNS internodes and disrupted juxtaparanodes." Mol Cell Neurosci **39**(3): 478-490.

Savvaki, M., K. Theodorakis, L. Zoupi, A. Stamatakis, S. Tivodar, K. Kyriacou, F. Stylianopoulou and D. Karagogeos (2010). "The expression of TAG-1 in glial cells is sufficient for the formation of the juxtaparanodal complex and the phenotypic rescue of tag-1 homozygous mutants in the CNS." J Neurosci **30**(42): 13943-13954.

Schafer, D. P. and M. N. Rasband (2006). "Glial regulation of the axonal membrane at nodes of Ranvier." Curr Opin Neurobiol **16**(5): 508-514.

Scherberich, A., R. P. Tucker, E. Samandari, M. Brown-Luedi, D. Martin and R. Chiquet-Ehrismann (2004). "Murine tenascin-W: a novel mammalian tenascin expressed in kidney and at sites of bone and smooth muscle development." J Cell Sci **117**(Pt 4): 571-581.

Serada, S., M. Fujimoto, M. Mihara, N. Koike, Y. Ohsugi, S. Nomura, H. Yoshida, T. Nishikawa, F. Terabe, T. Ohkawara, T. Takahashi, B. Ripley, A. Kimura, T. Kishimoto and T. Naka (2008). "IL-6 blockade inhibits the induction of myelin antigen-specific Th17 cells and Th1 cells in experimental autoimmune encephalomyelitis." Proc Natl Acad Sci U S A **105**(26): 9041-9046.

Shen, S., J. Li and P. Casaccia-Bonnefil (2005). "Histone modifications affect timing of oligodendrocyte progenitor differentiation in the developing rat brain." J Cell Biol **169**(4): 577-589.

Sherman, D. L. and P. J. Brophy (2005). "Mechanisms of axon ensheathment and myelin growth." Nat Rev Neurosci **6**(9): 683-690.

Shi, J., A. Marinovich and B. A. Barres (1998). "Purification and characterization of adult oligodendrocyte precursor cells from the rat optic nerve." J Neurosci **18**(12): 4627-4636.

Shooter, E. M. (2001). "Early days of the nerve growth factor proteins." Annu Rev Neurosci **24**: 601-629.

Silver, J. and J. H. Miller (2004). "Regeneration beyond the glial scar." Nat Rev Neurosci **5**(2): 146-156.

Simon, C., M. Gotz and L. Dimou (2011). "Progenitors in the adult cerebral cortex: cell cycle properties and regulation by physiological stimuli and injury." Glia **59**(6): 869-881.

Simons, M., T. Misgeld and M. Kerschensteiner (2014). "A unified cell biological perspective on axon-myelin injury." J Cell Biol **206**(3): 335-345.

Skripuletz, T., V. Gudi, D. Hackstette and M. Stangel (2011). "De- and remyelination in the CNS white and grey matter induced by cuprizone: the old, the new, and the unexpected." Histol Histopathol **26**(12): 1585-1597.

Skripuletz, T., D. Hackstette, K. Bauer, V. Gudi, R. Pul, E. Voss, K. Berger, M. Kipp, W. Baumgartner and M. Stangel (2013). "Astrocytes regulate myelin clearance through recruitment of microglia during cuprizone-induced demyelination." Brain **136**(Pt 1): 147-167.

Sloane, J. A., C. Batt, Y. Ma, Z. M. Harris, B. Trapp and T. Vartanian (2010). "Hyaluronan blocks oligodendrocyte progenitor maturation and remyelination through TLR2." Proc Natl Acad Sci U S A **107**(25): 11555-11560.

Snaidero, N. and M. Simons (2014). "Myelination at a glance." J Cell Sci **127**(Pt 14): 2999-3004.

Sofroniew, M. V. and H. V. Vinters (2010). "Astrocytes: biology and pathology." Acta Neuropathol **119**(1): 7-35.

Soulet, D. and S. Rivest (2008). "Microglia." Curr Biol **18**(12): R506-508.

Speight, J. L., L. Yao, I. Rozenberg and P. Bernd (1993). "Early embryonic quail dorsal root ganglia exhibit high affinity nerve growth factor binding and NGF responsiveness--absence of NGF receptors on migrating neural crest cells." Brain Res Dev Brain Res **75**(1): 55-64.

Stankoff, B., M. S. Aigrot, F. Noel, A. Wattilliaux, B. Zalc and C. Lubetzki (2002). "Ciliary neurotrophic factor (CNTF) enhances myelin formation: a novel role for CNTF and CNTF-related molecules." J Neurosci **22**(21): 9221-9227.

Streit, W. J. (2002). "Microglia as neuroprotective, immunocompetent cells of the CNS." Glia **40**(2): 133-139.

Strohmaier, C., B. D. Carter, R. Urfer, Y. A. Barde and G. Dechant (1996). "A splice variant of the neurotrophin receptor trkB with increased specificity for brain-derived neurotrophic factor." EMBO J **15**(13): 3332-3337.

Susuki, K. and M. N. Rasband (2008). "Molecular mechanisms of node of Ranvier formation." Curr Opin Cell Biol **20**(6): 616-623.

Susuki, K. and M. N. Rasband (2008). "Spectrin and ankyrin-based cytoskeletons at polarized domains in myelinated axons." Exp Biol Med (Maywood) **233**(4): 394-400.

Takano, R., S. Hisahara, K. Namikawa, H. Kiyama, H. Okano and M. Miura (2000). "Nerve growth factor protects oligodendrocytes from tumor necrosis factor-alpha-induced injury through Akt-mediated signaling mechanisms." J Biol Chem **275**(21): 16360-16365.

Tamashiro, T. T., C. L. Dalgard and K. R. Byrnes (2012). "Primary microglia isolation from mixed glial cell cultures of neonatal rat brain tissue." J Vis Exp(66): e3814.

Taveggia, C., P. Thaker, A. Petrylak, G. L. Caporaso, A. Toews, D. L. Falls, S. Einheber and J. L. Salzer (2008). "Type III neuregulin-1 promotes oligodendrocyte myelination." Glia **56**(3): 284-293.

Tissir, F. and A. M. Goffinet (2003). "Reelin and brain development." Nat Rev Neurosci **4**(6): 496-505.

Traka, M., J. L. Dupree, B. Popko and D. Karagogeos (2002). "The neuronal adhesion protein TAG-1 is expressed by Schwann cells and oligodendrocytes and is localized to the juxtaparanodal region of myelinated fibers." J Neurosci **22**(8): 3016-3024.

Traka, M., L. Goutebroze, N. Denisenko, M. Bessa, A. Nifli, S. Havaki, Y. Iwakura, F. Fukamauchi, K. Watanabe, B. Soliven, J. A. Girault and D. Karagogeos (2003). "Association of TAG-1 with Caspr2 is essential for the molecular organization of juxtaparanodal regions of myelinated fibers." J Cell Biol **162**(6): 1161-1172.

Trapp, B. D. (2004). "Pathogenesis of multiple sclerosis: the eyes only see what the mind is prepared to comprehend." Ann Neurol **55**(4): 455-457.

Trapp, B. D., A. Nishiyama, D. Cheng and W. Macklin (1997). "Differentiation and death of premyelinating oligodendrocytes in developing rodent brain." J Cell Biol **137**(2): 459-468.

Trebst, C., F. Konig, R. Ransohoff, W. Bruck and M. Stangel (2008). "CCR5 expression on macrophages/microglia is associated with early remyelination in multiple sclerosis lesions." Mult Scler **14**(6): 728-733.

Trigos, A. S., M. Longart, L. Garcia, C. Castillo, P. Forsyth and R. Medina (2015). "ProNGF derived from rat sciatic nerves downregulates neurite elongation and axon specification in PC12 cells." Front Cell Neurosci **9**: 364.

Tucker, R. P., K. Drabikowski, J. F. Hess, J. Ferralli, R. Chiquet-Ehrismann and J. C. Adams (2006). "Phylogenetic analysis of the tenascin gene family: evidence of origin early in the chordate lineage." BMC Evol Biol **6**: 60.

Tzimourakas, A., S. Giasemi, M. Mouratidou and D. Karagogeos (2007). "Structure-function analysis of protein complexes involved in the molecular architecture of juxtaparanodal regions of myelinated fibers." Biotechnol J **2**(5): 577-583.

Ultsch, M. H., C. Wiesmann, L. C. Simmons, J. Henrich, M. Yang, D. Reilly, S. H. Bass and A. M. de Vos (1999). "Crystal structures of the neurotrophin-binding domain of TrkA, TrkB and TrkC." J Mol Biol **290**(1): 149-159.

Vabnick, I., S. D. Novakovic, S. R. Levinson, M. Schachner and P. Shrager (1996). "The clustering of axonal sodium channels during development of the peripheral nervous system." J Neurosci **16**(16): 4914-4922.

Vabnick, I., J. S. Trimmer, T. L. Schwarz, S. R. Levinson, D. Risal and P. Shrager (1999). "Dynamic potassium channel distributions during axonal development prevent aberrant firing patterns." J Neurosci **19**(2): 747-758.

Villoslada, P., S. L. Hauser, I. Bartke, J. Unger, N. Heald, D. Rosenberg, S. W. Cheung, W. C. Mobley, S. Fisher and C. P. Genain (2000). "Human nerve growth factor protects common marmosets against autoimmune encephalomyelitis by switching the balance of T helper cell type 1 and 2 cytokines within the central nervous system." J Exp Med **191**(10): 1799-1806.

Wang, C., G. Rougon and J. Z. Kiss (1994). "Requirement of polysialic acid for the migration of the O-2A glial progenitor cell from neurohypophyseal explants." J Neurosci **14**(7): 4446-4457.

Wang, H., S. Liu, Y. Tian, X. Wu, Y. He, C. Li, M. Namaka, J. Kong, H. Li and L. Xiao (2015). "Quetiapine Inhibits Microglial Activation by Neutralizing Abnormal STIM1-Mediated Intercellular Calcium Homeostasis and Promotes Myelin Repair in a Cuprizone-Induced Mouse Model of Demyelination." Front Cell Neurosci **9**: 492.

Wang, L., X. Chang, L. She, D. Xu, W. Huang and M. M. Poo (2015). "Autocrine action of BDNF on dendrite development of adult-born hippocampal neurons." J Neurosci **35**(22): 8384-8393.

Wang, Y., X. Cheng, Q. He, Y. Zheng, D. H. Kim, S. R. Whittemore and Q. L. Cao (2011). "Astrocytes from the contused spinal cord inhibit oligodendrocyte differentiation of adult oligodendrocyte precursor cells by increasing the expression of bone morphogenetic proteins." J Neurosci **31**(16): 6053-6058.

Wang, Y., C. Hagel, W. Hamel, S. Muller, L. Kluwe and M. Westphal (1998). "Trk A, B, and C are commonly expressed in human astrocytes and astrocytic gliomas but not by human oligodendrocytes and oligodendroglioma." Acta Neuropathol **96**(4): 357-364.

Warf, B. C., J. Fok-Seang and R. H. Miller (1991). "Evidence for the ventral origin of oligodendrocyte precursors in the rat spinal cord." J Neurosci **11**(8): 2477-2488.

Watkins, T. A., B. Emery, S. Mulinyawe and B. A. Barres (2008). "Distinct stages of myelination regulated by gamma-secretase and astrocytes in a rapidly myelinating CNS coculture system." Neuron **60**(4): 555-569.

Weeber, E. J., U. Beffert, C. Jones, J. M. Christian, E. Forster, J. D. Sweatt and J. Herz (2002). "Reelin and ApoE receptors cooperate to enhance hippocampal synaptic plasticity and learning." J Biol Chem **277**(42): 39944-39952.

Xiao, Z. C., D. S. Ragsdale, J. D. Malhotra, L. N. Mattei, P. E. Braun, M. Schachner and L. L. Isom (1999). "Tenascin-R is a functional modulator of sodium channel beta subunits." J Biol Chem **274**(37): 26511-26517.

Xing, Y. L., P. T. Roth, J. A. Stratton, B. H. Chuang, J. Danne, S. L. Ellis, S. W. Ng, T. J. Kilpatrick and T. D. Merson (2014). "Adult neural precursor cells from the subventricular zone contribute significantly to oligodendrocyte regeneration and remyelination." J Neurosci **34**(42): 14128-14146.

Yajima, K. and K. Suzuki (1979). "Demyelination and remyelination in the rat central nervous system following ethidium bromide injection." Lab Invest **41**(5): 385-392.

Yang, J., L. C. Harte-Hargrove, C. J. Siao, T. Marinic, R. Clarke, Q. Ma, D. Jing, J. J. Lafrancois, K. G. Bath, W. Mark, D. Ballon, F. S. Lee, H. E. Scharfman and B. L. Hempstead (2014). "proBDNF negatively regulates neuronal remodeling, synaptic transmission, and synaptic plasticity in hippocampus." Cell Rep **7**(3): 796-806.

Yao, R. and G. M. Cooper (1995). "Regulation of the Ras signaling pathway by GTPase-activating protein in PC12 cells." Oncogene **11**(8): 1607-1614.

Yates, M. A., Y. Li, P. Chlebeck, T. Proctor, A. A. Vandenbark and H. Offner (2010). "Progesterone treatment reduces disease severity and increases IL-10 in experimental autoimmune encephalomyelitis." J Neuroimmunol **220**(1-2): 136-139.

Yin, X., R. C. Baek, D. A. Kirschner, A. Peterson, Y. Fujii, K. A. Nave, W. B. Macklin and B. D. Trapp (2006). "Evolution of a neuroprotective function of central nervous system myelin." J Cell Biol **172**(3): 469-478.

Yoon, S. O., P. Casaccia-Bonnefil, B. Carter and M. V. Chao (1998). "Competitive signaling between TrkA and p75 nerve growth factor receptors determines cell survival." J Neurosci **18**(9): 3273-3281.

Yorek, M. A., L. J. Coppey, J. S. Gellett, E. P. Davidson, X. Bing, D. D. Lund and J. S. Dillon (2002). "Effect of treatment of diabetic rats with dehydroepiandrosterone on vascular and neural function." Am J Physiol Endocrinol Metab **283**(5): E1067-1075.

Yoshikawa, K., S. Palumbo, C. D. Toscano and F. Bosetti (2011). "Inhibition of 5-lipoxygenase activity in mice during cuprizone-induced demyelination attenuates neuroinflammation, motor dysfunction and axonal damage." Prostaglandins Leukot Essent Fatty Acids **85**(1): 43-52.

Young, K. M., K. Psachoulia, R. B. Tripathi, S. J. Dunn, L. Cossell, D. Attwell, K. Tohyama and W. D. Richardson (2013). "Oligodendrocyte dynamics in the healthy adult CNS: evidence for myelin remodeling." Neuron **77**(5): 873-885.

Zalc, B. and D. R. Colman (2000). "Origins of vertebrate success." Science **288**(5464): 271-272.

Zawadzka, M., L. E. Rivers, S. P. Fancy, C. Zhao, R. Tripathi, F. Jamen, K. Young, A. Goncharevich, H. Pohl, M. Rizzi, D. H. Rowitch, N. Kessaris, U. Suter, W. D. Richardson and R. J. Franklin (2010). "CNS-resident glial progenitor/stem cells produce Schwann cells as well as oligodendrocytes during repair of CNS demyelination." Cell Stem Cell **6**(6): 578-590.

Zeger, M., G. Popken, J. Zhang, S. Xuan, Q. R. Lu, M. H. Schwab, K. A. Nave, D. Rowitch, A. J. D'Ercole and P. Ye (2007). "Insulin-like growth factor type 1 receptor signaling in the cells of oligodendrocyte lineage is required for normal in vivo oligodendrocyte development and myelination." Glia **55**(4): 400-411.

Zhao, L., M. L. Yeh and E. S. Levine (2015). "Role for Endogenous BDNF in Endocannabinoid-Mediated Long-Term Depression at Neocortical Inhibitory Synapses." eNeuro **2**(2).

Zoupi, L., M. Savvaki and D. Karagogeos (2011). "Axons and myelinating glia: An intimate contact." IUBMB Life **63**(9): 730-735.

Zwain, I. H. and S. S. Yen (1999). "Neurosteroidogenesis in astrocytes, oligodendrocytes, and neurons of cerebral cortex of rat brain." Endocrinology **140**(8): 3843-3852.

APPENDIX

Table 1. Primary antibodies used in the study

Antibody/Epitope	Source	Type	Directed against (species)	Working dilution	Application
α-IBA1	Wako Chemicals	Rabbit, polyclonal	Human, mouse, rat, rabbit	1:500	ICC, IHC
α-MBP	Serotec	Rat, monoclonal	Human, mouse, rat, rabbit	1:200	ICC, IHC
α-Caspase3	Millipore	Rabbit, polyclonal	Human, mouse, rat, rabbit	1 :100	ICC
α-Ki67	Novocastra	Rat, monoclonal	Human, mouse, rat, rabbit	1 :200	ICC
α-TrkA	Millipore	Rabbit, polyclonal	Human, mouse, rat, rabbit	1 :100 (ICC, IHC) 1:2000 (WB)	ICC, IHC, WB
α-$p75^{NTR}$	Promega	Rabbit, polyclonal	Human, mouse, rat, rabbit	1 :200 (ICC, IHC) 1:5000 (WB)	ICC, IHC, WB
α-APC (clone CC-1)	Calbiochem	Mouse, monoclonal	Human, mouse, rat	1:100	ICC, IHC
α-PDGFRα	Millipore	Rat, monoclonal	Mouse, rat	1:100	IHC
α-GFAP	Sigma	Mouse, monoclonal	Human, mouse, rat, pig	1:2000	ICC, IHC

TG2 (α-TAG1)	Traka et al, 2002	Rabbit, polyclonal	Human, mouse, rat	1:2000	WB
α -TNR	Ratjen et al, 2002	Mouse, monoclonal	Human, mouse, rat	1:1000	WB
α-MAP1B	Santa Cruz Biotechnology	Mouse, monoclonal	Human, mouse, rat	1:500	WB
α-MAP2	Cell Signaling	Mouse, monoclonal	Human, mouse, rat	1:5000	WB
α-Reelin E4	Developmental Studies Hybridoma Bank	Mouse, monoclonal	Human, mouse, rat	1:1000	WB
α-GAPDH	Santa Cruz Biotechnology	Mouse, monoclonal	Human, mouse, rat	1:3000	WB
α-γ tubulin	Sigma Aldrich	Mouse, monoclonal	Human, mouse, rat	1:4000	WB

ICC: Immunocytochemistry; IHC: Immunohistochemistry; WB: Western blot

Table 2. Secondary antibodies and fluorescent-conjugated probes used in the study

Antibody/Epitope	Source	Working dilution	Application
α-rabbit IgG-Cy3®	Jackson ImmunoResearch Laboratories	1:800	ICC, IHC
α-rat IgG-Alexa Fluor® 488 or 555	Molecular Probes, Thermo	1:800	ICC, IHC
α-mouse IgG-Alexa Fluor® 488 or 555	Molecular Probes, Thermo Fisher Scientific	1:800	ICC, IHC
α-rabbit IgG horseradish-conjugated	Jackson ImmunoResearch Laboratories	1:5000	WB
α-mouse IgG horseradish-conjugated	Jackson ImmunoResearch Laboratories	1:5000	WB

ICC: Immunocytochemistry; IHC: Immunohistochemistry; WB: Western blot